

**Development of a Molecular Spaceframe. Study towards
the synthesis of molecular building blocks for this
new material concept.**

Proefschrift voorgelegd tot het behalen van de graad van
Doctor in de Wetenschappen, richting Scheikunde,
te verdedigen door

Joachim VAN DIJK

Promotor : Prof. dr. D. Vanderzande

UNIVERSITEITSBIBLIOTHEEK LUC



03 04 0067583 8

161191



24 JUN 2003



541.64
VAND
2003

luc.luc

547.69
- synthese methoden
- vertaalde structuren
- complex set
2003

Faculteit Wetenschappen

**Development of a Molecular Spaceframe. Study towards
the synthesis of molecular building blocks for this new
material concept.**

031191

Proefschrift voorgelegd tot het behalen van de graad van
Doctor in de Wetenschappen, richting Scheikunde,
te verdedigen door

Joachim VAN DIJK

Promotor : Prof. dr. D. Vanderzande



24 JUN 2003



Instituut voor Materiaalonderzoek



According to the guidelines of the Limburgs Universitair Centrum, a copy
this publication has been filed in the Royal Library Albert I, Brussels, as publicat
D/2003/2451,

Voorwoord

Gelukkig is het maken van een doctoraatsthesis niet het werk van slechts één persoon, vandaar dat een woord van mijn oprechte dank aan diegene die hieraan meegewerkt hebben en dan bedoel ik niet enkel inhoudelijk, hier zeker op zijn plaats is. Dit onderdeel van het wetenschappelijk proefschrift heeft, wetenschappelijk gezien, geen enkele waarde maar wordt toch het meest gelezen. Waarschijnlijk is dit onderdeel voor de meesten dan ook het interessantste. Daarom heb ik in dit voorwoord niet enkel een woord van dank, maar eveneens een aantal aspecten die me zijn bijgebleven en ervaringen van de laatste vijf jaar, vermeld.

Laat ik beginnen met de twee mensen die hun vertrouwen in mij hebben gesteld en van wie ik de kans gekregen heb om aan dit project te mogen beginnen. Professor dr. Dirk Vanderzande, mijn promotor, dank ik voor het aanbieden van de mogelijkheid om hier in het verre Limburg te kunnen doctoreren. Niet alleen zijn wetenschappelijke inventiviteit zijn enthousiasme voor de scheikunde maar ook het statement "Shit Happens" en het beeld van het bijna nader kennis maken met de Demer tijdens één van de barbecues zullen mij nog lang bijblijven. Professor dr. Jan Gelan ben ik eveneens erkentelijk voor het aanbieden van de mogelijkheid om te doctoreren aan het LUC. Spijtig dat ik niet een jaartje eerder hier ben kunnen beginnen, die Jungle Party's had ik wel willen meemaken.

De mensen van het DSM-team Prof dr. Jos Put, dr. Ing. Roelof Marissen, dr. Ronald Lange, Loek Steffanie en Betty Coussens dank ik om dit project. DSM dank ik eveneens voor de financiële steun.

Professor dr Luc Van Meervelt die mij uit de nood heeft geholpen door een x-straal diffractie voor me op te nemen ben ik eveneens erkentelijk.

Professor dr. Ulrich Schubert van de TU/e ben ik dank verschuldigd voor het ter beschikking stellen van de apparatuur en een aantal producten.

Dr. Peter Adriaensens dank ik omdat hij ondanks alle drukte toch steeds eventjes tijd vrij kon maken als ik problemen had met het ene of het andere spectrum alsook Jan Czech die steeds de massa van mijn 'lastige' producten opnam en als dit niet lukte waren er nog steeds dr. Jean-Paul Noben en Erik Royackers die het voor mij probeerde. Huguette Penxten die steeds bereid was om met een glimlach en de nodige apparatuur IR en UV's op te nemen, bedankt. Guy Reggers dank ik voor de TGA en DSC's.

De volgende mensen van het labo dank ik en zal ik zeker niet gauw vergeten. De volgorde van opsomming geeft natuurlijk niet de mate van hun belangrijkheid weer.

Dr. Laurence Lutsen, dank ik voor het organiseren van het evenement van het jaar; met name de labokuis. De Post-it papiertjes 's morgens op mijn bureau waren voor mij steeds een aangename verrassing.

Wojtek, because you are not able to read Dutch, I thank you in english. Thanks for the photos you gave me, I don't know when you leave but anyway: have a safe trip back to Poland.

Stijn bedankt voor die keren dat ik bij je mocht blijven logeren, vooral die keer met Annie was te gek. En wat onze trekkasten betreft, die pasten perfect naast elkaar, die waren beide even slordig.

Annie, meest behulpzame van het labo, als het nog eens -ik weet niet meer welke- kermis is ginder laat maar iets weten dan. Misschien kunnen we dan 's morgens lekkere krwazants van ginder eten.

Sofie, de stralende glimlach waar je me 's morgens mee begroet zal ik missen alsook de koffie die je voor me ging halen. Gelukkig dat je geen diwaterstofperoxide voor me moest meebrengen hé.

Kristof, gij zijt natuurlijk ook een goei koffiëmadam. Als je naar een ander appartement verhuist bent kom ik nog wel eens dag zeggen tegen de geburen, bedankt dat ik toch nog mocht blijven logeren.

Veerle, 75 is Beslist een goed jaar dat zie je aan je. Bedankt voor die ene GPC die je voor me kon opnemen alsook voor het Sinterklaas spelen want volgens mij ben jij dat al wel eens geweest.

Hilde, als ik ooit een ongeluk heb met de auto hoop ik dat je langs rijdt euh... ik bedoel stopt. Veel geluk met de trouw!

Fil, spijtig dat je niet kon blijven in Warwick, gelukkig is nu uiteindelijk alles in orde gekomen. Nog veel geluk met de duiven en dan vooral als ik inzet natuurlijk. Hopelijk lukt dat spelen beter als met de gouden 11 en op de beurs.

Lien, geweldige wedstrijd die je samen met Ine georganiseerd hebt maar ik zou hem toch elke morgen weer opnieuw laten beginnen je weet maar nooit of er iets veranderd is.

Liesbet, alias bigfoot, ocharme nog in geen enkel dankwoord expliciet vermeld, zonder haar hadden we dit jaar waarschijnlijk geen labo week-end gehad, alvast veel geluk met de (uiteindelijke) trouw.

Els, spijtig dat we voor die verre verplaatsingen niet regelmatig hebben kunnen carpoolen, dat had nog wat meer in onze portemonné gescheelt hé.

Ine, als ik ooit in pan sta met de auto spring ik met veel plezier de trein op want dat is sinds kort toch zóveel mooier geworden. Ik denk dat ik een abonnement ga nemen. X.

Lieve, ook al zit je niet meet op't labo, bedankt om me je luisterend oor aan te bieden en als je nog eens iemand zoekt om de Colonisten te spelen, je weet me wel te vinden hé.

Anne, die geweldige foto's die er van ons samen genomen zijn gedurende die vijf jaar daar kun je nog prijzen mee winnen, met wat dat laat ik wijselijk in het midden.

Dams, Geel zal altijd minder goed zijn dan KV gelijk in welke klasse ze spelen. Volgend jaar is het waarschijnlijk terug fuif van de voetbal, misschien kan je is overwegen langs te komen? Tof dat je hier aan het LUC gebleven bent om samen met mij te doppen maat.

Robby, kamergenoot, de crash na het verblijf in de Vil, pukkelpop verleden jaar en nog een hele boel meer, zal ik me nog lang herinneren. Nog veel succes bij het VITO en veel leuke momenten met Zamira en de (voorlopige) scampi.

Duysens, lekker beest zoals sommigen je blijkbaar noemde, je was een schitterende gebuur, bedankt voor het luisterend oor en voor al die geweldige uitvluchten die je steeds wist te verzinnen om niet mee te moeten gaan batmintonnen of naar de bbq komen, nog veel wandelplezier.

Bobby, met je lekkere kippebillen spijtig dat we is niet een keer samen zijn kunnen uitgaan, dat zou pas ramvet geweest zijn.

Ook mensen die niet tot 'het labo' behoren ben ik dankbaar. Sali, altijd bereidt om een leuke babbel, als ik ooit een privé chauffeur nodig heb weet ik je wel te vinden. Kristel, niet enkel bedankt voor het snel maken van bestellingen maar ook voor de vele snoepjes alsook voor de opvang van mijn voormalige twee poezen. Steven Nys, als je volgend jaar bij KVM komt spelen kom ik zeker voor je supporteren. Eugene we worden beide te oud voor de voetbal maar 't was toch plezant. Koen, niet enkel voor zaken zoals computers aan de praat krijgen maar ook voor andere dingen zoals o.a. het labo van blaaspipen voorzien voor het labo week-endje konden we steeds bij je terecht. Jos, op het LUC ben je mijn naamgenoot bedankt voor de schitterende destillatie opstelling die je voor me hebt gemaakt.

Al de mensen van het SBG secretariaat die ervoor gezorgd hebben dat alle administratieve zaken geregeld werden, bedankt.

Ook de leden van de andere onderzoeksgroepen dank ik voor de leuke momenten tijdens de labo week-ends en tijdens allerlei feestjes. VW, Fox, James, Geert, Goeshjoe, de vakantie in Polen, de koers in Frankrijk waren toch wel 'sterk' hé; Cola, Fanta, Fucky Fucky, Sprite...?

Als laatste maar zeker niet de minste, integendeel, zou ik nog enkele mensen van 'thuis' willen bedanken. Mam, pap bedankt voor de mogelijkheid om te kunnen verder studeren zonder jullie steun zou dit alles niet gelukt zijn. Liesbeth ik weet niet waar we zullen staan als dit boekje uiteindelijk gedrukt is maar ik hoop uit de grond van mijn hart dat we dit gedeelte op onze oude dag SAMEN kunnen nalezen ook al is het met één oog en moet ik het je, of jij het mij, voorlezen. Vassie als je dit leest zijn twee van de drie "moeilijke zaken" achter de rug, nu alleen dat laatste nog. Hilde, de jaren van mijn doctoraat zijn zeker niet de gemakkelijkste geweest, toch bedankt om me er, in de mate van het mogelijke, op te wijzen dat dat wel in orde zou komen, ik wens je nog veel gelukkige jaren met Dirk.

Al de andere vrienden en vriendinnen diegene hun naam ik hier moeilijk allemaal kan vermelden en die zich steeds afgevraagd hebben wat ik nu juist deed op het LUC, wel zie hier het resultaat. Veel leesplezier en voor de analfabeten onder jullie niet getreurd er staan genoeg "prentjes" in om te bekijken.

Ik hoop dat ik in de toekomst in een even aangename werksfeer mag terechtkomen. Hoogst waarschijnlijk heb ik in dit voorwoord niet steeds de juiste woorden gevonden om mijn oprechte dank en respect uit te drukken, vandaar dat ik dit hele voorwoord misschien beter had kunnen samenvatten als: bedankt allemaal.

TABLE OF CONTENTS

CHAPTER ONE GENERAL INTRODUCTION

1.1	INTRODUCTION	1
1.2	PROPERTIES OF MOLECULAR SPACEFRAME	4
1.2.1	Calculational Details	4
	<i>1.2.1.1 The force field approach</i>	4
	<i>1.2.1.2 Molecular mechanics and dynamics calculations</i>	5
1.2.2	Isostatic And Hyperstatic Spaceframe	6
1.2.3	Structure	8
1.2.4.	Density	12
1.2.5	Bulk Modulus	13
1.2.6	Thermal Expansion Coefficient	16
1.3	APPLICATIONS	17
1.4	REFERENCES	19

CHAPTER TWO SYNTHESIS OF MOLECULAR RODS

2.1	CHOICE OF MOLECULAR RODS	21
2.1.1	Introduction	21
2.1.2	Oligophenylenes	23
	<i>2.1.2.1 Synthetic method towards oligo-p-phenylenes</i>	25

2.1.2.2	<i>Targeted and random synthesis</i>	28
2.1.3	Terpyridines	30
2.1.3.1	<i>History and properties of</i> <i>2,2':6',2''-terpyridine</i>	30
2.1.3.2	<i>Choice of terpyridines</i>	32
2.2	SYNTHESIS OF MOLECULAR RODS	34
2.2.1	Synthesis Of Oligophenylenes	34
2.2.1.1	<i>Synthesis of 4-bromo-2,5,2'',5''-tetra-n-hexyl-</i> <i>4'''-trimethylsilyltetraphenyl</i>	34
2.2.2	Synthesis Of Terpyridines	40
2.2.2.1	<i>Synthesis of 4'-(4-ethynylphenyl)-2,2':6',2''-</i> <i>terpyridine</i>	40
2.2.3	Synthesis Of Bis-terpyridines	43
2.2.3.1	<i>Synthesis of bis[(2,2':6',2''-terpiridin-4'-yl)</i> <i>phenyl]-ethyne</i>	43
2.2.3.2	<i>Synthesis of 1,4-bis(2,2':6',2''-terpiridin-4'-yl)-</i> <i>benzene</i>	44
2.2.3.2	<i>Synthesis of 1,4-di[4'-(4-ethynylphenyl)-</i> <i>2,2':6',2''-terpyridine]-2-(3,7-dimethyloctyl-5-</i> <i>methoxy-benzene</i>	46
2.3	CONCLUSIONS	48
2.4	REFERENCES	49

CHAPTER THREE SYNTHESIS OF MOLECULAR KNOTS

3.1	INTRODUCTION	53
3.2	CHOICE OF MOLECULAR KNOTS	54
3.2.1	Diamantane	54
3.2.2	1,1'-Biadamantane and derivatives	56
3.2.3	Adamantane and adamantane derivatives	58
3.2.4	Silsesquioxane	63
3.2.4.1	<i>Reactions of functionalized aryl-substituted</i> <i>silsesquioxanes</i>	67
3.3	SYNTHESIS OF MOLECULAR KNOTS	69

3.3.1	Synthesis of 1,1'-biadamantane and derivatives as six-functionalized molecular knots	69
3.3.2	Synthesis of adamantane derivatives as four-functionalized molecular knots	72
3.3.2.1	<i>Derivatization reactions of 1,3,5,7-tetrakis(4-iodophenyl)adamantane</i>	76
3.3.2.2	<i>Synthesis of 1,3,5,7-tetrakis(1,3-dibromophenyl)adamantane</i>	84
3.3.3	Synthesis Of Silsesquioxanes	88
3.3.3.1	<i>Synthesis of octaphenylpentacyclo-[9.5.1.1^{3,9}.1^{5,17}.1^{7,13}]-octasiloxane</i>	88
3.3.3.2	<i>Synthesis octa(p-chlorophenyl)pentacyclo-[9.5.1.1^{3,9}.1^{5,15}.1^{7,13}]-octasiloxane</i>	91
3.4	CONCLUSIONS	101
3.5	REFERENCES	102

CHAPTER FOUR COMPLEXATION AND NETWORK FORMATION

4.1	INTRODUCTION	107
4.2	SYNTHESIS OF COMPLEXES	111
4.2.1	Synthesis Of Monocomplexes	111
4.2.1.1	<i>Synthesis of homoleptic complexes</i>	111
4.2.1.2	<i>Synthesis of heteroleptic complexes</i>	116
4.2.2	Synthesis Of Dicomplexes	117
4.2.3	Synthesis Of Tetracomplexes	120
4.3	SYNTHESIS OF NETWORKS	123
4.4	REFERENCES	127

CHAPTER FIVE CONCLUSIONS AND FUTURE PERSPECTIVES

5.1	INTRODUCTION	129
5.2	MOLECULAR RODS	129
	5.2.1 Molecular Rods: Oligophenylenes	129
	5.2.2 Molecular Rods: Terpyridines	131
5.3	MOLECULAR KNOTS	136
	5.3.1 Molecular Knots: Adamantane And Derivatives	136
	5.3.2 Molecular Knots: Silsesquioxanes	137
5.4	GENERAL CONCLUSIONS	139
5.5	REFERENCES	141

CHAPTER SIX EXPERIMENTAL PART

6.1	GENERAL REMARKS AND INSTRUMENTATION	143
6.2	SYNTHESIS OF OLYGOPHENYLENES	144
6.3	SYNTHESIS OF TERPYRIDINES	150
6.4	SYNTHESIS OF ADAMANTANES	154
6.5	SYNTHESIS OF SILSESQUIOXANES	162
6.6	SYNTHESIS OF COMPLEXES	165
6.7	SYNTHESIS OF PRODUCTS CHAPTER FIVE	169

I

CHAPTER ONE: GENERAL INTRODUCTION

1.1 INTRODUCTION

There is a permanent need for the development of new concepts and routes towards new and advanced material systems. Sometimes the macroscopic world can be used to inspire us for such new concepts. Dr. Ing. Roelof Marissen (DSM Research and Delft University of Technology, The Netherlands) suggested in 1998 investigating whether the principles of macroscopic mechanical engineering could be translated to molecular scale, provided that sufficient analogy was present between the type of molecules and the type of macroscopic structure. A very efficient macroscopic structure for mechanical strength and low density is a spaceframe. Spaceframes consist of rods, connected to each other with knots. Our ultimate interest is in the use of these molecular rods and knots as modules in the controlled construction of molecular networks and scaffolds. The construction of such structures, consisting of rigid bars (rods) which are connected via functionalized corners (knots) should result in a stiff and very strong entity as we can see, for example, in the construction of hoisting-cranes.

Translation of this macroscopic principle to the molecular level should result in an isotropic polymeric material, which is very strong and stiff, and which possesses a low density. A possible advantage of this polymeric construction is its self-restoring and potentially self-healing property. Molecules, in contradiction with metal tubes, possess high elasticity, so they can return to their original structure after being twisted or buckled.

The use of molecular rods as construction elements depends critically on the ability to adjust the length of the rod to a desired value, to attach the desired terminal connectors, and to ensure sufficient rigidity. Molecular rods offer the opportunity to position two knots at a known distance apart and connect them by a medium whose properties can be controlled at least to some degree. The degree of interaction between the knots can be studied and provides information about the coupling of the knots to the rod, ultimately contributing to the theory of chemical bonding.

Interest in these rigid rod molecules is a phenomenon of the past decade. If we limit our horizon to well-characterized and pure individual molecular structures, very few rigid rod molecules were known before the Nineties^{1,2}. It has been primarily driven by interest in two areas; firstly in long-distance interaction phenomena such as electron and energy transfer, magnetic coupling of transition metal atoms, etc... and secondly in the use of molecular rods as connectors for the construction of supramolecular assemblies and giant molecules³. Since the intention of this work was to construct a rigid molecular spaceframe, we exemplify their uses and potential uses by considering them as spacers and construction elements in giant molecules and supramolecular assemblies.

To realize the purpose described above, development of some well-defined monodispers rods and knots which possess high rigidity and high stiffness is essential. For this reason molecular rods may not possess flexible bonds along their axis. Flexible chains are only attached as side chains for increasing the solubility of the molecular rods. The molecular rods must also have the ability to attach in high numbers to the multifunctionalized molecular knots. Of all rigid rods known at present, oligo-*p*-phenylenes (Figure 1.1) (A) and bisterpyridines (Figure 1.1) (B) seem to be the most accessible and convenient rigid rods that could be used as rigid linkers between molecular knots.

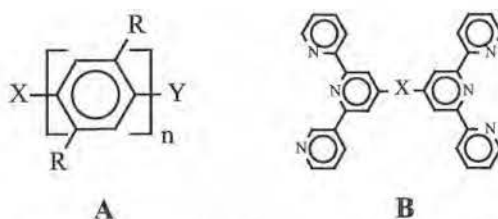


Figure 1.1: Oligo-*p*-phenylenes and bisterpyridines

Both of these will be attached differently to the molecular knots. The oligo-*p*-phenylenes will be attached through a covalent bonding mechanism and the terpyridines via complexation reactions.

For the molecular knot a six-functionality is required as a minimum in order to create strong rigid molecular spaceframes. The reason for this is explained in Chapter 1.2. Silsesquioxane- and adamantane-like structures are proposed as suitable rigid knots because these structures can be provided with a suitable functionality.

Silsesquioxane-like structures are suggested since there is a possibility that they could combine features of organic materials (rods) with those of ceramics (silsesquioxane core). Octafunctional octahedral silsesquioxanes $[\text{RSiO}_{1.5}]_8$ (POSS) or cubic silsesquioxanes (cubes) (Figure 1.2) represent three-dimensional nanobuilding blocks that offer the potential to construct a wide variety of materials, nanometer by nanometer, with precise control/tailoring of nanoarchitecture and properties⁴⁻¹⁴.

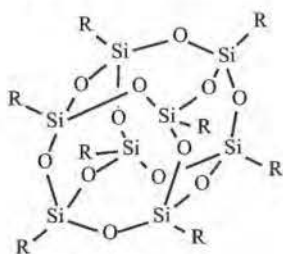


Figure 1.2: Octafunctional octahedral silsesquioxanes $[\text{RSiO}_{1.5}]_8$

POSS thermoplastic nanocomposites have been developed that provide robust materials with a wide range of novel properties including resistance to atomic oxygen⁴⁻⁸.

As rigid molecular knot adamantane-like structures were also proposed, since adamantane (Figure 1.3) has good chemical and thermal stability and possesses an extreme hardness, it can be thought of as the “repeat unit” of diamond.

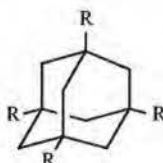


Figure 1.3: Tetra-R-adamantane

In 1933, this substance was isolated from the petroleum of Hodinin in Czechoslovakia by *Landa*¹⁵, and was named adamantane from the Greek for diamond. The unique structure of adamantane is reflected in highly unusual physical and chemical properties¹⁶.

In summary the objective of this project is a molecular translation of a macroscopic architectural principle for the preparation of stable structures. The resulting material would be the first of a new class of materials, which would have improved mechanical properties at lower density than the polymer systems known at present.

1.2 PROPERTIES OF MOLECULAR SPACEFRAME

1.2.1 Computational Details

1.2.1.1 The force field approach

Considering the size of the molecules of interest, they can at present only be modelled by using force field methods.

Force field methods find their origin in classical mechanics and consider a molecule as an ensemble of balls and springs, the balls representing the atoms, the springs representing the bonds between the atoms. The potential energy of the system is then described via a set of parameterized functions having a similar form to classical mechanics. This set of functions and parameters define the forcefield. In the current modelling study two forcefields have been employed namely CVFF (Consistent Valence Force Field) and PCFF. In CVFF the analytical form of the energy expression is

$$E_p = \sum_b D_b [1 - e^{-\alpha(b-b_0)}] + \sum_\theta H_\theta (\theta - \theta_0)^2 + \sum_\phi H_\phi [1 + s \cos(n\phi)] + \sum_x H_x \chi^2$$

(1) (2) (3) (4)

$$+ \sum_i \sum_{j>i} \varepsilon \left[\left(\frac{r_{ij}^*}{r_{ij}} \right)^{12} - 2 \left(\frac{r_{ij}^*}{r_{ij}} \right)^6 \right] + \sum_i \sum_{j>i} \frac{q_i q_j}{\varepsilon r_{ij}}$$

(5) (6)

Equation 1.1: Energy expression

Terms (1)-(4) represents the energy of deformation of bond length (1), bond angle (2), torsion angles (3) and out-of-plane interactions (4). Terms (5) and (6) describe the non-bond interactions. The van der Waals interactions are represented by the Lennard-Jones potential (5) and the electrostatic interactions by the Coulombic term (6). ε is the dielectric constant. The forcefield contains the parameters D_b , α , b_0 , H_θ , θ_0 , etc. CVFF also offers a set of parameters to describe the bond deformation by a harmonic function instead of the Morse potential (1). These harmonic functions are computationally much less expensive. A much more complicated expression containing even more parameters is used by PCFF.

1.2.1.2 Molecular mechanics and dynamics calculations

In a molecular mechanics calculation, the potential energy function (Equation 1.1) is minimised with respect to the atomic or alternatively the

internal co-ordinates. A molecular dynamics run solves the classical equations of motion for a system of atoms interacting according to the potential energy function (Equation 1.1) i.e.

$$\underline{F}_i(t) = m_i \underline{a}_i$$

With $\underline{F}_i(t)$ is the force, m_i the mass and \underline{a}_i the acceleration of atom i . $\underline{F}_i(t)$ is directly computed from the derivative of the potential energy function with respect to the co-ordinates \underline{r}_i :

$$\underline{F}_i(t) = -\frac{\partial E_p}{\partial \underline{r}_i}$$

The initial co-ordinates are usually obtained via energy minimisation and the initial velocities are generated by a random number generator and a random seed from the Gaussian distribution of their x, y and z components at a given temperature.

All minimisation runs in the current modelling study were carried out until the maximum energy derivative was less than 0.1 kcal/molÅ. Molecular dynamics runs have been carried out at different temperatures using a time step of one femtosecond. Direct velocity scaling controlled the temperature and the equations of motion were integrated using the default Verlet velocity integrator. In both the minimisation and dynamics runs the summation method for evaluating the non-bonded interactions was set to no cut-off and the dielectric constant to 1.0.

Starting structures for the simulations were generated by means of the building facilities of the InsightII package from Molecular Simulations; actual simulations were carried out by the MSI Discover program version 97.0.

1.2.2 Isostatic And Hyperstatic Spaceframe

In order to be mechanically effective, macroscopic spaceframes have to fulfil the following requirement:

$$3k \leq r + 6 \quad (k \text{ is the number of knots and } r \text{ is the number of rods})$$

The spaceframe is called isostatic for $3k = r+6$ and hyperstatic for $3k < r+6$. In isostatic and hyperstatic spaceframes, the rods are no longer loaded in bending, but are only loaded by normal tension and compression forces, which can be carried much more than bending loads. The structure should additionally be irregular, in that different rods should not provide the same mechanical function, because in that case several rods would act as one single rod. A simple example is two parallel rods between the same knots. These two rods can act as one. As a material can be considered as a structure containing an extremely large number of molecular structural elements and the presently considered materials contain an almost infinite number of molecular rods and knots, this material can be considered to be a molecular space frame. For an infinite number of rods, the constant 6 may be neglected and the above equation reduces to:

$$3k \leq r$$

So the number of rods should be three times (or larger) the number of knots. Because every rod is connected to two knots (at its ends), the average functionality in a molecular spaceframe should be 6.

The considerations above indicate that a molecular spaceframe consisting of rigid rods and highly functional (>6) molecular knots, should result in a material with an extremely low density, and still high mechanical properties, because the molecular rods would be loaded in the most efficient way, namely in almost pure tension and compression. Moreover (and unlike conventional polymers), those loads would be carried by covalent bonds. Unlike fibres like Dyneema, the material is expected to be isotropic; i.e. whereas Dyneema (and other similar fibres) can only carry loads in one direction (fibre direction, c.q. stretch direction), the molecular spaceframe should have the ability to carry loads in all directions. In addition, good compression strength might be possible.

During the course of 1999 it became clear that knots made of an eight-functional cubic oligosilsesquioxane, and rods made of oligo-*p*-phenylene could be made with a reasonable chance of success. Consequently, sufficient detailed knowledge of the chemistry of the anticipated material was available to be able to make a molecular theoretical model.

Molecular modelling allows a check of the validity of the hypothesis regarding the translation of macroscopic insights to molecular structures as it allows the properties of the molecular structure to be estimated. A molecular modelling study of the expected molecular spaceframe material was therefore undertaken. The molecular modelling was done by Betty Coussens at DSM Research (The Netherlands)

1.2.3 Structure

One of the first important questions regarding the molecular spaceframe is whether the structure will implode due to attractive atomic interactions or not. Usually polymers with such a low density definitely would. On the other hand, the spaceframe with high knot functionality may be expected to remain stable. In order to answer this question with molecular modelling, it should be realised that two types of molecular spaceframe can be distinguished (Figure 1.4 and 1.5). Structure 1.4 is a very regular periodic structure whereas structure 1.5 is a random one. Due to its specific periodicity it can be expected that structure 1.4 will easily collapse in one direction whereas structure 1.5 will not.

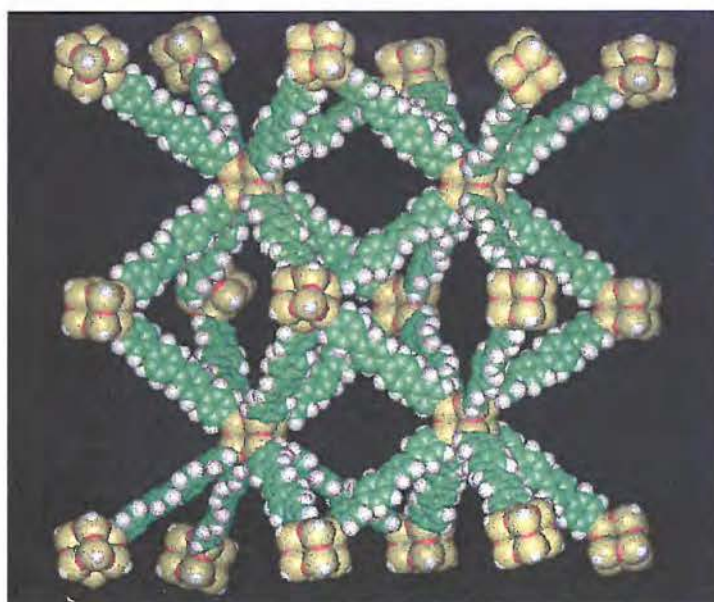


Figure 1.4: Periodic structure

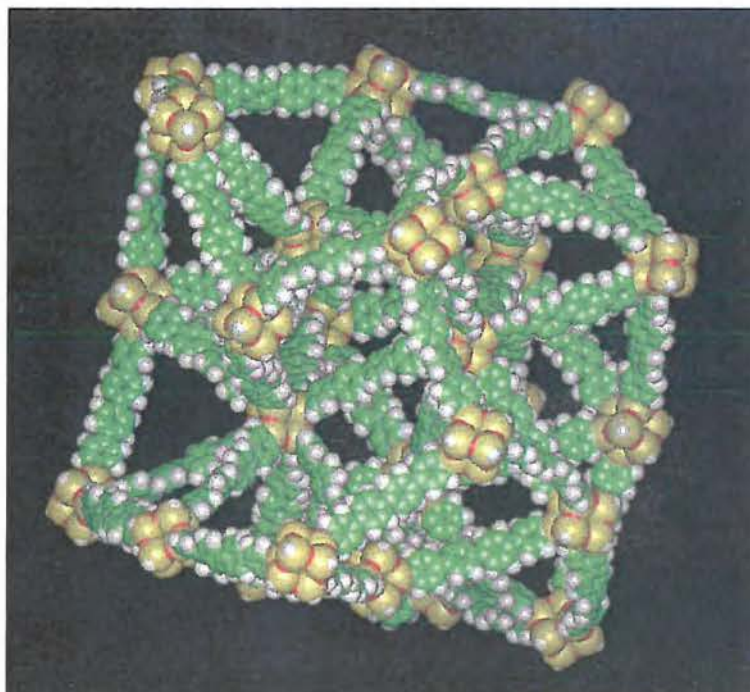


Figure 1.5: Random structure

The yellow coloured spheres represent the silicon atoms of the cubic silsesquioxane cage, the green sticks the phenylene rods which link these cages to one another and the white spheres represent the hydrogen atoms.

In order to verify the importance of random character for having a molecular spaceframe that will not easily implode, both models were first subjected to a molecular dynamics run at 350 K using the CVFF forcefield with the harmonic potentials for describing bond deformation. The equilibration time was 5 ps and after equilibration every 1000th configuration was stored until a total of 500 configurations was generated. Configuration averages of both structures are shown in Figure 1.6 and 1.7. As can be seen, neither the periodic nor the random structure collapsed during the simulation.

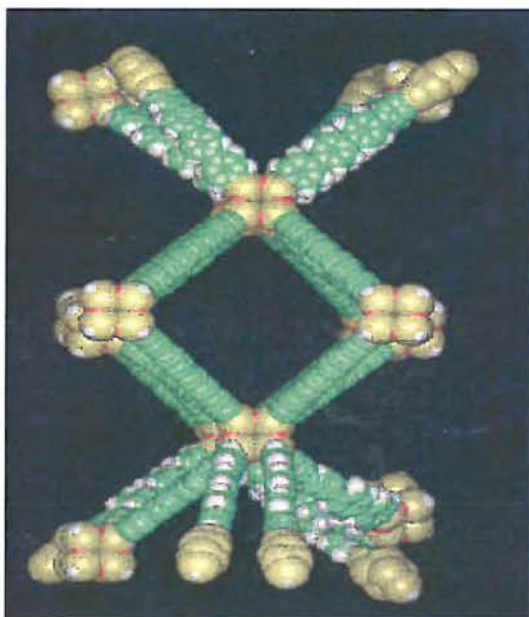


Figure 1.6: Configuration average of periodic structure as obtained from a molecular dynamics run at 350 K

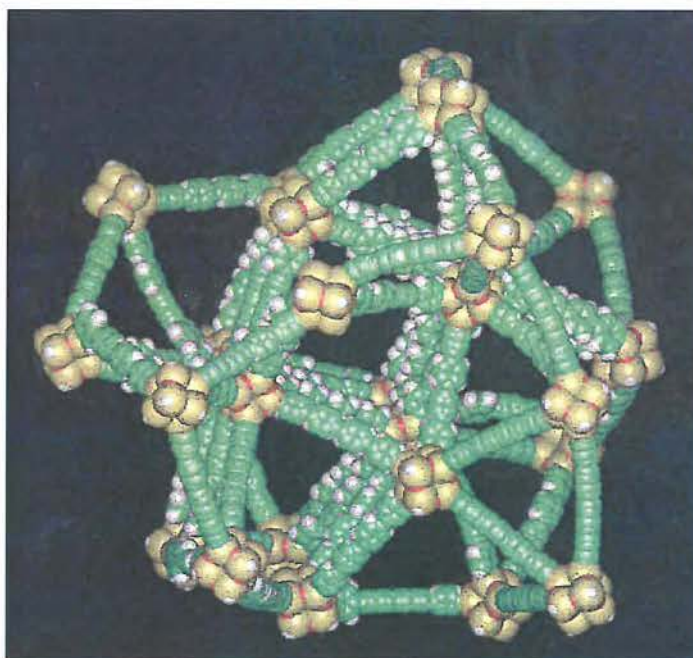


Figure 1.7: Configuration average of random structure as obtained from a molecular dynamics run at 350 K

Apparently, at 350 K, even in the periodic structure the attractive interactions between the atoms do not overcome the geometrical constraints due to the specific atomic hybridisation states. In a second set of simulations, the two molecular spaceframe models were subjected to a simulated annealing run. Again the CVFF forcefield with harmonic potentials was employed. The starting temperature was chosen to be 1500 K, the final temperature 300 K and the temperature step was 240 K. At each temperature, the simulation time was 5 ps. The structures obtained at 300 K were consequently subjected to new simulations in order to generate 500 configurations of them at room temperature. Average configurations obtained from these simulations are represented in Figures 1.8 and 1.9. It is clear that at higher temperatures the periodic structure does collapse and remains collapsed at 300 K, whereas the random one still remains intact.



Figure 1.8: Configuration average at 300K of periodic structure as obtained after a simulation annealing run with $T_{\text{start}} = 1500$ and $T_{\text{end}} = 300$ K



Figure 1.9: Configuration average at 300K of random structure as obtained after a simulation annealing run with $T_{\text{start}} = 1500$ and $T_{\text{end}} = 300$ K

It can thus be concluded that random character is indeed an important feature for obtaining a molecular spaceframe to avoid easy implosion.

1.2.4 Density

As already mentioned, another important feature of the molecular spaceframe is the fact that it is expected to have a very low density. To get a rough idea about the density of the spaceframe via molecular modelling, its molecular volume must be estimated. Considering the type of structure we have to deal with, this is not an easy task. The procedure we employed was to calculate the solvent accessible surface of the structure using a very large probe. We then calculated the volume inside this surface. The solvent accessible surface is defined as shown in Figure 1.10.

A sphere with a specific radius represents the solvent molecule and the surface is then obtained by rolling this sphere over the VDW surface. Solvent accessible surfaces are usually calculated using a sphere with a radius of 1.4 Å representing a molecule like water. However, in the case of random structure (Figure 1.10) having very big holes such a small radius would obviously not be appropriate as the calculated surface would then include the surface area inside these holes.

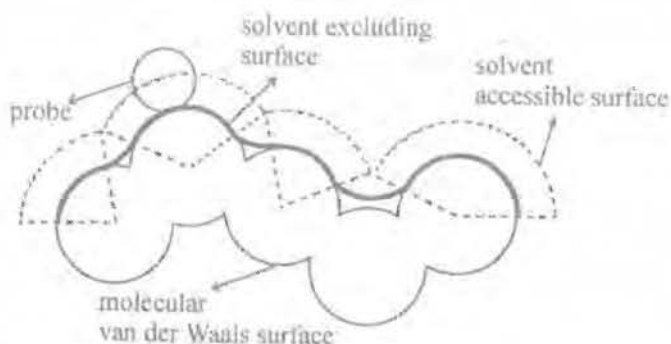


Figure 1.10: Definition of a solvent accessible surface

Therefore a much larger sphere of 10 Å was employed. Only one configuration of the spaceframe was investigated, as the solvent accessible surface is a property, which is hardly conformation dependent. The volume inside was calculated to be 98940 Å³. The mass of the random structure is 30820 g/mol and so its density is estimated to be ca. 0.5 g/cm³. This is of the same order of magnitude as a very microporous zeolite. The density is about a factor of two lower than the density of conventional polymers.

1.2.5 Bulk Modulus

For estimating the bulk modulus Coussens adapted the following procedure. Every 50th configuration out of 500 configurations generated via the molecular dynamics run at 350 K, was minimised using the CVFF forcefield. Obviously, the modulus depends on the curvature of the potential energy curve around the minimum and therefore Morse potentials for bond deformation instead of the harmonic functions were now employed.

For each configuration uniform scaling of all atomic co-ordinates then generated a compressed and expanded structure. A small scaling factor of 0.005 was used, i.e. the co-ordinates of the compressed and expanded structures were generated as:

$$p_{\text{compressed}} = p_{\text{min}} - p_{\text{min}}0.005$$
$$p_{\text{expanded}} = p_{\text{min}} + p_{\text{min}}0.005$$

With $p = x, y, z$ and p_{min} denoting the co-ordinates of the minimum energy structure. Scaling was performed by means of a simple FORTRAN program developed at DSM. Next, the compressed and expanded structures were minimised keeping all outer Si atoms of the structure fixed. (It turned out that during the minimization runs with the Si atoms fixed, the non-bonded interactions with these fixed atoms were not taken in account. This bug was reported to MSI. In order to obtain the correct potential energies of the distorted structures single point calculations on the minimized structures had to be performed with all input lines specifying the fixed Si atoms removed). The bulk modulus, K , for compression and expansion of each configuration was subsequently obtained as:

$$K = \frac{p}{dV/V_0} \quad \text{with} \quad p = \frac{dE_p}{dV}$$

In the above equations p is the hydrostatic pressure, dV is the change in volume as a consequence of compression or expansion, V_0 is the volume of the minimum energy configuration (i.e. 98940 \AA^3 , see Chapter 1.2.4) and dE_p is the change in potential energy as a result of the deformation. The obtained bulk moduli are tabulated as obtained via compression and expansion of ten configurations of structure 1.5 (Figure 1.5)

Configuration	Compressed	Expanded
1	5.5	5.9
2	5.6	5.8
3	5.5	5.8
4	5.4	5.6
5	5.3	5.7
6	5.4	5.7
7	5.6	5.9
8	5.6	5.8
9	5.7	5.9
10	5.6	5.9
Average	5.5	5.8

Table 1.1: Bulk moduli (GPa)

The bulk moduli of all configurations are roughly identical and the average values are calculated to be 5.5 GPa for compression and 5.8 GPa for expansion. The bulk modulus is thus estimated to be a factor of two higher than for common polymers, the latter being in the order of only 3 GPa. In contrast to conventional materials showing a slightly higher stiffness in compression the molecular spaceframe appears to have the highest bulk modulus for expansion. However, this result can easily be understood. The spaceframe material has a slight “heritage of implosion tendency” which supports compressive deformation and reduces compression stiffness. Obviously this trend is small, considering the small difference between expansion and compression modulus.

It must be realized that the above procedure for estimation of the bulk modulus is very crude, the simulation error probably being in the order of 1.5-2 GPa. In order to understand whether the procedure would indeed yield an acceptable accuracy, it was tested on polyethylene. The results of this testing showed an acceptable agreement between theory and experiment.

1.2.6 Thermal Expansion Coefficient

In order to estimate the thermal expansion coefficient, molecular dynamics simulations were performed at 50, 200 and 350 K. Equilibration times at each temperature were 5 ps after which every 1000th configuration was stored until a total of 500 configurations were generated. In these simulations bond deformation was described by a Morse potential. At each temperature, the set of 500 configurations was then used to calculate the average radius of gyration of the molecular spaceframe. This radius is defined by:

$$R_g^2 = \frac{\sum_i m_i (r_i - r_{cm})^2}{\sum_i m_i}$$

The above summations run over the total number of atoms, m_i is the mass of atom i , r_i the position vector of atom i and r_{cm} the position vector of the center of the mass. The calculated radii are given in Table 1.2

T (K)	R_g (Å)	R_η (Å)	V_η (Å ³)
50	28.19	36.39	201853
200	28.13	36.32	200690
350	27.73	35.80	192193

Table 1.2: Average radii of gyration, hydrodynamic radii and hydrodynamic volumes as obtained from molecular dynamics simulations

From these radii a so-called hydrodynamic radius R_η can be obtained from the relation:

$$R_\eta = \sqrt{5/3} R_g$$

This hydrodynamic radius R_η can then be used to calculate the hydrodynamic volume V_η of the spaceframe at three different temperatures, i.e.

$$V_\eta = \frac{4}{3} \pi R_\eta^3$$

These volumes are also included in Table 1.2. The expansion coefficient can then be derived as:

$$\alpha = \frac{1}{V} \left(\frac{dV}{dT} \right)$$

From the volume change obtained due to the temperature increase from 50 to 200 K the expansion coefficient is found to be $-3.8 \cdot 10^{-5} \text{ } ^\circ\text{C}^{-1}$; the volume change due to the temperature increase from 200 to 350 results in $-2.8 \cdot 10^{-4} \text{ } ^\circ\text{C}^{-1}$. A small shrinkage is thus observed. Again this trend is opposite to that of conventional materials for which negative coefficients of expansion are rare. The calculations show that the trend to collapse increases at high temperatures. The small negative thermal expansion coefficient is again a slight “heritage of implosion tendency”.

1.3 APPLICATIONS

In material development there always has been, and always will be, a drive towards lighter and stronger materials. Thermally stable polymers have received extensive interest over the past decade due to increasing demands for high-temperature polymers as replacements for metals or ceramics in automotive, aerospace, and microelectronic industries. These high-performance polymers are used in applications demanding structural integrity and an excellent combination of chemical, physical, and mechanical properties at elevated temperatures.

The technology, which combines features of organic polymers with those of ceramics, could prove revolutionary. It could lead to e.g. significantly less expensive rocket and aircraft hot parts, find uses in all sorts of consumer products, and usher in the first new wave of high-performance polymer applications since the 1950s. Because the organic molecules are bound to more heat-resistant inorganic molecules, they remain in place even at temperatures that would unravel conventional polymers. In many cases, POSS polymer nanocomposites retain their properties even past their decomposition point.

While high temperatures oxidize organic molecules on the surfaces, the oxidatively stable POSS remain in place. They anchor the resulting organic char, which forms a flammability barrier, and also provide structural support as temperature continues to rise. POSS does more than extend resin temperature ranges. It makes them stronger, lighter, and more durable.

1.4 REFERENCES

1. Kaszynski P.; Michl J.; *J. Am. Chem. Soc.*, **1988**, 110, 5225.
2. Zimmerman H. E.; Goldman T. D.; Hirzel T. K.; Schmidt S. P.; *J. Org. Chem.*, **1980**, 45, 3933.
3. Stang P. J.; Otenyuk B.; *Acc. Chem. Rev.*, **1997**, 30, 502.
4. Lichtenhan J. D.; Otonari Y. A.; Carr M. J. *Macromolecules*, **1995**, 28, 8435.
5. Feher F. J.; Budzichowski T. A.; *J. Organometal. Chem.*, **1989**, 379, 33.
6. Feher F. J.; Soulivong D.; Eklud A. G.; Wyngham K. D.; *Chem. Commun.*, **1997**, 1185
7. Jeon H. G.; Mather P. T.; Haddad T. S.; *Polym. Int.*, **2000**, 49, 453.
8. Gilman J. W.; Schlitzere D. S.; Lichtenhan J. D.; *J. Appl. Polym. Sci.*, **1996**, 60, 591.
9. Sellinger A.; Laine R. M.; *Macromolecules*, **1996**, 29, 2327.
10. Sellinger A.; Laine R. M.; *Chem. Mater.*, **1996**, 8, 1592.
11. Sellinger A.; Laine R. M.; Chu V.; Viney C.; *J. Polym. Sci. Part A: Polym Chem.*, **1994**, 32, 3069.
12. Zhang C.; Babonneau F.; Bonhomme C.; Laine R. M.; Soles C. L.; Hristov H. A.; Yee A. F.; *J Am. Chem. Soc.*, **1998**, 120 (33), 8380.
13. Laine R. M.; Choi J.; Lee I.; *Adv. Mater.*, **2001**, 13, 800.
14. Zhang C.; Laine R. M.; *J Am. Chem. Soc.*, **2000**, 122 (29), 6979.
15. Landa S.; Machacek V.; *Collection Czech. Chem. Commun.*, **1963**, 5, 1.
16. Raymond C. Fort; Jr, Paul Von R. Schleyer, *Chem. Rev.*, **1964**, 64, 277-300.

II

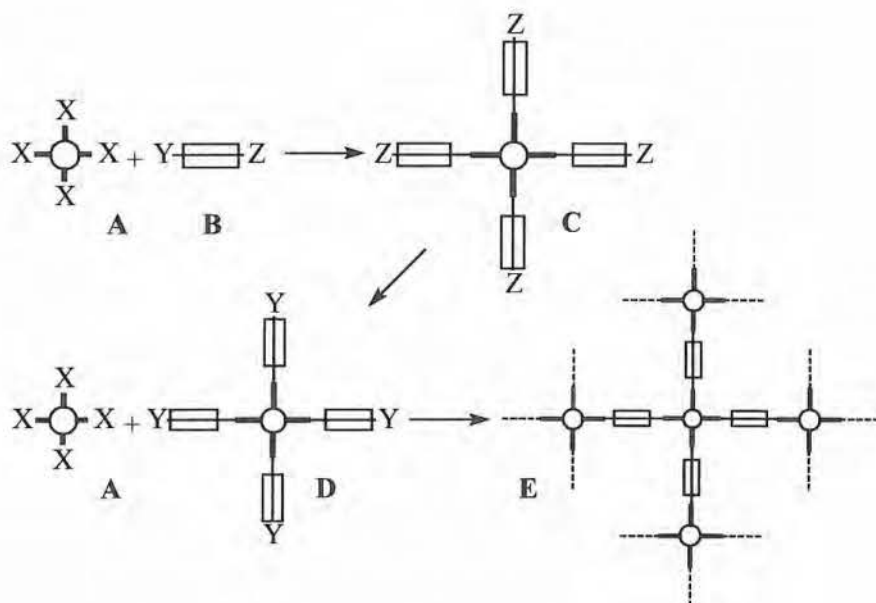
CHAPTER TWO: SYNTHESIS OF MOLECULAR RODS

2.1 CHOICE OF MOLECULAR RODS

2.1.1 Introduction

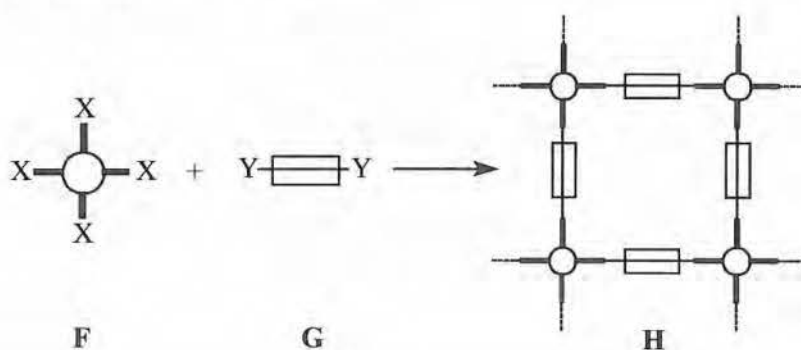
Of all rigid rods known at present (cubanes¹⁻⁴, staffanes⁵⁻⁸, oligoynes⁹⁻¹⁹, cumulenes²⁰⁻²², ...), oligophenylenes and terpyridines (Chapter 2.1.3) seem to be the most accessible and convenient rigid rods that could be used as rigid linkers between molecular knots.

If we represent the molecular knots as **A**, with suitable groups X (e.g. acetylene) present for coupling with molecular rods, two different ways to build up a molecular network are investigated. The first approach (Scheme 2.1) is the use of oligophenylene telechelics **B** where Y is a group that can couple (e.g. bromine) with the X group present on the molecular knot to give **C** and Z is a protection group (e.g. trimethylsilyl) to prevent coupling of two oligophenylene units to one another. After coupling, the protection group must be possible to remove easily or to be exchanged, both in high yields, to provide another potential group for coupling (e.g. iodine). This extended molecular knot **D** can couple again with **A** to give a molecular network **E**.



Scheme 2.1: Network formation via coupling reactions

In the second approach (Scheme 2.2) we wanted to use complexation as a coupling method for the synthesis of highly rigid networks. The use of terpyridine derivatives offers here the possibility to use complexation reactions for coupling terpyridines to one another.



Scheme 2.2: Network formation via complexation

F represents a multifunctionalized molecular knot which can couple with the molecular rod **G**. **G** represents a bisterpyridine of which **Y** is a terpyridine metal complex which was in essential ruthenium. Both of them, **F** and **G**, can couple to one another to give molecular networks **H**. This will be explained in chapter four.

2.1.2 Oligophenylenes

Along with ethyne, *p*-phenylene represents the oldest and cheapest monomer for the construction of rigid rods. Oligo-*p*-phenylenes are among the most thermally stable rods in the molecular construction kit, and the high molecular weight polymers were reported to be stable up to 800 or 900 °C²³. Functionalized oligo-*p*-phenylenes have gained some importance as main-chain-stiffening building blocks in semiflexible polymers like aromatic polyesters²⁴⁻²⁶ and polyimides^{27,28}.

Oligo-*p*-phenylenes have existed for a long time, but only a few molecules are available with axial functionalization at the termini, required for use in a molecular construction kit. The synthesis of 2''-5''-dihexyl-4-bromo-*p*-pentaphenyl (Figure 2.1) for example is described in literature by *Galda and Rehahn*²⁹ who prepared a series of oligomers up to fifteen phenyl units.

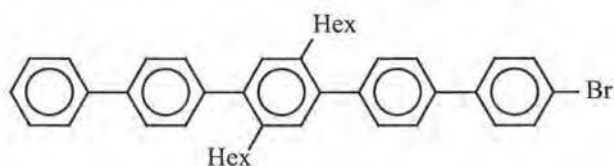


Figure 2.1: 2''-5''-Di-*n*-hexyl-4-bromo-*p*-pentaphenyl

The disadvantage of this *p*-pentaphenyl for use in a molecular construction kit is the mono-functionalized termini. Predicted synthesis problems for the functionalization of the other termini (exclusive in para-position) forced us to search for another way to synthesize unsymmetrical oligophenylenes. Extensive literature search showed that the best access, towards these unsymmetrical oligophenylenes, is described by the group of *Schlüter et al*^{30,31}.

Schlüters group has described the synthesis of individual oligomers having up to 16 repeating units with excellent yields. These rods are monodisperse and have different functionalized termini (oligophenylene telechelics). Therefore 4-bromo-2,5,2'',5''-tetra-*n*-hexyl-4'''-trimethylsilyl-tetraphenyl which is suitable as rigid soluble axial terminated rod (Figure 2.2), is prepared according to a procedure in the literature^{30,31}.

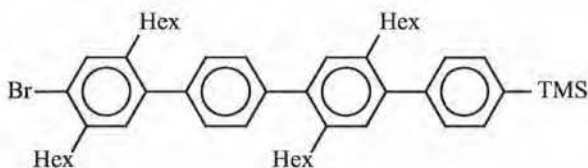
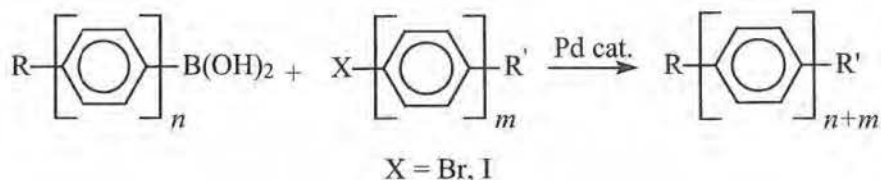


Figure 2.2: 4-Bromo-2,5,2'',5''-tetra-*n*-hexyl-4'''-trimethylsilyltetraphenyl

In order to keep this rigid oligo-*p*-phenylene soluble, this building block was provided with flexible hexyl side chains. Indeed, oligo-*p*-phenylenes have a serious drawback; their solubility decreases dramatically with the number of benzene rings. For example, although *p*-terphenyl dissolves in toluene up to 8.5g L⁻¹, *p*-sexiphenyl has a solubility³² less than 10 mg L⁻¹. The attachment of lateral alkyl groups to the oligo-*p*-phenylenes increases their solubility. The solubilizing effect of the alkyl groups depends on their length: the longer the alkyl chains the higher the solubility of the *n*-alkyl-oligo-*p*-phenylenes. Except solubility, two other primary difficulties are encountered in the synthesis of molecular rods, namely the difficult separations and purifications, and demanding characterisation. Of the three primary obstacles, low solubility is probably the most significant. If a mixture of high molecular weight molecules cannot be dissolved there is very little hope of separating and purifying the components and a full characterisation of the mixture will be very difficult. The chief tool that has been used over the years to increase solubility of molecular rods is the attachment of a sufficient number of flexible side chains.

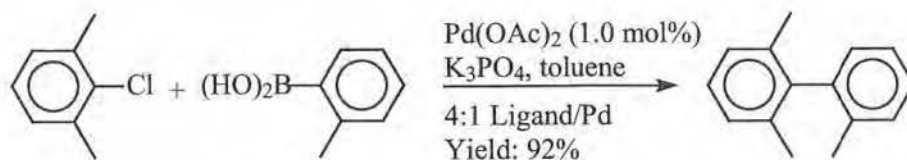
2.1.2.1 Synthetic method towards oligo-*p*-phenylenes

Presently, the most versatile step-by-step approach to oligo-*p*-phenylenes includes a palladium-catalyzed unsymmetrical coupling of arylboronic acids with aryl bromides or aryl iodides called Suzuki cross-coupling reaction^{29,31,33-35} (Scheme 2.3).



Scheme 2.3: Suzuki cross-coupling reaction

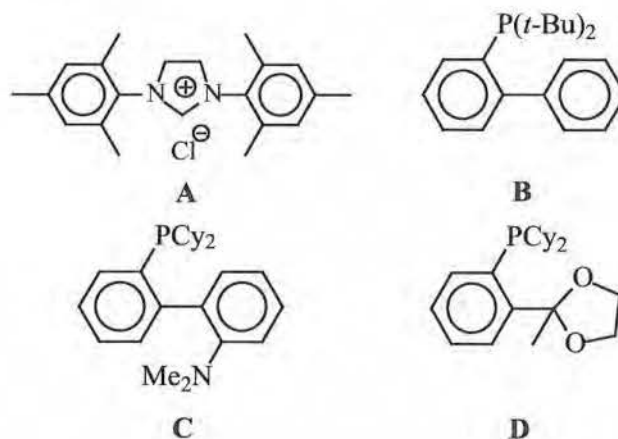
The Suzuki cross-coupling reaction – the palladium catalyzed coupling reaction of an organoboron reagent with aryl- or alkenylhalide – is among the most powerful and versatile methods for carbon-carbon bond formation³⁶. The scope of the reaction is broad, and its exceptional tolerance of functional groups (e.g. esters, ethers, NH₂, NO₂, CF₃, CN, CHO, ketones,...) and the ability to couple sterically demanding substrates (Scheme 2.4) with yields of more than 90% makes the reaction useful in diverse areas of chemistry.



Scheme 2.4: Suzuki reaction with sterical hindered substrates

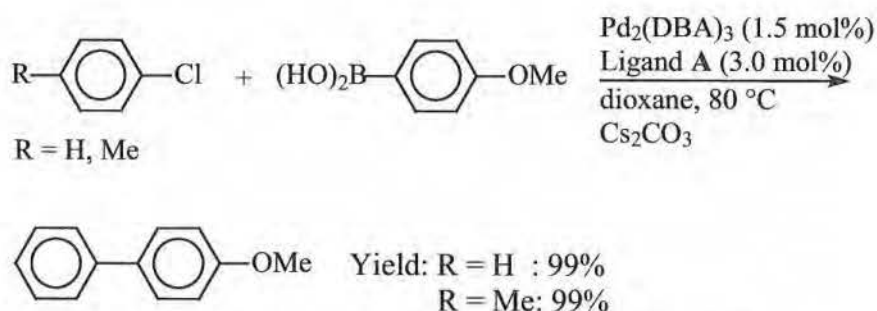
While aryl and alkenyl bromides, iodides and triflates are commonly used in Suzuki reactions, until recently, aryl and alkenyl chlorides (Scheme 2.4), which are often the least expensive and most accessible coupling partners, have rarely been used. The decreased reactivity of aryl chlorides in Pd-catalyzed reactions is usually attributed to their reluctance towards oxidative addition to Pd (0)³⁷. Progress in the development of catalysts that

transform aryl chlorides in Suzuki reactions has been rapid. While the catalytic systems, that were developed initially, were effective only for aryl chlorides activated by an electron withdrawing functional group, more recent catalysts (Scheme 2.5) allow even electron-rich aryl chlorides to react efficiently under conditions that are mild and with yields that rival those of aryl bromides, iodides and triflates.



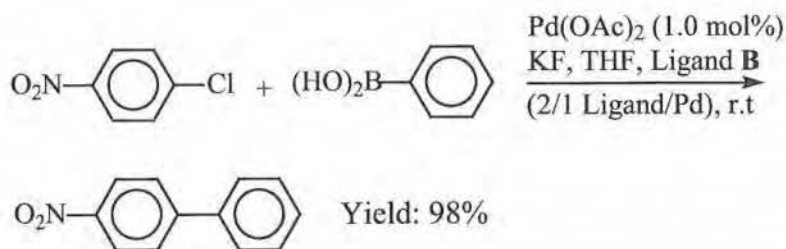
Scheme 2.5: High effective Pd-catalysts

*Trudell, Nolan and coworkers*³⁸ have found that Suzuki reactions of aryl boronic acids and non-activated aryl chlorides occur at 80 °C and with high yields if catalytic amounts of Pd₂(DBA)₃ and the sterically encumbered imidazolium salt **A** are combined with Cs₂CO₃ in dioxane (Scheme 2.6).



Scheme 2.6: Suzuki reaction with Pd-catalyst based on *N*-heterocyclic carbene ligands

More recent work of *Stephen L. Buchwald and coworkers*^{39,40} has shown that the combination of Pd(OAc)₂ and biphenyl-based ligand **B** gives an exceptional catalyst for the Suzuki reactions of both aryl bromides and chlorides (Scheme 2.7). With a relatively low catalyst loading (0.5-1.5 mol% Pd), it is possible to couple a large variety of aryl chlorides with phenylboronic acid derivatives at room temperature.



Scheme 2.7: Suzuki reaction with Pd-catalyst based on biphenyl phosphine ligands

They also reported that the combination of Pd(OAc)₂ and 2-dimethylamino-2'-dicyclohexylbiphenyl **C** is highly effective for the Suzuki reactions of aryl chlorides⁴¹. For the first time, it was found that Suzuki reactions of phenylboronic acid derivatives with aryl chlorides, including those substituted by electron donating and *ortho*-methyl substituents, could be carried out at room temperature. The utility of ligand **C** is further increased by its stability in air. The material is a white, crystalline solid that is easily handled and stored in air.

Bei, Guram and co-workers^{42,43} showed that the combination of phenyl backbone derived P-O ligand **D** with Pd₂(DBA)₃ gives an efficient catalyst for Suzuki reactions of a variety of arylboronic acids and aryl chlorides, if CsF was used in dioxane and reactions were carried out between 100-110 °C. The catalytic system is sufficiently active to permit *ortho*-substitution on both of the coupling partners. Both electron donating and withdrawing functional groups were tolerated.

Thus in principle aryl chlorides can be coupled with arylboronic acids efficiently. This will be considered in the course of this work.

2.1.2.2 Targeted and random synthesis

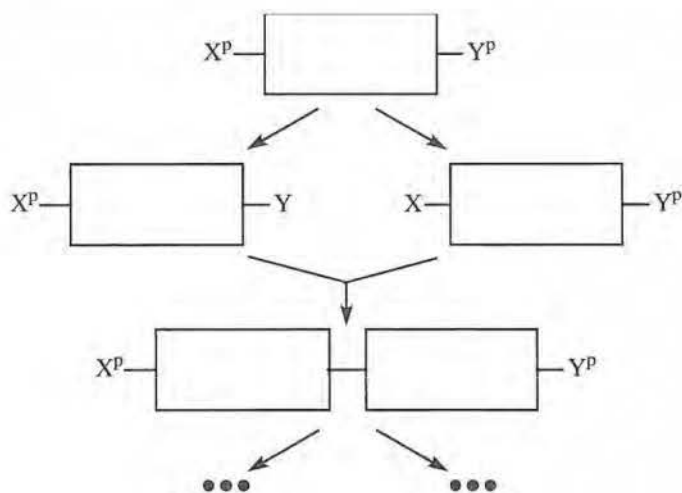
For the synthesis of rods with a predetermined length, in principle, two different approaches exist: targeted and random synthesis.

Targeted synthesis usually involves a long series of controlled steps in which modules are transformed or combined such that only one oligomer is involved in each reaction and the target product, a rod of particular length, is the only product. The advantage of the targeted method is the relatively simple purification of the resulting oligomers. There are three different approaches for the preparation of these rods with predetermined length. In the divergent approach, one module is added at a time, and in the convergent approach, large species of the rod are coupled. A combination of the divergent and convergent approaches leads to “iterative” synthesis⁴⁴⁻⁴⁷, which permits exponential growth of the oligomeric chain with high overall yields of individual oligomers.

Random synthesis converts a module or a shorter rod into a mixture of oligomers whose length distribution can be controlled to some extent by the choice of the mechanism of oligomerization and the reaction conditions. The advantage of the random method is the minimal number of synthetic steps needed, most of the time only one. The disadvantages are often the difficult separation and low yields of the individual oligomers.

Methods for the preparation of the axial rods are dominated by metal catalyzed coupling reactions⁴⁸. Because there are an immense number of available metal-containing catalysts, the coupling reactions can usually be tuned to give good yield and selectivity. Recently the metal-catalyzed coupling reactions are well worked out for the coupling of aryl, vinyl, ethynyl, and carboranyl groups to each other and less so to other cage modules.

The approach we will focus on is the versatile and easy method of soluble *n*-alkyl substituted oligo-*p*-phenylenes, the so-called “repetitive synthesis growth” strategy (Scheme 2.8).



Scheme 2.8: Repetitive synthesis growth strategy

This strategy has the advantage that exponential growth patterns can be executed. X and Y represent functional groups that can be used to connect two molecules. The P represents an orthogonal protecting group, which was in our case trimethylsilyl (TMS), or bromo. TMS can be easily converted into, for example, iodo or bromo functions. These TMS functions act as placeholders ensuring completely ipso substitution. The bromo protective group can be converted into boronic acid or TMS. With the Suzuki cross-coupling reaction of boronic acids and aromatic halides the two building blocks can be attached to each other. This proceeds regioselectively and with high yields. The coupling reactions are highly sensitive to the nature of the halogen involved. Iodo aromatics couple significantly faster than bromo aromatics. Thus molecules containing both bromo and iodo functions undergo coupling on the iodo site first. To prove a successful strategy, high yields of all reactions and substitutions were necessary.

2.1.3 Terpyridines

2.1.3.1 History and properties of 2,2':6',2''-terpyridine

The synthesis of terpyridine and bisterpyridine derivatives was the second route considered for producing rigid axial terminated rods. The terdentate ligand 2,2':6',2''-terpyridine (Figure 2.3) was first isolated in the thirties by *Morgan and Burstall*⁴⁹ as one of the many products from the reaction of pyridine with iron(III) chloride⁵⁰⁻⁵³.

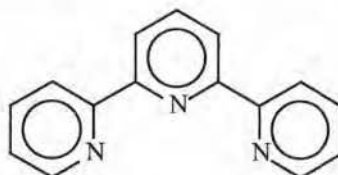


Figure 2.3: 2,2':6',2''-Terpyridine

Since then, there have been many investigations of this metal-complexing ligand, and its complexes. These studies include complex formation, photochemical properties and most recently their use as building blocks for novel supramolecular structures such as dendrimers⁵⁴, double helicates⁵⁵ and ordered architectures on surfaces⁵⁶.

2,2':6',2''-Terpyridine commonly behaves as a chelating terdentate ligand within the majority of complexes exhibiting 1:1 or 1:2 metal:ligand ratios. The 1:2 complexes are invariably based upon an octahedral geometry. These geometrical properties have been utilized in the synthesis of macrocyclic derivatives⁵⁷, and for the preparation of highly structured polymers based upon such building blocks⁵⁸. The majority of transition metal complexes incorporate metal ions in the +2 or +3 oxidation state, in basically octahedral, tetrahedral, or squareplanar geometries. Low oxidation states are characterized by an excess of electron density at the metal atom. Stabilization may be achieved using ligands capable of reducing that electron density. One of the simplest ways to reduce the electron density is to design ligands with low-lying vacant orbitals of suitable symmetry for overlap with filled metal orbitals. This results in the transfer of electron density from the metal to the ligand (back-donation).

In general, ligand non-bonding or π anti-bonding orbitals have the correct symmetry for such overlap. Similarly, metal ions in high oxidation states may be stabilized by powerful σ - or π -donor ligands. The oligopyridines are ideally suited to such roles; they possess a filled highest occupied molecular orbital (HOMO) and a vacant lowest unoccupied molecular orbital (LUMO) of suitable energies for interaction with metal d orbitals⁵⁹. They are thus capable of stabilizing both high and low oxidation states of metal ions.

The use of 4'-substituted terpyridines allows the development of oligomers and three dimensional arrays in which a linear arrangement of substituents about the metal centre is achieved, with a 90° angle between the planes of the two 2,2':6',2''-terpyridine ligands at each metal centre (Figure 2.4)

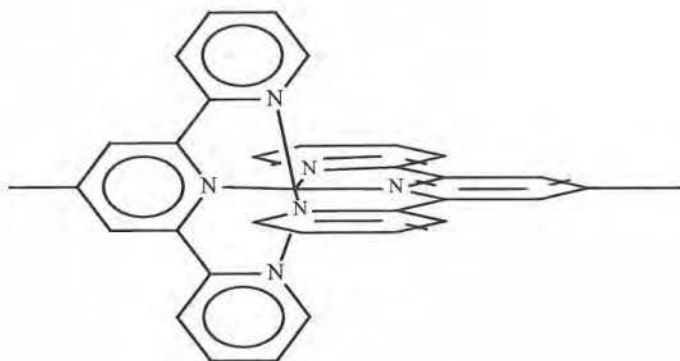


Figure 2.4: Co-ordination of terpyridine ligands around a metal

The geometries of complexes incorporating relatively inflexible polydentate ligands are predominantly determined by the configuration of the ligand e.g. a planar pentadentate ligand cannot form octahedral complexes. This apparently obvious observation has a number of far-reaching consequences. A compromise between the optimum geometry for the metal ion and for the ligand must be reached. This may be expressed as a distorted geometry about the metal or as a distortion of the ligand. Upon co-ordination to a metal center, the terpyridine ligand undergoes a number of significant changes. The most obvious results from the adoption of the *cis,cis*-configuration, in contrast to the *trans,trans*-equilibrium solution structure. It is also apparent that for terpyridine to act as an efficient terdentate, it is necessary

to distort (Figure 2.5) the ligand and reduce the interannular angle between the central and terminal pyridine rings.

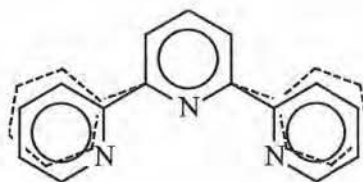


Figure 2.5: The distortion of 2,2':6',2''-terpyridine ligand upon coordination to a metal ion in a planar terdentate mode

The dihedral angle between the terminal and central rings increases from 5.7° to 7.1° in the complex, while the C-C-N angles reduce from 116° in the free ligand to 114° in the complex⁶⁰.

2.1.3.2 Choice of terpyridines

In order to synthesize terpyridine derivatives bearing suitable functional groups at the 4' position, it is essential to have an efficient and flexible preparative method at our disposal. From the synthetic routes available for the synthesis of 4' substituted terpyridines⁶¹⁻⁶⁴ the procedure of *Akermark et al*⁶⁵ was selected. This approach allows gram-scale preparation of 4'-(*p*-bromophenyl)-2,2':6',2''-terpyridine (Figure 2.6).

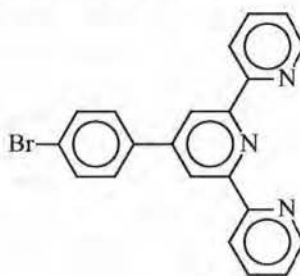


Figure 2.6: 4'-(*p*-Bromophenyl)-2,2':6',2''-terpyridine

Potentially this functionalized terpyridine is the ideal precursor to any bridging multi-terpyridine ligand.

It can lead to bis-terpyridine systems with various aromatic or saturated spacers as well as to bridging multichelates by connecting several such terpyridines units.

Therefore 4'-(4-ethynylphenyl)-2,2':6',2''-terpyridine (Figure 2.7) was prepared from 4'-(*p*-bromophenyl)-2,2':6',2''-terpyridine (Figure 2.6) according to procedures^{66,67} in the literature.

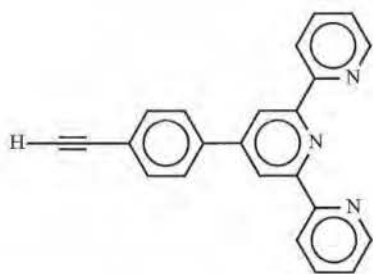


Figure 2.7: 4'-(4-Ethynylphenyl)-2,2':6',2''-terpyridine

These acetylene and bromine terminated terpyridines can be attached to each other via a palladium catalyzed reaction to give bis[(2,2':6',2''-terpyridin-4'-yl)phenyl]ethyne⁶⁸ (Figure 2.8).

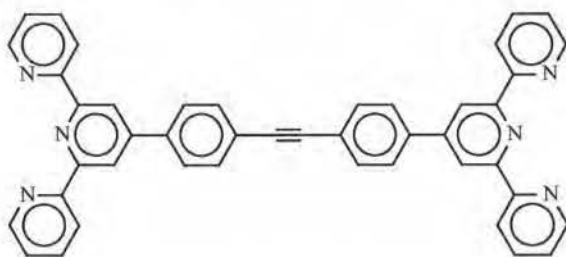


Figure 2.8: Bis[(2,2':6',2''-terpyridin-4'-yl)phenyl]ethyne

To check the influence of the spacer between the two terpyridyl termini on the density of the networks, we also synthesized 1,4-bis(2,2':6',2''-terpyridin-4'-yl)benzene⁶⁹, (Figure 2.9) a molecular rod based on two terpyridyl termini bridged by a spacer consisting of a phenylene module.

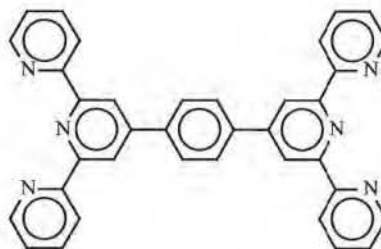


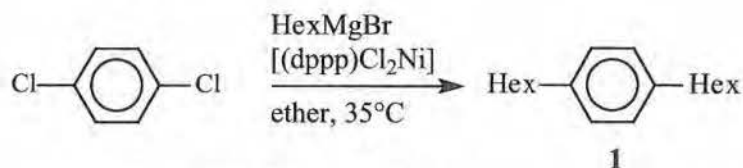
Figure 2.9: 1,4-Bis(2,2':6',2''-terpyridin-4'-yl)benzene

2.2 SYNTHESIS OF MOLECULAR RODS

2.2.1 Synthesis Of Oligophenylenes

2.2.1.1 Synthesis of 4-bromo-2,5,2'',5''-tetra-*n*-hexyl-4'''-trimethylsilyltetra-phenyl

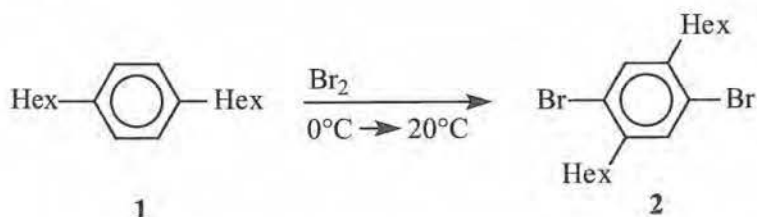
n-Hexylmagnesium bromide is coupled with commercially available 1,4-dichlorobenzene (Scheme 2.9) under nickel catalysis, giving 1,4-dihexylbenzene⁷⁰ (**1**) with yields of more than 80%.



Scheme 2.9: Synthesis of 1,4-dihexylbenzene

(dppp)Cl₂Ni [dppp = 1,3-bis(diphenylphosphino)propane] is an effective catalyst in this coupling reaction; no positional scrambling of the hexyl substituent attached to the benzene ring or isomerization of the primary substituents to secondary ones is observed.

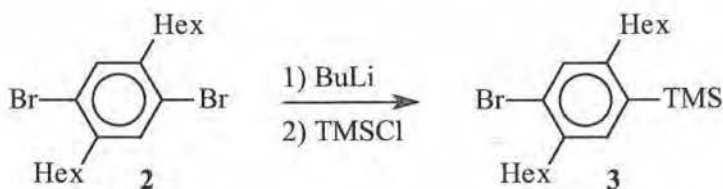
In the next step 1,4-dihexylbenzene (**1**) is brominated under rigorous exclusion of light (Scheme 2.10). The bromine was added dropwise to an ice-cooled solution of 1,4-dihexylbenzene (**1**) and stirred for 24 hours at room temperature.



Scheme 2.10: Synthesis of 2,5-dibromo-1,4-dihexylbenzene

The product (**2**) of the reaction was exclusively brominated at the opposite carbons C-2 and C-5 and was produced with yields of up to 80% after recrystallization.

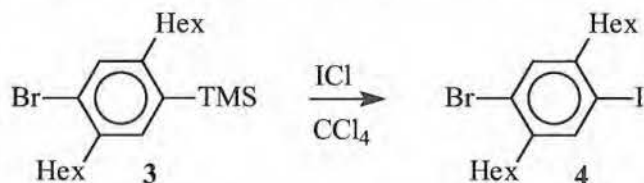
The lithiation of 2,5-dibromo-1,4-dihexylbenzene (**2**) (Scheme 2.11) is performed in diethyl ether at -78°C using an excess of butyllithium. A clean monolithiation could be achieved as indicated by the very high yield of more than 90% of the quenching product 1-bromo-2,5-di-*n*-hexyl-4-trimethylsilylbenzene (**3**).



Scheme 2.11: Synthesis of 1-bromo-2,5-di-*n*-hexyl-4-trimethylsilylbenzene

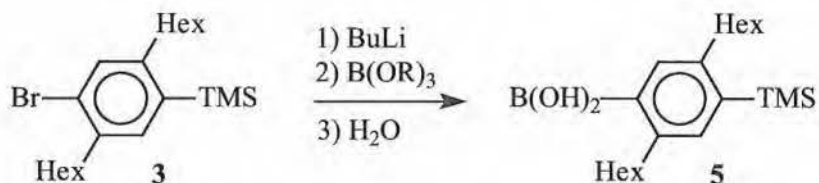
1-bromo-2,5-di-*n*-hexyl-4-trimethylsilylbenzene (**3**) is the molecular building block of all monomers needed for the construction of various biphenyls. The bromine function can be converted into boronic acid or TMS, and the trimethylsilyl can be converted into an iodine or boronic acid function.

The iodo function of 4-bromo-2,5-di-*n*-hexyl-1-iodobenzene (**4**) is introduced by *ipso* iododesilylation (Scheme 2.12) of 1-bromo-2,5-di-*n*-hexyl-4-trimethylsilylbenzene (**3**) with iodine monochloride. This conversion proceeds cleanly and gives the product with yields of more than 95%.



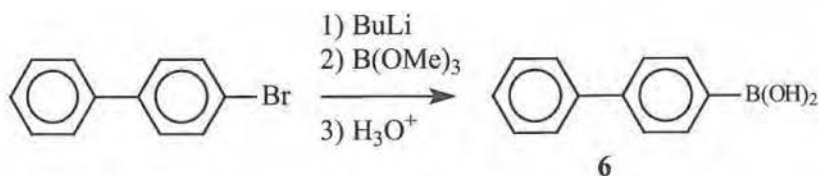
Scheme 2.12: Synthesis of 4-bromo-2,5-di-*n*-hexyl-1-iodobenzene

The boronic acid of 2,5-di-*n*-hexyl-4-trimethylsilylbenzene (**3**) (Scheme 2.13) is generated from the corresponding bromoarene after lithiation, boronation of the lithiated intermediate with triisopropyl borate and hydrolysis of the resulting boronic acid ester, and give 2,5-di-*n*-hexyl-4-trimethylsilylbenzene-1-boronic acid (**5**) with yields of up to 80%.



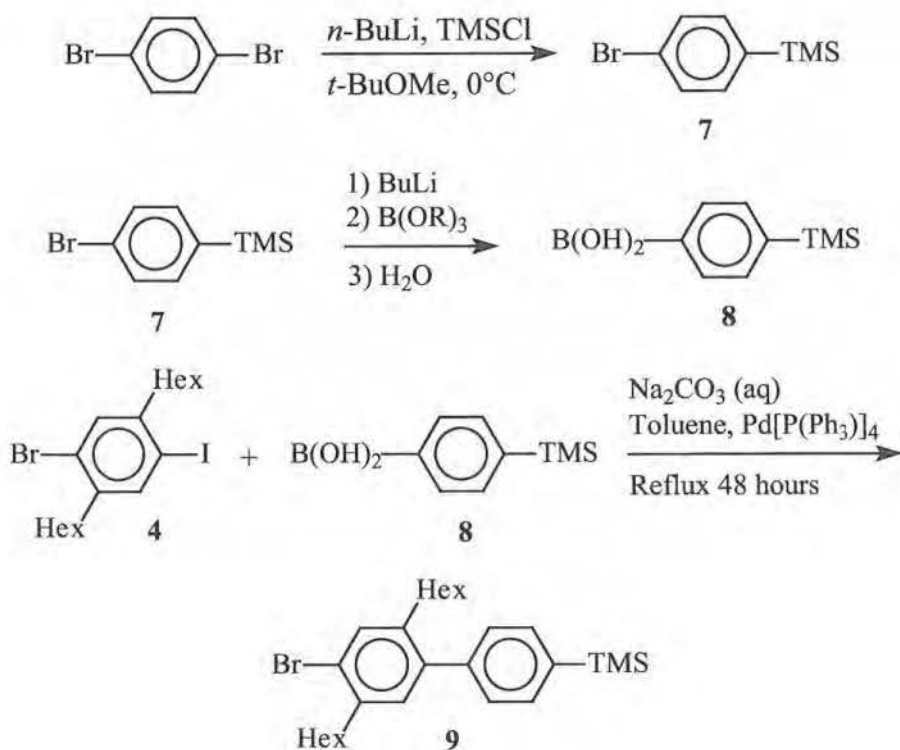
Scheme 2.13: Synthesis of 2,5-di-*n*-hexyl-4-trimethylsilylbenzene-1-boronic acid

Triisopropyl borate is used instead of trimethylborate because the literature³¹ describes that the yields are approximately 20% higher when using triisopropyl borate. This was also experienced in our lab with the synthesis of 4-biphenylboronic acid (**6**) (Scheme 2.14) which was prepared out of 4-bromobiphenyl via boronation of the lithiated intermediate with trimethylborate and hydrolysis of the resulting boronic acid ester. Yields of only 30% could be achieved.



Scheme 2.14: Synthesis of 4-biphenylboronic acid

For the synthesis of the biphenyl derivative (**9**), 4-trimethylsilylbenzene-1-boronic acid (**8**) was prepared from commercially available 1,4-dibromobenzene (Scheme 2.15) with yields of more than 90%.



Scheme 2.15: Synthesis of 4-bromo-2,5-di-*n*-hexyl-4'-trimethylsilylbiphenyl

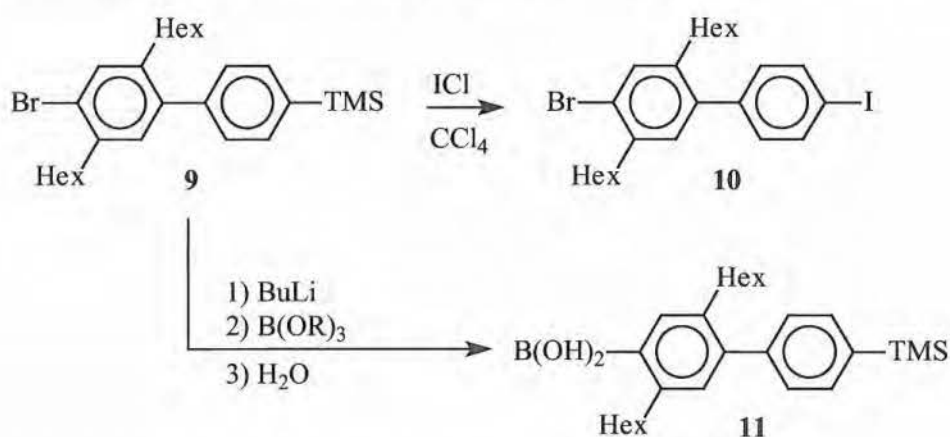
When converting 1,4-dibromobenzene to 1-bromo-4-trimethylsilylbenzene (**7**) the use of an appropriate solvent is necessary. *t*-Butyl methyl ether provided bromine lithium exchange and silylation with high yield, which was

not observed when other solvents were used. For example, according to literature⁷¹, the treatment of 1,4-dibromobenzene in tetrahydrofuran with *n*-butyllithium at 0°C followed by addition of chlorotrimethylsilane, did not lead to the desired product.

1-Bromo-4-trimethylsilylbenzene (7) was converted to 4-trimethylsilylbenzene-1-boronic acid (8) via consecutive lithiation, boronation and hydrolysis of the bromine with yields up to 80%. This 4-trimethylsilylbenzene-1-boronic acid (8) was then coupled with 4-bromo-2,5-di-*n*-hexyl-1-iodobenzene (4) via a palladium catalyzed reaction with tetrakis(triphenylphosphine)-palladium(0) as catalyst to give 4-bromo-2,5-di-*n*-hexyl-4'-trimethylsilylbiphenyl (9) with yields of around 90%.

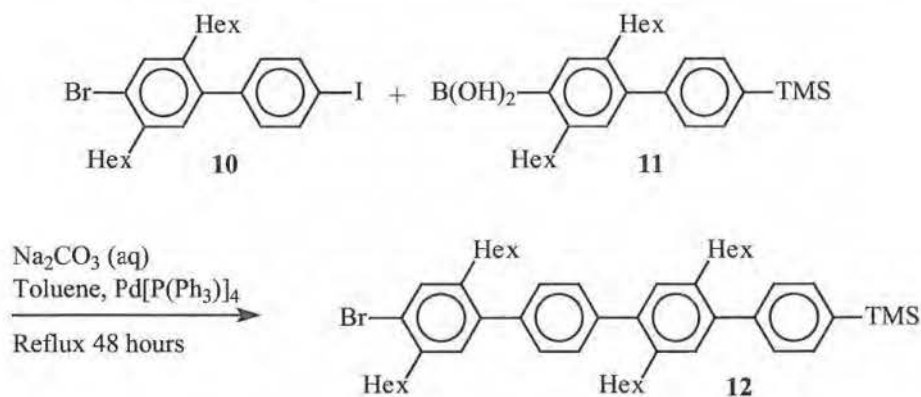
All boronic acids tend to form cyclic anhydrides (boroxines) and, depending upon solvent polarity and water content, exist as mixtures of the monomeric and trimeric forms. When NMR spectra were recorded in either chloroform or DMSO the cyclic trimer and the monomeric species were respectively favoured. Thus when taking a ¹H-NMR in chloroform no signals of the boronic acid hydrogens could be detected in contradiction with DMSO where the signals were visible. The EI mass spectra showed the correct ion peak of the trimer at a mass of MS (EI, *m/e*) = 474 (*M*⁺).

The biphenyls needed for the synthesis of 4-bromo-2,5,2'',5''-tetra-*n*-hexyl-4'''-trimethylsilyltetraphenyl (11) (Scheme 2.16) were prepared following the same procedures as used for the monomers (4,5).



Scheme 2.16: Synthesis of biphenyls

The trimethylsilyl function at the terminus of the biphenyl derivative (**9**) is easily and cleanly converted into an iodine function with iodine monochloride via *ipso* iododesilylation of 4-bromo-2,5-di-*n*-hexyl-4'-trimethylsilylbiphenyl (**10**) with yields of more than 85%. The bromo protective group is converted into boronic acid giving 2,5-di-*n*-hexyl-4'-trimethylsilylbiphenyl-4-boronic acid (**11**) with 65% yield.



Scheme 2.17: Synthesis of 4-bromo-2,5,2'',5''-tetra-*n*-hexyl-4'''-trimethylsilyltetraphenyl

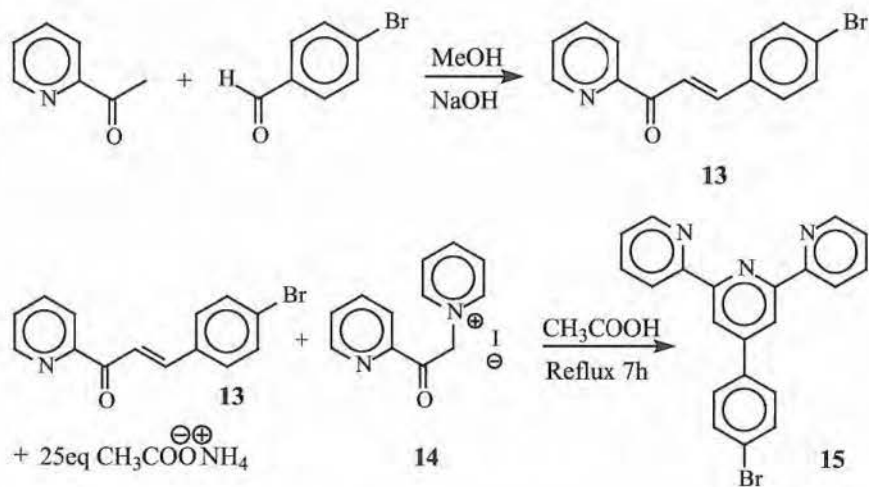
Finally the Suzuki cross-coupling of the boronic acid (**11**) and iodine (**10**) under palladium catalysis gives 4-bromo-2,5,2'',5''-tetra-*n*-hexyl-4'''-trimethylsilyltetraphenyl (**12**) with 66% yield.

Exactly the same reaction procedures could be repeated to achieve for example the octaphenyl. This rigid, soluble 4-bromo-2,5,2'',5''-tetra-*n*-hexyl-4'''-trimethylsilyltetraphenyl (**12**) (**B** in scheme 2.1) can now act as rigid rod. The TMS (**Z**) act as a protective group and the bromine (**Y**) as a potential coupling place. This bromine function can couple with the unprotected acetylenes present on the molecular knot **A** via palladium catalyzed reactions to give the extended molecular knot **C**. The trimethylsilyl function can easily be converted into an iodine function in high yields to give **D**. This iodine function on the extended knot **D** can again couple with the acetylenes on the knot **A** to obtain a molecular network.

2.2.2 Synthesis Of Terpyridines

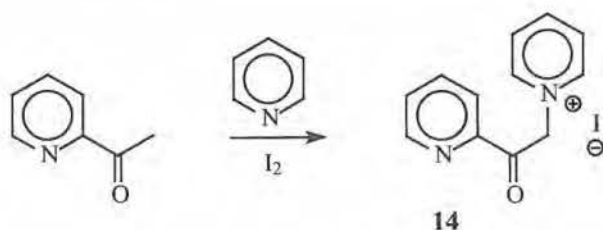
2.2.2.1 Synthesis of 4'-(4''-bromophenyl)-2,2':6',2''-terpyridine

The commercial availability of different *para*-substituted benzaldehydes allows the synthesis of various 4'-aryl-2,2':6',2''-terpyridines. For our purposes__ 4'-(4''-bromophenyl)-2,2':6',2''-terpyridine (**15**) is prepared (Scheme 2.18) in a two step aldol condensation using ammonium acetate both as a base and ring closure agent. In the literature⁶⁵ it was mentioned that a one step aldol condensation of 2-acetylpyridine and 4-bromobenzaldehyde would give low yields of the desired terpyridine due to facile formation of polycondensation products.



Scheme 2.18: Synthesis of 4'-(4''-bromophenyl)-2,2':6',2''-terpyridine

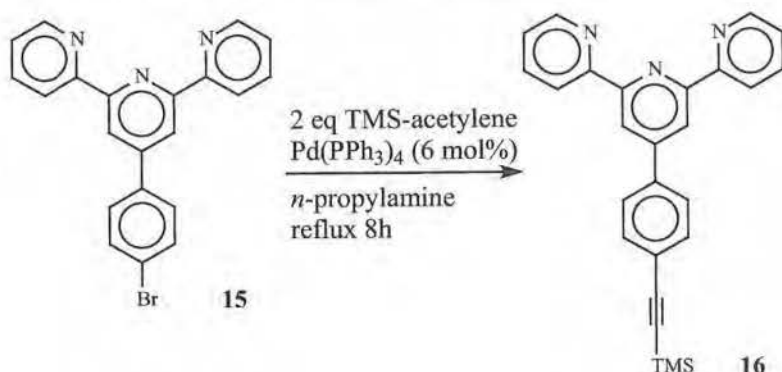
E)-3-(4''-Bromophenyl)-1-(pyrid-2'-yl)prop-2-enone (**13**) is formed by a Claisen-Schmidt reaction of 2-acetylpyridine with 4-bromobenzaldehyde and isolated with a yield of 66% after two recrystallizations. This azachalcone (**13**) is condensed with N-[2-(pyrid-2'-yl)-2-oxoethyl]pyridinium iodide (**14**) (Scheme 2.19) a Kröhnke-type nucleophile⁷².



Scheme 2.19: Synthesis of N-[2-(pyrid-2'-yl)-2-oxoethyl]pyridinium iodide

For the preparation of the pyridinium salt (**14**) the Ortoleva-King-reaction⁷³ is used where iodine, pyridine and 2-acetylpyridine are refluxed to precipitate the salt. After standing overnight the crystals were filtered and washed with pyridine. The crystals were recrystallized twice from ethanol/water and achieved with yields of around 75%.

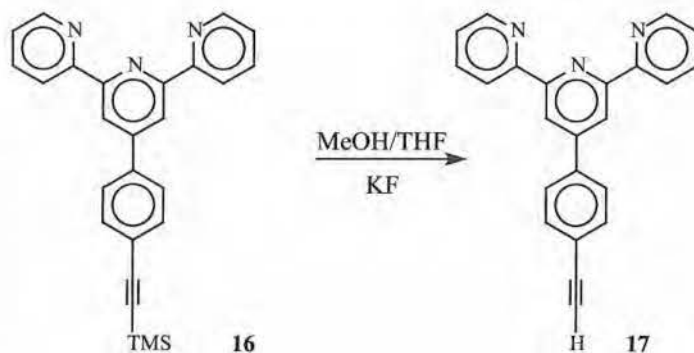
The bromine function of 4'-(4'''-bromophenyl)-2,2':6',2''-terpyridine (**15**) can couple easily and in high yields with unprotected acetylenes (Scheme 2.20). The transformation of the bromo-function into trimethylsilyl-acetylene was performed in *n*-propylamine with [Pd(PPh₃)₄] at 60°C in a high yield reaction; yields of more than 90% could be reached.



Scheme 2.20: Synthesis of 4'-[4-{2-(trimethylsilyl)-1-ethynyl}phenyl]-2,2':6',2''-terpyridine

In contradiction with literature procedures⁶⁶, where it is mentioned that 4'-[4-{2-(trimethylsilyl)-1-ethynyl}phenyl]-2,2':6',2''-terpyridine (**16**)

precipitated out of the solution as a white powder, the solution stayed clear after reflux overnight. After chromatographic separation on silicagel, with chloroform as eluent and recrystallization in acetonitrile white needles were obtained.



Scheme 2.21: Synthesis of 4'-(4-ethynylphenyl)-2,2':6',2''-terpyridine

The deprotection of the trimethylsilyl group with KF in a mixture of methanol and tetrahydrofuran gave excellent yields (>95%) of the unprotected acetylene (**17**). This can be used for coupling reactions with, for example, aryl bromides and iodides using tetrakis(triphenylphosphine) palladium [Pd(PPh₃)₄] as catalyst and *n*-propyl amine as solvent.

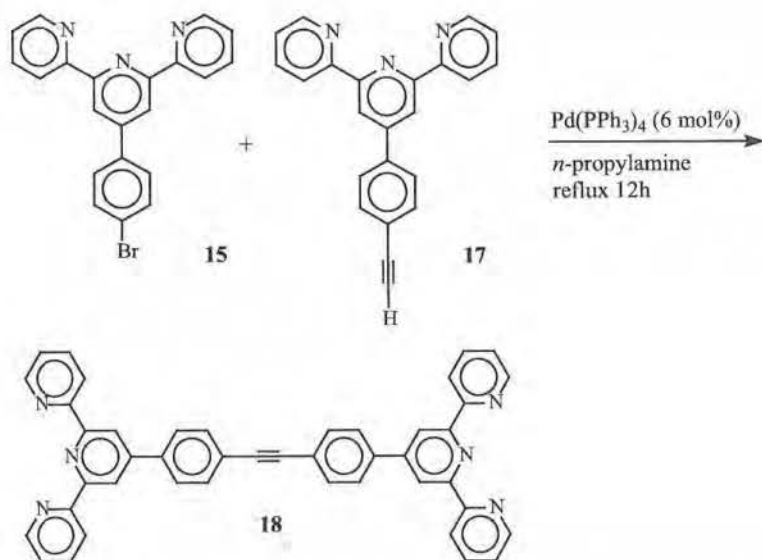
4'-(4-Ethynylphenyl)-2,2':6',2''-terpyridine (**17**) (Scheme 2.21) can easily couple to aryl bromides or iodides present on our molecular knot via a palladium catalyzed reaction (see also Chapter 3). This ligand (**17**) can act as half-rod between our molecular knots and because of the possibility to form very stable metal complexes it can form linkages between two half-rods almost as strong as covalent bonds. We wanted to use the metal ligand interaction as a non-covalent binding force to assemble non-covalent well-defined and ordered systems.

4'-(4-Ethynylphenyl)-2,2':6',2''-terpyridine (**17**) and 4'-(4'''-bromophenyl)-2,2':6',2''-terpyridine (**15**) are obtained as two building blocks for the synthesis of bisterpyridine: bis[(2,2':6',2''-terpyridin-4'-yl)phenyl]ethyne (**18**) (See Scheme 2.22).

2.2.3 Synthesis Of Bis-terpyridines

2.2.3.1 Synthesis of bis[(2,2':6',2''-terpyridin-4'-yl)phenyl]ethyne

The palladium-catalyzed reaction between the ethynylated derivatives of terpyridine and the corresponding terpyridine halides provides access to various homo-tritopic and hetero tritopic ligands. Therefore 4'-(4-ethynylphenyl)-2,2':6',2''-terpyridine (**17**) and 4'-(4'''-bromophenyl)-2,2':6',2''-terpyridine (**15**) (Scheme 2.22) were refluxed in *n*-propylamine in the presence of tetrakis(triphenylphosphine)-palladium(0) for 12 hours. During that time a yellow precipitate was formed.



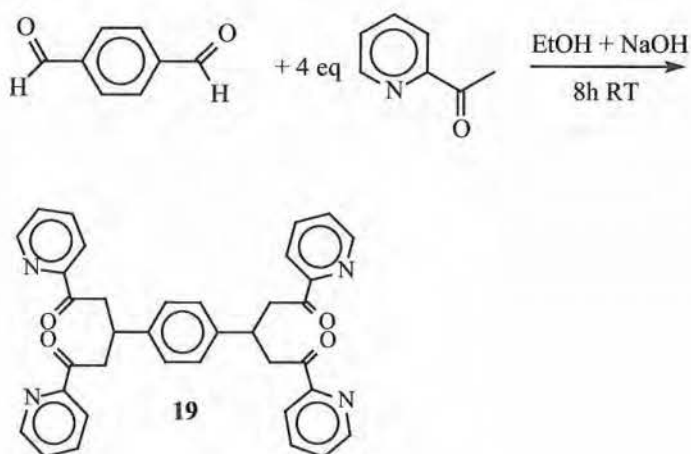
Scheme 2.22: Synthesis of bis[(2,2':6',2''-terpyridin-4'-yl)phenyl]ethyne

The yellow precipitate was filtered off and washed with *n*-propylamine to give bis[(2,2':6',2''-terpyridin-4'-yl)phenyl]ethyne (**18**) as a slightly yellow coloured solid with a yield of 95%. To check the influence of the spacer (two phenylene and one acetylene modules) between the two terpyridyl termini of bis[(2,2':6',2''-terpyridin-4'-yl)phenyl]ethyne (**18**) on the density of the networks, the synthesis of 1,4-bis(2,2':6',2''-terpyridin-4'-yl)benzene (**20**)

(See Scheme 2.24) was planned and executed. The spacer of 1,4-bis(2,2':6',2''-terpyridin-4'-yl)benzene (**20**) consist on one phenylene module.

2.2.3.2 Synthesis of 1,4-bis(2,2':6',2''-terpyridin-4'-yl)benzene

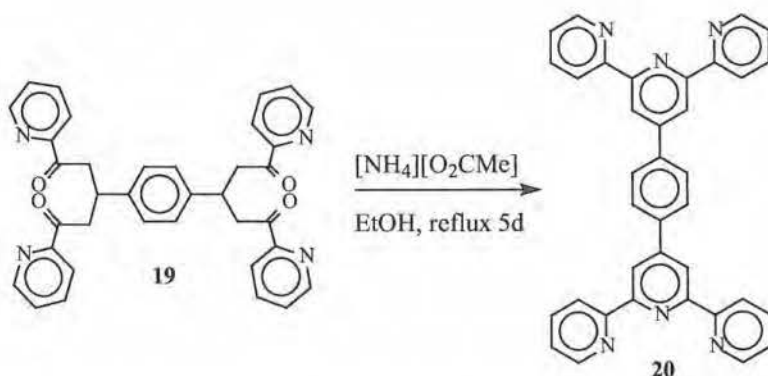
2-Acetylpyridine was added to a stirred solution of benzene-1,4-dicarbaldehyde in warm ethanol (Scheme 2.23). Aqueous sodium hydroxide was added and the mixture was stirred for eight hours at room temperature, during which a white precipitate was formed.



Scheme 2.23: Synthesis of 1,4-bis[1,5-dioxo-1,5-bis(2-pyridyl)pentan-3-yl]benzene

The precipitate was filtered off and washed with ethanol to give 1,4-bis[1,5-dioxo-1,5-bis(2-pyridyl)pentan-3-yl]benzene (**19**). A yield of 47% could be reached in contradiction with literature where yields of up to 65 % were reported.

This tetra-ketone 1,4-bis[1,5-dioxo-1,5-bis(2-pyridyl)pentan-3-yl]benzene (**19**) was added to a suspension of ammonium acetate in ethanol and refluxed for five days (Scheme 2.24).



Scheme 2.24: Synthesis of 1,4-bis(2,2':6',2''-terpyridin-4'-yl)benzene

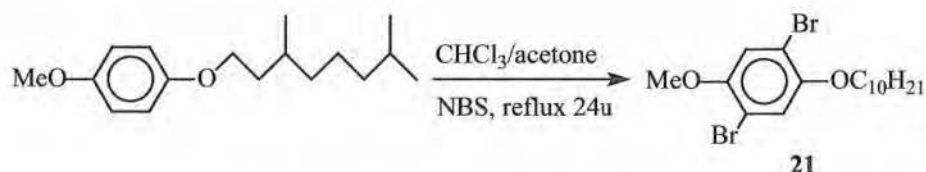
After the reaction mixture was cooled, the solid product was collected and washed well with ethanol. In contradiction with literature⁶⁹, the product was not an off-white solid but a brown powder and the yields were again not as high as reported. Yields of only 19% were achieved in contradiction with literature where a yield of 40 % was reported.

1,4-bis(2,2':6',2''-terpyridin-4'-yl)benzene (**20**) and bis[(2,2':6',2''-terpyridin-4'-yl)phenyl]ethyne (**18**) are both only slightly soluble in most organic solvents. This and also the very low yields of the reactions needed for the synthesis of 1,4-bis(2,2':6',2''-terpyridin-4'-yl)benzene (**20**) forced us to look for the synthesis of a more soluble bisterpyridine. Earlier results (Scheme 2.22) showed that palladium catalyzed coupling reactions of bromines with acetylenes gave high yields of the corresponding coupling product. Therefore 1,4-di[4'-(4-ethynylphenyl)-2,2':6',2''-terpyridine]-2-(3,7-dimethyloctyl-5-methoxybenzene (**22**) is prepared (See Scheme 2.26). It is expected to be more soluble than the two other (**18,20**) bisterpyridines due to the alkyl side chains. The reason 1,4-di[4'-(4-ethynylphenyl)-2,2':6',2''-terpyridine]-2-(3,7-dimethyloctyl-5-methoxybenzene (**22**) was chosen, was the commercial availability of 1,4-dibromo-2-(3,7-dimethyloctyl)-4-methoxybenzene and the availability of 4'-(4-ethynylphenyl)-2,2':6',2''-terpyridine (**17**) which was already prepared before, for the synthesis of bisterpyridine bis[(2,2':6',2''-terpyridin-4'-yl)phenyl]ethyne (**18**).

2.2.3.3 Synthesis of 1,4-di[4'-(4-ethynylphenyl)-2,2':6',2''-terpyridine]-2-(3,7-dimethyloctyl-5-methoxybenzene)

1,4-Di[4'-(4-ethynylphenyl)-2,2':6',2''-terpyridine]-2-(3,7-dimethyloctyl)-5-methoxybenzene (**22**) (Scheme 2.26) is prepared via the same literature procedures as used for the synthesis of bis[(2,2':6',2''-terpyridin-4'-yl)phenyl]ethyne (Scheme 2.22). Again high yields could be obtained when the acetylene was coupled with the arylbromide under palladium catalysis.

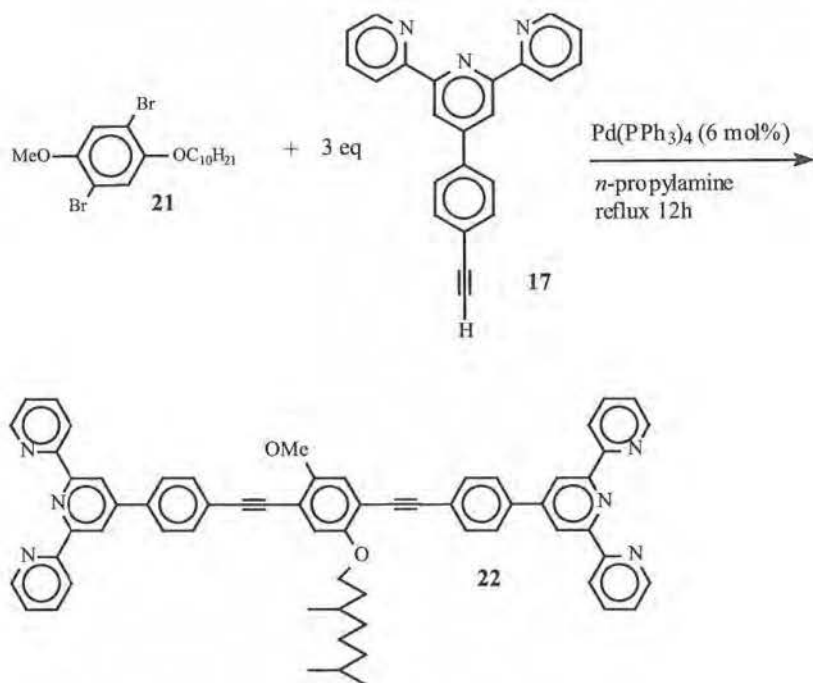
1-(3,7-dimethyloctyl)-4-methoxybenzene was purchased via Covion and is refluxed for 24 hours in a mixture of acetone and chloroform with N-bromosuccinimide (NBS) (Scheme 2.25).



Scheme 2.25: Synthesis of 1,4-dibromo-2-(3,7-dimethyloctyl)-5-methoxybenzene

After 24 hours reflux another portion of NBS is added and the mixture is refluxed during another 16 hours. Chromatographic separation on silicagel with CHCl₃/hexane (3:7) gave 1,4-dibromo-2-(3,7-dimethyloctyl)-5-methoxybenzene (**21**) as a colourless oil with 76% yield.

The dibromide 1,4-dibromo-2-(3,7-dimethyloctyl)-5-methoxybenzene (**21**) and three equivalents of 4'-(4-ethynylphenyl)-2,2':6',2''-terpyridine (**17**) in *n*-propylamine were refluxed for 12 hours under palladium catalysis (Scheme 2.26).



Scheme 2.26: Synthesis of 1,4-di[4'-(4-ethynylphenyl)-2,2':6',2''-terpyridine]-2-(3,7-dimethyloctyl)-5-methoxybenzene

The yellow solid was filtered off and washed thoroughly with cold *n*-propylamine. The filtrate was partly evaporated and the solid that precipitated was again filtered off. Chromatographic separation of the solids on silicagel with chloroform as eluent gave 1,4-di[4'-(4-ethynylphenyl)-2,2':6',2''-terpyridine]-2-(3,7-dimethyloctyl)-5-methoxybenzene (**22**) as a yellow solid with yields of more than 90%. The product was pure on NMR spectra, and all the ¹H-NMR-signals could be assigned. MALDI-TOF-MS experiments showed the correct signal at *m/z*: 926.

2.3 CONCLUSIONS

4-Bromo-2,5,2'',5''-tetra-*n*-hexyl-4'''-trimethylsilyl-tetraphenyl (**12**) is prepared in gram quantities and can now be used as a rigid soluble rod between molecular knots. These rigid molecular knots will be discussed in chapter three.

1,4-Di[4'-(4-ethynylphenyl)-2,2':6',2''-terpyridine]-2-(3,7-dimethyloctyl)-5-methoxybenzene (**22**) is also prepared in gram quantities and can now be used for network formation via complexation which will be explained in chapter four. The two other bisterpyridines; 1,4-bis(2,2':6',2''-terpyridin-4'-yl)benzene (**20**) and bis[(2,2':6',2''-terpyridin-4'-yl)phenyl]ethyne (**18**) were too insoluble to be used as linkers between different molecular knots.

2.4 REFERENCES

1. Kaszynski P., Michl J., In *Advances in Strain in Organic Chemistry*, JAI Press Inc., London, **1995**, 4, 283.
2. Della E. W., Lochert I. J., *Org. Prep. Proc. Int.*, **1996**, 28, 411.
3. Kaszynski P., Friedli A. C., Michl J., *J. Am. Chem. Soc.*, **1992**, 114, 601.
4. Wiberg K. B., Waddell S. T., Laidig K., *Tetrahedron Lett.*, **1986**, 27, 1553.
5. Eaton P. E., Cole T. W., Jr., *J. Am. Chem. Soc.*, **1964**, 86, 962.
6. Griffin G. W., Marchard A. P., *Chem. Rev.*, **1989**, 89, 997.
7. Eaton P. E., *Angew. Chem. Int Ed. Engl.*, **1992**, 31, 1421.
8. Hassenrück K., Radziszewski J. G., Balaji V., Murthy G. S., McKinley, A. J., David D. E., Lynch V. M., Martin H.-D., Michl J., *J. Am. Chem. Soc.*, **1990**, 112, 873.
9. Glaser C., *Ann. Chem.*, **1870**, 154, 137.
10. Behr O. M., Eglinton, G., Galbraith A. R. Raphael R. A., *J. Chem. Soc.*, **1960**, 3614.
11. Hay A. S., *J. Org. Chem.*, **1962**, 27, 3320.
12. Wright M. E., Porsch M. J., Buckley C., Cochran B. B., *J. Am. Chem. Soc.*, **1997**, 119, 8393.
13. Bohlmann F., Herbst P., Gleinig H., *Chem. Ber.*, **1961**, 94, 948.
14. Berscheid R., Vögtle F., *Synthesis*, **1992**, 58.
15. Black H. K., Horn D. H. S., Weedon B. G. L., *J. Chem. Soc.*, **1954**, 1704.
16. Miller J. A., Zweifel G., *Synthesis*, **1983**, 128.
17. Kitamura T., Lee C. H., Taniguchi H., Masumoto M., Sano Y., *J. Org. Chem.*, **1994**, 59, 8053.
18. Stille J. K., *Angew. Chem. Int Ed. Engl.*, **1986**, 25, 508.
19. Eastmond R., Johnson T. R., Walton D. R. M., *Tetrahedron*, **1972**, 28, 4601.
20. Karich G., Jochims J. C., *Chem. Ber.*, **1977**, 110, 2680.
21. Komatsu K., Kamo H., Tsuji R., Takeuchi K., *J. Org. Chem.*, **1993**, 58, 3219.
22. Rutledge T. F., *Acetylenes and Allenes*, Reinhold: New York, **1969**.

23. Wallenberger F. T., *Angew. Chem. Int Ed. Engl.*, **1964**, 3, 460.
24. Kallitsis J. K., Rehahn M., Wegner G., *Makromol. Chem.*, **1992**, 193, 1021.
25. Kallitsis J. K., Wegner G., Pakula T., *Makromol. Chem.*, **1992**, 193, 1031.
26. Kallitsis J. K., Kakali F., Gravalos K. V., *Makromolecules*, **1994**, 27, 4507.
27. Helmer-Metzmann F., Rehahn M., Schmitz L., Ballauff M., Wegner G., *Makromol. Chem.*, **1992**, 193, 1847.
28. Schmitz L., Ballauff M., *Polymer*, **1995**, 36, 879.
29. Patrick Galda, Matthias Rehahn, *Synthesis (papers)*, **1996**, 614-620.
30. Volker Hensel, A.-Dieter Schlüter, *Liebigs Ann. Recueil*, **1997**, 303-309.
31. Petra Liess, Volker Hensel, A.-Dieter Schlüter, *Liebigs Ann.*, **1996**, 1037-1040.
32. Kern W., Seibel M., Wirth H. O., *Makromol. Chem.*, **1959**, 29, 165.
33. Lamba J. J. S., Tour J. M., *J. Am. Chem. Soc.*, **1994**, 116, 11723.
34. Scherf U., Müllen K., *Synthesis*, **1992**, 23.
35. Goldfinger M. B., Swager T. M., *J. Am. Chem. Soc.*, **1994**, 116, 7895.
36. Suzuki A., *J. Organomet. Chem.*, **1999**, 576, 147-168.
37. Grushin V. V., Alper H., *Chem. Rev.*, **1994**, 94, 1047-1062.
38. Zhang, C.; Huang, J.; Trudell, M. L.; Nolan, S. P. *J. Organomet. Chem.*, **1999**, 64, 3804.
39. Wolfe, J. P.; Buchwald, S. L. *Angew. Chem. Int Ed.*, **1999**, 38, 2413.
40. Wolfe, J. P.; Singer, R. A.; Yang, B. H.; Buchwald, S. L. *J. Am. Chem. Soc.*, **1999**, 121, 9550.
41. Old, D. W.; Wolfe, J. P.; Buchwald, S. L. *J. Am. Chem. Soc.*, **1998**, 120, 9722.
42. Bei, X.; Turner, H. W.; Weinberg, H.; Guram, A. S. *J. Org. Chem.*, **1999**, 64, 6797.
43. Bei, X.; Crevier, T.; Guram, A. S.; Jandeleit, B.; Powers, T. S.; Turner, H. W.; Uno, T.; Weinberg, W. H. *Tetrahedron Lett*, **1999**, 40, 3855.
44. Feuerbacher N.; Vögtle F., *Top Curr. Res.*, **1998**, 197, 1.
45. Feuerbacher N.; Vögtle F., Windscheidt J., Pötsch E., Nieger M. *Synthesis*, **1999**, 117.

46. Petra Liess, Volker Hensel, A.-Dieter Schlüter, *Liebigs Ann.*, **1996**, 1037-1040.
47. Schumm J. S., Pearson D. L., Tour J. M., *Angew. Chem. Int Ed. Engl.*, **1994**, 33, 1360.
48. Diederich F., Stang P. J., Eds., Wiley-VCH: Weinheim, *Metal-Catalyzed Cross-Coupling reactions*, **1998**.
49. Morgan, G. T., Burstall F. H., *J. Chem. Soc.* **1931**, 20.
50. Morgan, G. T., Burstall F. H., *J. Indian Chem. Soc., Ray Commem.*, **1933**, 1.
51. Morgan, G. T., Burstall F. H., *J. Chem. Soc.* **1934**, 1499.
52. Morgan, G. T., Burstall F. H., *J. Chem. Soc.* **1932**, 20.
53. Morgan, G. T., Burstall F. H., *J. Chem. Soc.* **1938**, 1672.
54. (a) Newkome G. R., He E., Godinez L. A., *Makromolekules*, **1998**, 31, 4382. (b) Schubert U. S., Weidl C. H., Moorefield C. N., Baker G. R., Newkome G. R., *Polym. Prepr.*, **1999**, 40, 940.
55. Lehn J.-M., *Supramolecular Chemistry, Concepts and perspectives*, VCH: Weinheim, **1995**.
56. (a) Salditt T., An Q. R., Plech A., Eschbaumer C., Schubert U. S., *Chem. Commun.*, **1998**, 2731. (b) Schubert U. S., Eschbaumer C., An Q. R., Salditt T., *J. Incl. Phenom.*, **1999**, 32, 35.
57. (a) Constable E. C., Lewis J., *Polyhedron*, **1982**, 303. (b) Constable E. C., Lewis J., Liptrot M. C., Raithby P. R., Schröder M., *Polyhedron*, **1983**, 2, 301. (c) Constable E. C., Lewis J., Liptrot M. C., Raithby P. R., Schröder M., *J. Chem. Soc. Dalton Trans.*, **1984**, 2177. (d) Constable E. C., Khan F. K., Lewis J., Liptrot M. C., Raithby P. R., *J. Chem. Soc. Dalton Trans.*, **1985**, 333. (e) Constable E. C., Holmes J. M., McQueen R. C. S., *J. Chem. Soc. Dalton Trans.*, **1987**, 5. (f) Constable E. C., Holmes J. M., *Polyhedron*, **1988**, 7, 2531. (g) Bell T. W., Firestone A., *J. Org. Chem.*, **1986**, 51, 1342. (h) Newkome G. R., Hager D. C., Kiefer G. E., *J. Org. Chem.*, **1986**, 51, 850. (i) Thummel R. P., Jahng Y., *J. Org. Chem.*, **1985**, 50, 2407.
58. Constable E. C., Cargill Thompson A. M. W., Tocher D. A., *Supramolecular Chemistry*, Balzani V., De Cola L. Eds., NATO ASI Series, Kluwer, Dordrecht, **1992**, 219.
59. Kovac B., Klasine L. Z., *Naturforsch., A*, **1978**, 23A, 247.

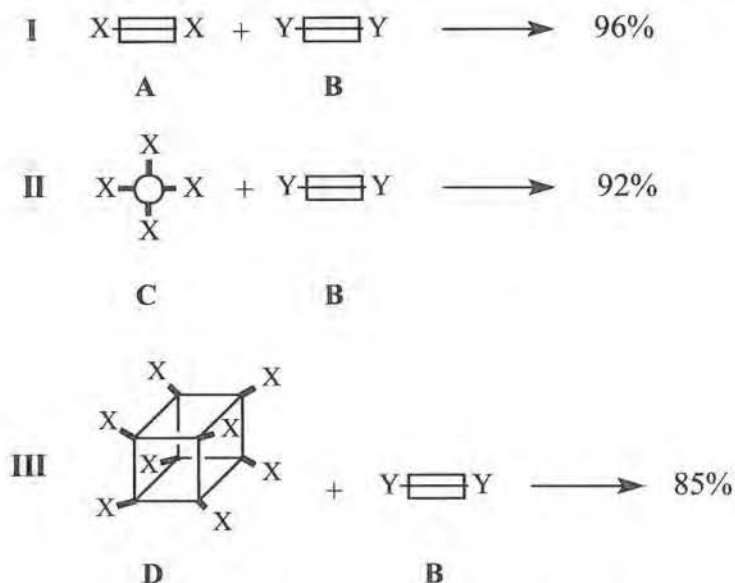
60. E. C. Constable, *advances in inorganic chemistry and radiochemistry*, **1986**, 30, 69-121.
61. Francis H. Case, Thomas J. Kasper, *J. Am. Chem. Soc.*, **1956**, 78, 5842.
62. Kevin T. Potts, Michael J. C., Philip R., George T., *J. Org. Chem.*, **1982**, 47, 3027.
63. Werner Spahni, Gion Calzefferri, *Helvetica Chimica Acta*, **1984**, 67, 450-454.
64. Veli-Matti M., Matti H., Jouko K., Harri T., *Helvetica Chimica Acta*, **1993**, 76, 1361.
65. Peter Korall, Anna Börje, Per-Ola Nouby, Björk Akermark, *Acta Chemica Scandinavica*, **1997**, 51, 760-766.
66. Vincent Grosshenny, Francisco M. Romero, Raymond Ziessel, *J. Org. Chem.*, **1997**, 62, 1491-1500.
67. Vincent Grosshenny, Raymond Ziessel, *Journal of Organometallic Chemistry*, **1993**, 453, C19-C22.
68. Vincent Grosshenny, Francisco M. Romero, Raymond Ziessel, *J. Org. Chem.*, **1997**, 62, 1491-1500.
69. Edwin C. Constable, Alexander M. W., Cargill Thompson, *J. Chem. Soc. Dalton. Trans.*, **1992**, 3467-3475.
70. Matthias Rehahn, Arnulf-Dieter Schlüter, W. James Feast, *Synthesis*, **1988**, 386-388.
71. John C-Amedio Jr., George T. Lee, Kapa Prasad, Oljan Repic, *Synthetic communications*, **1995**, 25(17), 2599-2612.
72. (a) Kröhnke F., *Angew. Chem.*, **1963**, 4, 181-224. Kröhnke F., *Angew. Chem. Int. Ed.*, **1963**, 2, 386. Haasnoot C. A. G., De Leeuw F. A. A. M., Altona C., *Tetrahedron*, **1980**, 36, 2783.
73. Kröhnke F., Gross K. F., *Chem. Ber.*, **1959**, 92, 22.

III

CHAPTER THREE: SYNTHESIS OF MOLECULAR KNOTS

3.1 INTRODUCTION

In order to achieve rigid and stiff networks, the two building blocks; the knots as well as the rods, have to be rigid. To be an efficient molecular knot for the formation of highly rigid molecular networks, the functionality of the knot has to be high enough (at least six). From a synthesis viewpoint it is of course true that the higher the functionality of the knot, the more difficult it is to obtain a full functionalization of the knots with the rods (Scheme 3.1).



Scheme 3.1: Coupling of knots with different functionalized rods

If we consider **A** as a bi-functional molecular knot and **B** as a molecular rod and the yield of the coupling of X with Y is e.g. 98%, the yield of the coupling reaction – to get a linear building block B-A-B – of **A** with **B** would theoretically be 96%. If we consider that the yield for the coupling of X with Y is the same for system **II** and **III**, the yield will decrease to 92% for **II** and to 85 % for **III**. For this reason high yield coupling reactions are needed between X and Y. (Imagine when the yield for the coupling of X with Y would be only 80%, the yield would decrease from 64% and 41% to only 17%, respectively.)

Two types of molecular knots were investigated. First of all the synthesis of knots where X represents an aryl halide, halide, acetylene or a boronic acid and secondly where X represents a terpyridine. In this way we can use either coupling reactions for the network formation if X is an aryl halide, halide, acetylene or a boronic acid and Y is a suitable coupling partner, or we can use complexation reactions if X and Y are terpyridines. This network formation via complexation will be discussed in detail later in chapter four.

Lower as well as higher functionalized molecular knots were investigated. The synthesis of molecular knots with different levels of functionalization was considered. This is because for some cases lower functionalized molecular knots are more easily accessible and on the other hand could also provide useful information about the behaviour of the more highly functionalized molecular knots.

3.2 CHOICE OF MOLECULAR KNOTS

3.2.1 Diamantane

Our first intention was to start with the synthesis of diamantane derivatives and to use them, after functionalization, as molecular knots. Diamantane¹⁻³ (Figure 3.1) is a cycloaliphatic-cage hydrocarbon, containing an “extended-cage” adamantane structure⁴.

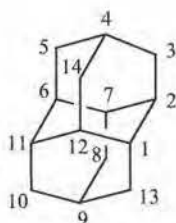


Figure 3.1: Diamantane

Diamantane has been investigated for many years. It was first synthesized in 1965 as congressane⁵ and later renamed to diamantane or pentacyclo[7.3.1.1^{4,12}.0^{2,7}.0^{6,11}]tetradecane. It became readily available⁶⁻⁸ in 1970. It's possible to synthesize diamantane in good yields by AlBr_3 -catalyzed isomerization of its strained polycyclic saturated precursors. For the functionalization⁹⁻¹³ of diamantane by ionic bromination, eight tertiary hydrogen atoms are present, which can be for example replaced by, for example bromine. Two types of bridgehead positions, named "medial" (C-1, -2, -6, -7, -11, -12) and "apical" (C-4, -9) are available for substitution. This substitution would give an octa-functionalized molecular knot (Figure 3.2) with eight bromines, more specifically, six "medial" and two "apical" bromines.

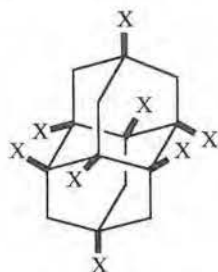
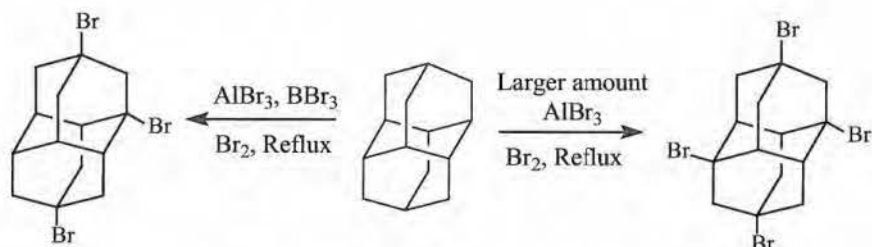


Figure 3.2: Octa-functionalized molecular knot

A literature search showed that 1,6-dibromodiamantane was the major product of diamantane bromination (with neat bromine) without using any catalyst^{8,14}, and that 4,9-dibromodiamantane was formed if the bromination was catalyzed by a small amount of AlBr_3 . (In the reaction mixture were also other dibromo derivatives present in small quantities.)

By the addition of bigger amounts of Lewis acid catalysts, and by increasing the severity of the reaction conditions, diamantane can be selectively tetra-brominated (Scheme 3.2) at the bridgehead positions. No higher substituted derivatives can be obtained.



Scheme 3.2: Synthesis of 1,4,6,9-tetrabromoadamantane.

No vicinal dibromoadamantanes have ever been observed as bromination or even as rearrangement products¹⁵, suggesting that substitution is strongly inhibited at the positions close to bromines already present. In general, polybromination of diamantane is controlled by inductive effects of the first bromine already present. Subsequent attack is at positions as far removed from the first bromine substituent as possible, but medial positions are inherently more reactive than apical ones. However, in our viewpoint the difference in reactivity is more related to sterical hindrance.

Because literature indicates that no higher functionalized diamantanes can be obtained, the synthesis of other highly functionalized rigid knots was investigated.

3.2.2 1,1'-Biadamantane and derivatives

Since, hexa- or octa-functionalization of diamantane was not possible, our attention shifted towards the synthesis of biadamantane derivatives. 1,1'-Biadamantane (Figure 3.3) has been prepared by *Landa and Hola*¹⁶ from 1-bromoadamantane and sodium in diethyl ether and later more efficiently prepared from 1-bromoadamantane and sodium dispersion in xylene or dioxane¹⁷, but more recent literature disputed the synthesis of biadamantane via this procedure¹⁸.

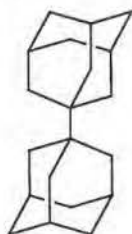


Figure 3.3: 1,1'-Biadamantane

1,1'-Biadamantane contains two adamantane units joined together at the tertiary carbon positions by a single bond. In contradiction with diamantane, 1,1'-biadamantane possesses only six tertiary hydrogen atoms. Between these six tertiary hydrogen atoms are present secondary hydrogen atoms, so the substitution is not inhibited due to sterical hindrance of nearby bromine atoms, as it is for diamantane. The functionalization of biadamantane would give a hexa-functionalized molecular knot (Figure 3.4).

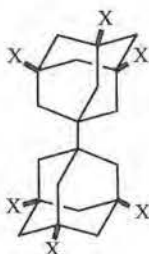


Figure 3.4: Hexa-functionalized 1,1'-biadamantane

A number of functionalization reactions, for the preparation of this hexa-functionalized molecular knot where X is chlorine or bromine, were investigated. These functionalization reactions should lead to 3,3',5,5',7,7'-hexachloro-1,1'-biadamantane and 3,3',5,5',7,7'-hexabromo-1,1'-biadamantane (Figure 3.5).

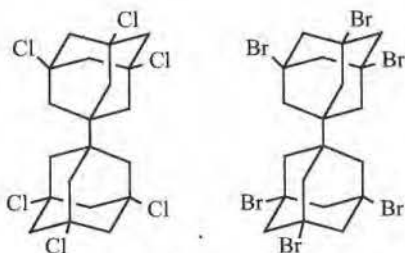


Figure 3.5: Hexachloro- and hexabromo-1,1'-biadamantane

These chlorine and bromine atoms could offer the possibility for coupling with the molecular rods.

Not only the functionalization of 1,1'-biadamantane, but also the functionalization of adamantane (Figure 3.6) was investigated for several reasons. First of all, because of the similarity in structure of biadamantane and adamantane, a similarity in reactivity can be expected. Furthermore the characterization of the less complex adamantane derivatives can facilitate the characterization of the more complex biadamantane derivatives. Secondly because adamantane derivatives such as adamantane and bromoadamantane are more readily commercially available, and 1,1'-biadamantane is not. Last but not least, concerning these functionalization reactions, the preparation of pure compounds requires a highly efficient synthetic methodology if high yields of a single polyfunctional product are to be obtained. The practical consequence of inefficient methodology was already illustrated by examining the functionalization of the knots. A problem related to this is that the isolation of pure Cl₆- or Br₆-biadamantane can be very difficult when reactions do not proceed to completion.

Consequently the synthesis of some adamantane derivatives was investigated first as the overall transformation (functionalization) requires for adamantane only four sequential chemical reactions that must proceed with high conversion instead of six.

3.2.3 Adamantane and adamantane derivatives

Adamantane²⁴ (Figure 3.6) or tricyclo[3.3.1.1^{3,7}]-decane can be readily prepared from tetrahydrodicyclopentadiene and aluminium trichloride or aluminium bromide^{25,26} and is now commercially available.

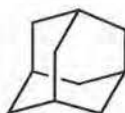


Figure 3.6: Adamantane

It is an ideal nucleus for four-directional rigid systems due to its rigid T_d symmetry, its all-hydrocarbon nature, its thermal stability and the fact that it can be selectively functionalized at the four tertiary positions (Figure 3.7).

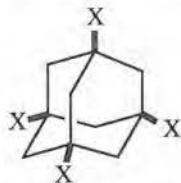


Figure 3.7: Tetra-functionalized molecular knot

This allows for controlled three-dimensional extension of adamantane's tetrahedral symmetry. We tried to synthesize three different tetra-functionalized adamantane derivatives. First of all if X is bromine this would give 1,3,5,7-tertrabromoadamantane (Figure 3.8).

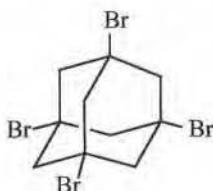


Figure 3.8: 1,3,5,7-Tertrabromoadamantane

The same as for the halogenated biadamantanes these bromine atoms could offer the possibility for coupling with molecular rods. In literature it is described that this tetra-functionalized molecular knot could be used for the synthesis of the octa-functionalized knot: 1,3,5,7-tetrakis(1,3-dibromophenyl)-adamantane (Figure 3.9).



Figure 3.9: 1,3,5,7-Tetrakis(1,3-dibromophenyl)adamantane

This rigid adamantane derivative possesses eight aromatic bromine atoms, which can couple via palladium catalyzed reactions. It is therefore a suitable multifunctional rigid knot. 4'-(4-Ethynylphenyl)-2,2':6',2''-terpyridine (17) (See pg 42 Chapter Two), one of our previous synthesized molecular rods, was a potential rigid extender of 1,3,5,7-tetrakis(1,3-dibromophenyl)adamantane. This coupling would lead to the formation of the octa-functionalized molecular knot (Figure 3.10). This rigid knot could be used for the formation of three-dimensional networks via complexation reactions.

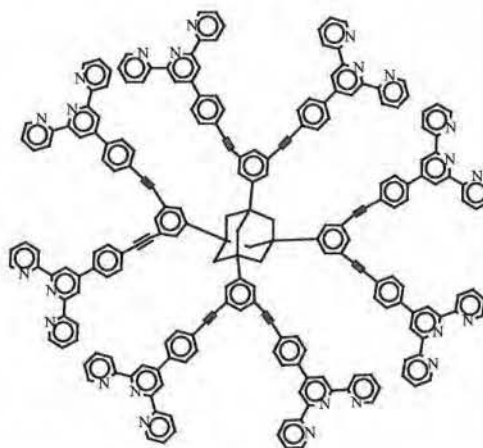


Figure 3.10: Octa-functionalized molecular knot

The second tetra-functionalized molecular knot we tried to synthesize was 1,3,5,7-tetrakis(4-iodophenyl)adamantane (Figure 3.11). The rigid extender of the adamantane core here is *p*-iodophenyl.

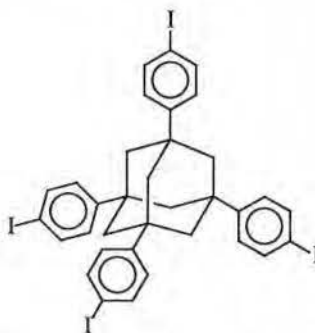


Figure 3.11: 1,3,5,7-Tetrakis(4-iodophenyl)adamantane

These aryl iodines possess good coupling properties because of their high reactivity in e.g. palladium catalyzed coupling reactions. Because of these good coupling properties 1,3,5,7-tetrakis(4-iodophenyl)adamantane can couple with the previous synthesized molecular rod 4'-(4-ethynylphenyl)-2,2':6',2''-terpyridine (**17**) (See pg 42 Chapter Two) to give 1,3,5,7-tetrakis[[4'-[4-{2-(phenyl)-1-ethynyl}phenyl]-2,2':6',2''-terpyridine]-adamantane (Figure 3.12)

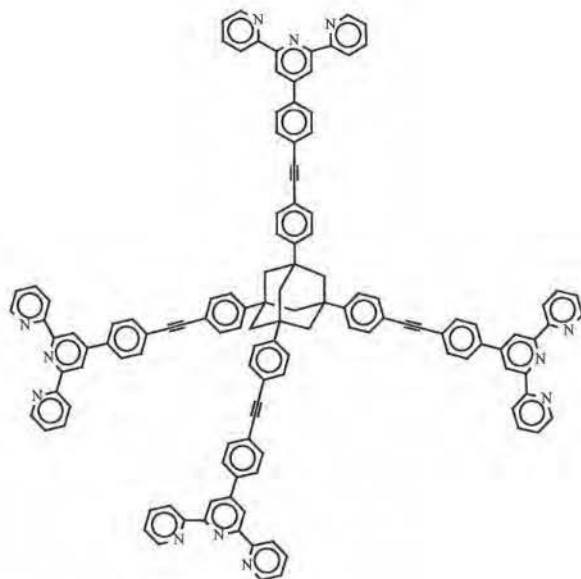


Figure 3.12: 1,3,5,7-Tetrakis[[4'-[4-{2-(phenyl)-1-ethynyl}phenyl]-2,2':6',2''-terpyridine]-adamantane

This tetra-functionalized knot could be used in complexation reactions for the formation of three-dimensional networks with various metals. These complexation reactions will be discussed later in chapter four.

Finally, we tried to synthesize 1,3,5,7-tetrakis(4-ethynyl)phenyl)-adamantane (Figure 3.13).

This rigid knot can couple with all kinds of aryl halides under palladium catalysis e.g. the rigid rod 4'-(4'''-bromophenyl)-2,2':6',2''-terpyridine (15) (See pg 40 Chapter Two) to give the same tetra-functionalized molecular knot 1,3,5,7-tetrakis[[4'-[4-{2-(phenyl)-1-ethynyl}phenyl]phenyl]-2,2':6',2''-terpyridine]-adamantane (Figure 3.12) as with the coupling of 1,3,5,7-tetrakis(4-iodophenyl)adamantane (Figure 3.11) and 4'-(4-ethynylphenyl)-2,2':6',2''-terpyridine (17) (See pg 42 Chapter Two).

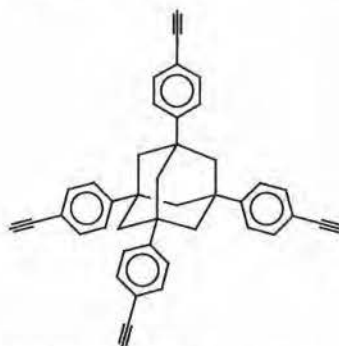


Figure 3.13: 1,3,5,7-Tetrakis(4-ethynyl)-phenyl)adamantane

If it is possible to synthesize 1,3,5,7-tetrakis(4-ethynyl)-phenyl)adamantane (Figure 3.13), another coupling method for the formation of the three dimensional networks can be considered. This tetra-functionalized molecular knot can couple with rigid bis-dienophyles e.g. 3,3'-(4,4'-biphenyl)-bis-(2.4.5-triphenyl-cyclopentadienon) (Figure 3.14) via Diels Alder reactions.

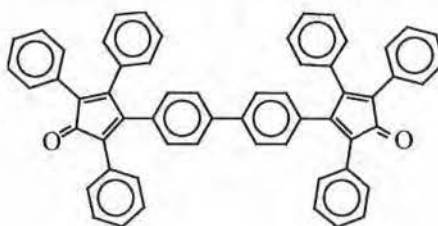


Figure 3.14: 3,3'-(4,4'-Biphenyl)-bis-(2.4.5-triphenyl-cyclopentadienon)

If this bis-dienophile can couple efficiently in high yield with 1,3,5,7-tetrakis(4-ethynyl)-phenyl)adamantane, rigid molecular networks can be formed.

3.2.4 Silsesquioxanes

Not only adamantane derivatives but also silsesquioxanes were simultaneously investigated for their potential use as highly functional rigid molecular knots. Silsesquioxanes, or T-resins are a class of compounds with the empirical formula $(\text{RSiO}_{1.5})_n$. They are synthesized by the hydrolytic condensation of tri-functional organosilicon monomers. Typical groups that may be hydrolyzed are alkoxy silanes²⁸, chlorosilanes^{29,30} and silanols³¹. These silsesquioxanes derive their name from the one and one half (1.5) or sesqui-stoichiometry of oxygen bound to silicon. While the alternate name “T-resin” is derived from the presence of three oxygen substituents on silicon (tri-substituted). Several structural representations of silsesquioxanes with the empirical formula $(\text{RSiO}_{1.5})_n$ are possible, with the two most common representations being a ladder-type structure (A) and a cubic structure (B) (Figure 3.15) containing eight silicon atoms placed at the vertices of the cube.

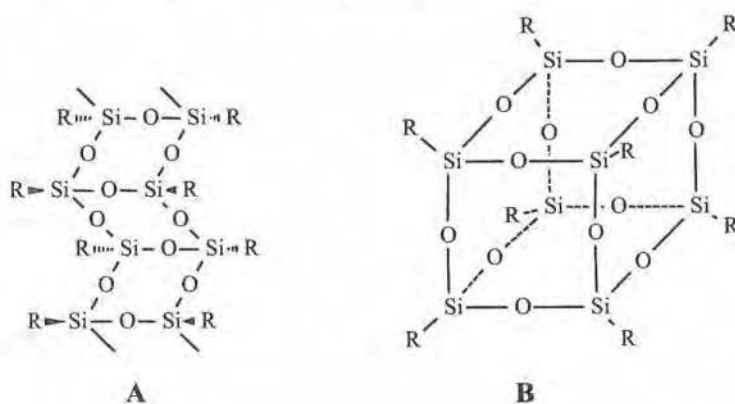


Figure 3.15: Representation silsesquioxane

This cubic structure is commonly called T_8 cube, and is usually drawn incorrectly with O-Si-O bond angles of 90° . The actual structure of a T_8 “cube” is more a Si-O framework as depicted in figure 3.16. However, the cubic structure B (Figure 3.15) is easier to visualize and will be used hereafter.

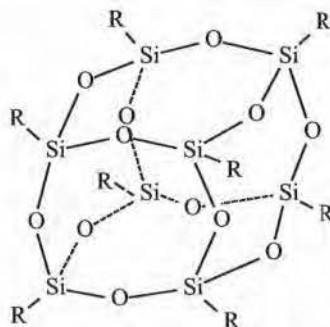


Figure 3.16: Actual structure T_8 “cube”

Substituents (R) on silicon can include hydrogen, alkyl, alkenyl, alkoxy and aryl. Due to organic substitution on silicon, many silsesquioxanes have reasonable solubility in common organic solvents.

Ladenburg first synthesized Silsesquioxanes in the late 1800s³². In the early 1900s, *Kipping* further studied the hydrolysis and condensation reactions of tri-functional silanes³³ and concluded that poly-condensation of “silicic acids” invariably leads to extremely complex mixtures of little synthetic value. Due to *Kipping*'s discovery, serious investigation into a controllable synthesis of silsesquioxanes was hindered for forty-five years until the work of *Brown and Vogt* in the 1960s³⁴⁻³⁶. *Brown and Vogt* synthesized octaphenylpentacyclo[9.5.1.1^{3,9}.1^{5,17}.1^{7,13}]octasiloxane (Figure 3.17) also called “phenyl- T_8 ”.

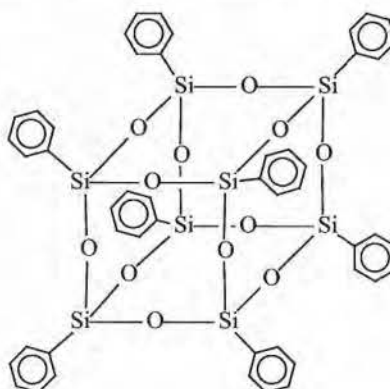


Figure 3.17: Octaphenylpentacyclo[9.5.1.1^{3,9}.1^{5,17}.1^{7,13}]octasiloxane

We repeated this synthesis because we wanted to functionalize this inorganic-organic hybrid in order to obtain 4-iodophenyl- T_8 (Figure 3.18).

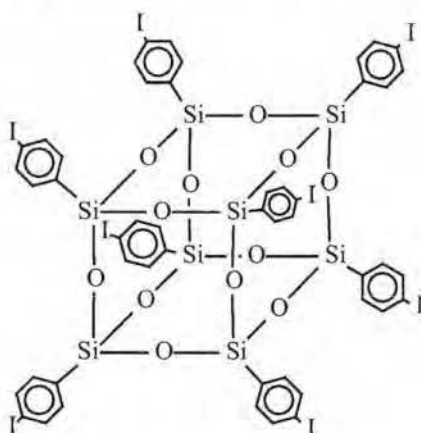


Figure 3.18: 4-Iodophenyl- T_8

4-Iodophenyl- T_8 would be a potential octa-functionalized molecular knot where the iodine atoms can couple with various organic substituents. The motivation to functionalize octaphenylpentacyclo-[9.5.1.1^{3,9}.1^{5,17}.1^{7,13}]-octasiloxane as a starting point was, that introduction of a halogen atom or a methyl substituent into the phenyl group of $C_6H_5SiCl_3$ would make the formation of the corresponding fully condensed phenylsilsesquioxanes much more difficult. This is mentioned in literature³⁷. Thus, e.g. octaphenylsilsesquioxanes with $X = Cl, Br$ and I , have not been described in literature³⁵ (Figure 3.19).

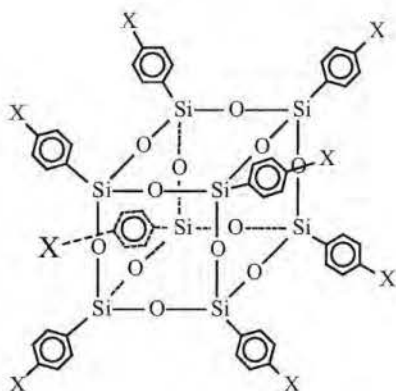


Figure 3.19: 4-X-phenyl- T_8

This rigid cubic $[\text{Si}_8\text{O}_{12}]$ core would offer us the possibility of generating porous, but still rigid materials due to geometric factors limiting the density with which corner-linked cubes can fill space. These compounds (Figure 3.19) can be considered as one of the products of complete hydrolytic condensation of the corresponding tri-functional monomers, XSiY_3 with $\text{Y} = \text{Hal}, \text{OH}, \text{OR}$. This hydrolytic poly-condensation strongly depend on the following factors:

- 1 Nature of solvent.
- 2 Concentration of the initial monomer in the solution.
- 3 Character of substituent X in the initial monomer.
- 4 Type of catalyst.
- 5 Addition of water.
- 6 Solubility of the polyhedral oligomers formed.
- 7 Nature of functional groups Y in the initial monomer.
- 8 Temperature.

These fully condensed octasilsesquioxanes with $\text{R} = \text{phenyl}$ and with a halogen atom at the 4-position, look very promising for the synthesis of a 3-dimensional network. This because of the eight fold functionalization and the symmetric position of the eight halogen atoms in space (Figure 3.20). This structure is from that point of view more favourable than diamantane and biadamantane. Until now little is published in the literature about these fully condensed octameric phenylsilsesquioxanes.

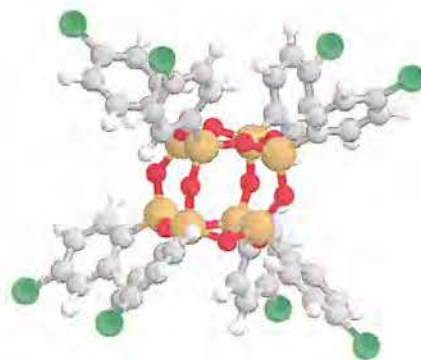


Figure 3.20: 3-D structure 4-chlorophenyl- T_8

A literature search (1967-1999) to find these octameric phenylsilsesquioxane and their analogues yielded only 16 hits in Beilstein and 22 hits in Chemical Abstracts. Most of these dealing with the synthesis of octaphenylsilsesquioxane.

If it would be possible to synthesize these *p*-halogenated octaphenylsilsesquioxanes, these fully condensed octa-functionalized molecular knots have to be stable under reaction conditions necessary for the formation of the networks. Therefore a few properties of the aryl-substituted phenylsilsesquioxanes have to be kept in mind.

3.2.4.1 Reactions of functionalized aryl-substituted silsesquioxanes

Except for reaction mixtures containing free fluoride, hydroxide and some strong basic reagents, $[\text{RSiO}_{3/2}]_n$ frameworks are stable in a wide range of reaction conditions and reagents, including acidic and strongly oxidizing environments. Most reasonable pendant group modifications can be performed without compromising the structural integrity of the frameworks. It is likely that any chemically reasonable pendant group modification can be accomplished, but three important characteristics of silsesquioxane frameworks can greatly complicate an otherwise "straightforward" organic transformation:

Silsesquioxane frameworks are strong electron-withdrawing substituents. In fact, the electron-withdrawing properties of Si_8O_{12} are comparable to a CF_3 group³⁸. Strong electron-withdrawing groups can make it very difficult to oxidize nearby functional groups or perform reactions that require cationic (or partially cationic) intermediates or transition states. The hydrolysis of $(\text{ICH}_2\text{C}_6\text{H}_4)_8\text{Si}_8\text{O}_{12}$, for example, is several orders of magnitude slower than hydrolysis of benzyl iodide and requires the use of a soluble silver salt, such as AgClO_4 , to obtain an acceptable reaction rate³⁸. (The corresponding chloride does not react with AgClO_4). In the light of the importance of choosing a synthetic methodology that proceeds cleanly and with very high conversion, the electron-withdrawing effects of a $[\text{SiO}_{3/2}]_n$ framework must be considered carefully when designing synthesis of new frameworks.

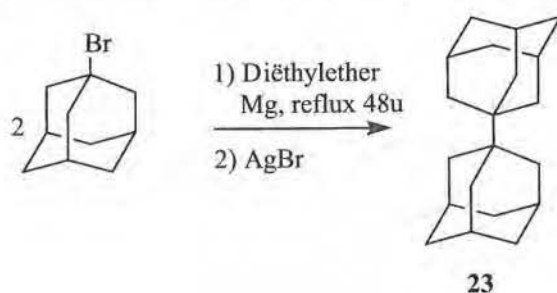
Silsesquioxane frameworks are susceptible to base-catalyzed redistribution and polymerization reactions. The reaction of a base or nucleophile with Si atoms of a fully condensed silsesquioxane framework is inefficient compared to reactions with pendant groups, but many reagents will initiate base-catalyzed redistribution or polymerization of frameworks upon prolonged reaction times and/or elevated reaction temperatures. Strong bases (e.g., NaOH) react rapidly with silsesquioxane frameworks, especially in polar aprotic solvents (e.g., DMF, DMSO). The reaction product in many cases is an ill-defined resin or “T-gel”, which sometimes (but not always) precipitates from solution. It is generally best to avoid the use of strong bases and to monitor the progress of reactions involving any reagent capable of generating a strong base via reaction with water (e.g., dialkylamides, alkoxides, NaH, alkyllithium and Grignard reactions). Weaker nucleophiles and bases - including tertiary amines, azide, cyanide, acetate, cyanate and conjugate bases of other weak acids- have also been observed to initiate base catalyzed redistribution or polymerization of the frameworks³⁹. Direct attack of these reagents on Si seems unlikely, hence most of these reagents probably destroy silsesquioxane frameworks by producing hydroxide from traces of water.

Highly symmetric, highly functionalized silsesquioxane frameworks can exhibit unexpected low solubility properties, and it is sometimes difficult to find an appropriate solvent for a chemical reaction. This can be a particularly difficult issue to solve when a reaction produces functional groups capable of forming strong intermolecular interactions. Oxidation reactions, which can produce strong hydrogen-bonded functional groups (e.g., COOH), and hydride reduction reactions, which often produce insoluble intermediates prior to aqueous work-up, are especially problematic because precipitation can occur at relatively low conversion. The poor solubility of many silsesquioxanes in non-polar solvents can also present problems.

3.3 SYNTHESIS OF MOLECULAR KNOTS

3.3.1 Synthesis of 1,1'-biadamantane and derivatives as six-functionalized molecular knots

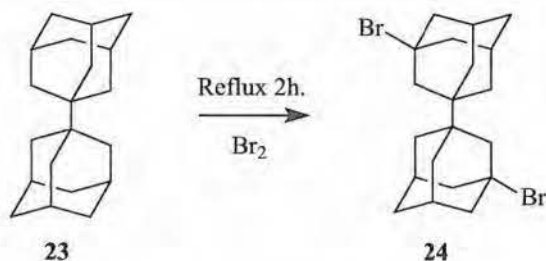
1,1'-Biadamantane (**23**) could be prepared via different literature procedures^{17,18,40-42}. In one of the methods we used commercially available 1-bromoadamantane was refluxed for two days in diethylether with magnesium (Scheme 3.3). Silver bromide was added and the mixture heated under reflux for a further 1 hour then water was added at a temperature of 0°C.



Scheme 3.3: Synthesis of 1,1'-biadamantane

After work up and recrystallization from benzene or methanol, 1,1'-biadamantane (**23**) was formed as white crystals with yields around 50%. The tertiary hydrogens can now be replaced by e.g. chlorine and bromine atoms via the same literature^{19,20a,21} procedures as described for the functionalization of adamantane^{20b-f} and so give rise to hexa-functionalized molecular knots.

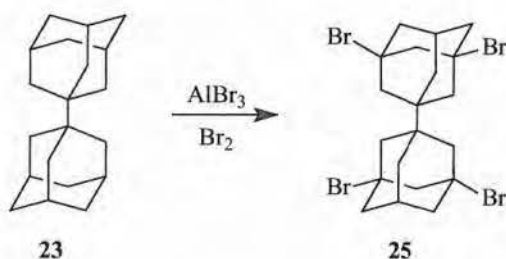
1,1'-Biadamantane could be di- tetra- or hexa-brominated depending on the reaction conditions used. Firstly, the bromination of 1,1'-biadamantane in the absence of added catalysts with elemental bromine gave 3,3'-dibromo-1,1'-biadamantane (**24**) (Scheme 3.4). No monobromo-biadamantane formation was observed.



Scheme 3.4: Synthesis of 3,3'-dibromo-1,1'-biadamantane

1,1'-Biadamantane (**23**) was charged into a flask fitted with a long reflux condenser and bromine was added with stirring. After 15 min hydrobromic acid evolution ceased and the mixture was then heated to reflux for 2 hours. Work up, precipitation with methanol and recrystallization from dioxane gave 3,3'-dibromo-1,1'-biadamantane (**24**) as white crystals. A yield of only 40% was obtained in contradiction with literature¹⁷ where a yield of 81% was reported.

Secondly, to obtain the tetra-functionalized knot, 1,1'-biadamantane (**23**) was treated with bromine containing a catalytic amount of aluminium bromide and stirred for 4 hours at room temperature. This gives 3,3',5,5'-tetrabromo-1,1'-biadamantane^{42b} (**25**) (Scheme 3.5).

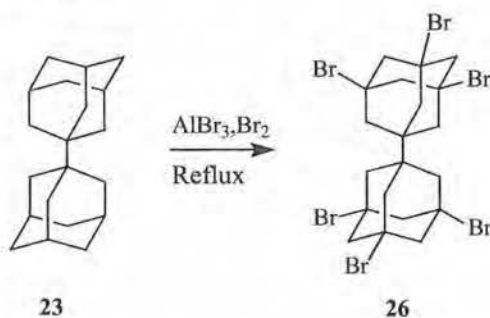


Scheme 3.5: Synthesis of 3,3',5,5'-tetrabromo-1,1'-biadamantane

The catalyst was destroyed by the addition of ice and the excess bromine present was destroyed by the addition, with stirring, of solid NaHSO₃. Recrystallization from a mixture of chloroform and acetone gave 3,3',5,5'-tetrabromo-1,1'-biadamantane (**25**) as an off-white solid with 80% yield.

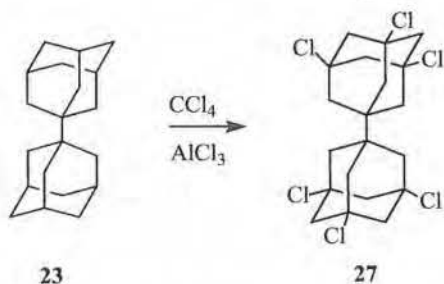
Consistent with the presence of a center of symmetry, its ^{13}C -NMR consisted of only seven resonances.

Finally, to obtain the hexa-functionalized molecular knot, we treated 1,1'-biadamantane (**23**) with bromine, aluminium bromide as catalyst and refluxed 6 hours this gave 3,3',5,5',7,7'-hexabromo-1,1'-biadamantane with 30% yield (**26**) (Scheme 3.6). The structure was assigned on the bases of its ^1H -NMR and mass spectrum.



Scheme 3.6: Synthesis of 3,3',5,5',7,7'-hexabromo-1,1'-biadamantane

But ^1H -NMR also showed evidence of the presence of 3,3',5,5'-tetrabromo-1,1'-biadamantane (**25**) in the reaction mixture. Recrystallization in different organic solvents, in order to separate the hexa- and tetrabromobiadamantane, failed. As purity of the knot is of utmost importance to be used as building block, we turned to the synthesis of 3,3',5,5',7,7'-hexachloro-1,1'-biadamantane (**27**) (Scheme 3.7).



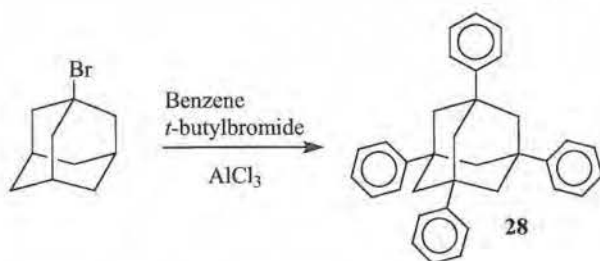
Scheme 3.7: Synthesis of 3,3',5,5',7,7'-hexachloro-1,1'-biadamantane

To a solution of 1,1'-biadamantane (**23**) in carbon tetrachloride, AlCl_3 was added. The reaction mixture was heated under reflux for three days, then cooled, and quenched with water. The liquid was decanted and the tarry residue was washed with dichloromethane. The combined organic extracts were washed successively with saturated sodium hydrogen carbonate, water and saturated sodium chloride and dried with MgSO_4 to give 3,3',5,5',7,7'-hexachloro-1,1'-biadamantane as an off-white solid with 57% yield. The EI mass spectra showed the correct ion peak at a mass of MS (EI, m/e) = 476 (M^+). But the same purification problems occur as for the hexabrominated biadamantane.

For this reason, and because of the easier accessibility of adamantane derivatives, attention was focused on the functionalization of commercially available adamantane and 1-bromoadamantane.

3.3.2. Synthesis of adamantane derivatives as four-functionalized molecular knots

Commercial available adamantane and 1-bromoadamantane could be used as starting materials for the synthesis of four-functional molecular knots. 1-bromoadamantane was used for the synthesis of 1,3,5,7-tetraphenyladamantane (**28**). This adamantane unit could be functionalized in the next step to give a tetra-functionalized molecular knot. Literature²² suggests that this 1,3,5,7-tetraphenyladamantane (**28**) could easily be prepared in multigram quantities (Scheme 3.8). The reaction involved the Friedel-Crafts reaction of the commercially available 1-bromoadamantane with benzene in the presence of *tert*-butylbromide. Relatively few reaction systems have been used for the introduction of functional groups at a tertiary carbon atom of saturated hydrocarbons. The abstraction of hydride ions and the formation of a reaction centre in these systems are usually initiated by hydrocarbon cations particularly by the most widely known *tert*-butyl cation⁴³. The reaction is performed in the presence of a high excess of the functionalization reagent. For the synthesis of 1,3,5,7-tetraphenyladamantane (**28**) the functionalization reagent benzene, is provided in very high excess, because it is used at the same time as a solvent.

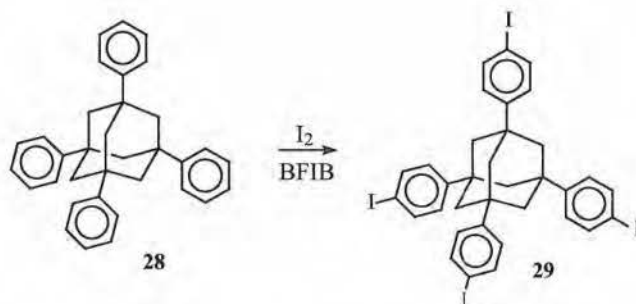


Scheme 3.8: Synthesis of 1,3,5,7-tetraphenyladamantane

To an ice cooled flask 1-bromo-10-adamantane, benzene and *tert*-butylbromide were added. AlCl_3 was added in portions to the chilled, stirred solution. The solution was allowed to warm to room temperature and refluxed for 2 hours. The heterogeneous reaction mixture was cooled to room temperature and poured into acidic ice. Benzene was added and the slurry stirred for 1 hour. The solution was filtered to remove the 1,3,5,7-tetraphenyladamantane and the residue washed with acetone. The solid was Soxhlet extracted overnight with chloroform and gave 1,3,5,7-tetraphenyladamantane with 66% yield.

1-Phenyladamantane, 1,3-diphenyladamantane and 1,3,5-triphenyladamantane were also formed during the reaction. Of all four products only the target compound, 1,3,5,7-tetraphenyladamantane (**28**), is insoluble in most organic solvents. This simplifies purification but limits further functionalization.

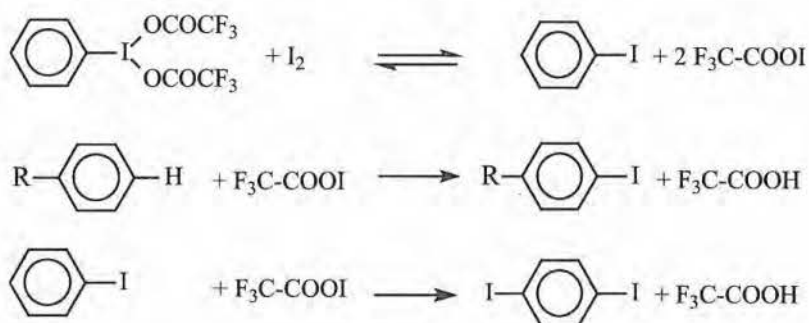
In 1,3,5,7-tetraphenyladamantane (**28**), the phenyl group act as rigid extender of adamantane's tetrahedral symmetry, reducing steric and electronic problems encountered when trying to react groups directly attached to the adamantane nucleus. This organic insoluble 1,3,5,7-tetraphenyladamantane (**28**) can now be used for the synthesis of 1,3,5,7-tetrakis(4-iodophenyl)adamantane (**29**) (Scheme 3.9) as described in literature^{22,23}. It is an ideal core for coupling reactions with, for example, boronic acids and acetylenes, due to the high reactivity of the iodine group for different coupling reactions in the presence of Pd catalysts.



Scheme 3.9: Synthesis of 1,3,5,7-tetrakis(4-iodophenyl)adamantane

1,3,5,7-Tetrakis(4-iodophenyl)adamantane (**29**) was formed with a yield of 58% in the two-phase reaction of 1,3,5,7-tetraphenyladamantane (**28**) with bis[trifluoroacetoxy]iodobenzene (BFIB) and iodine in CCl₄ or chloroform.

The mechanism of the reaction can be rationalized in terms of electrophilic aromatic substitution under the action of trifluoroacetylhypoiodide, resulting from the interaction of BFIB and iodine (Scheme 3.10).

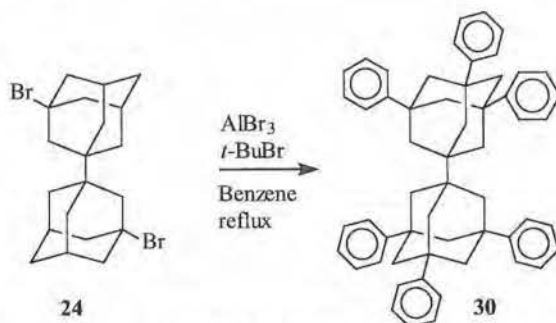


Scheme 3.10: Reaction course iodination.

Literature²² shows that to increase the yield, the reactants were ground together before the solvent was added. 1,3,5,7-Tetrakis(4-iodophenyl)adamantane (**29**) is soluble in the solvent used and was easily isolated from the insoluble starting material. The side product, 1,4-diiodo-benzene, was removed by recrystallization in a mixture of chloroform and methanol, this gave a white

crystalline product. The pure, all-para-substituted compound has been prepared in multigram quantities in this simple two-step route, starting from the commercially available 1-bromoadamantane. This opens a number of synthetic pathways to chain-extended tetrahedral compounds using a variety of aryl halide coupling reactions.

As we wanted to synthesize also more highly functionalized molecular knots, the kind of chemistry used for the synthesis of 1,3,5,7-tetraphenyladamantane (**28**) and 1,3,5,7-tetrakis(4-iodophenyl)adamantane (**29**) can be used for the synthesis of 3,3',5,5',7,7'-hexaphenyl-1,1'-biadamantane (**30**) (Scheme 3.11) and its iodinated derivative as well. Therefore 3,3'-dibromo-1,1'-biadamantane (**24**) was prepared because it is the molecule which shows most similarity to 1-bromoadamantane.



Scheme 3.11: Synthesis of 3,3',5,5',7,7'-hexaphenyl-1,1'-biadamantane

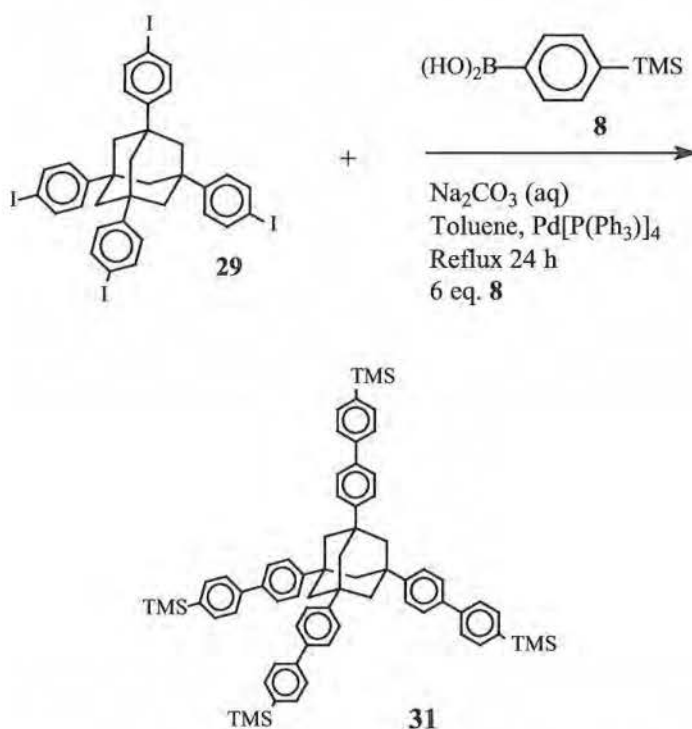
3,3'-Dibromo-1,1'-biadamantane (**24**), t -butylbromide and AlCl_3 were dissolved in benzene and refluxed for 24 hours. After work up, the reaction product was again treated with t -butylbromide and AlCl_3 in benzene and refluxed for another 12 hours. Recrystallization from o -dichlorobenzene gave 3,3',5,5',7,7'-hexaphenyl-1,1'-biadamantane (**30**) as a white powder with 21% yield.

In principle this 3,3',5,5',7,7'-hexaphenyl-1,1'-biadamantane (**30**) can be iodinated via the same procedures as we have used for the synthesis of 1,3,5,7-tetrakis(4-iodophenyl)adamantane (**29**) (Scheme 3.9). In view of the straightforward functionalization of 1,3,5,7-tetraphenyladamantane (**28**) no insurmountable problems are expected for the iodination of 3,3',5,5',7,7'-hexaphenyl-1,1'-biadamantane (**30**), in due time we will continue this reaction.

3.3.2.1 Derivatization reactions of 1,3,5,7-tetrakis(4-iodophenyl)adamantane

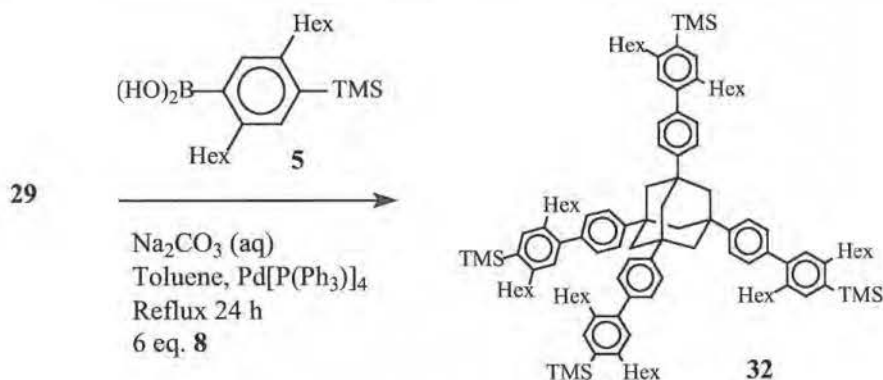
To investigate the derivatization properties of 1,3,5,7-tetrakis(4-iodophenyl)adamantane (**29**), it was first coupled with different arylboronic acids then with two different acetylene derivatives.

For the arylboronic acids, 4-trimethylsilylbenzene-1-boronic acid (**8**) and 2,5-di-*n*-hexyl-4-trimethylsilylbenzene-1-boronic acid (**5**) were used because they were already available since they were used for the synthesis of the molecular rods. For the first coupling reaction, 1,3,5,7-tetrakis(4-iodophenyl)adamantane (**29**) and an excess of 4-trimethylsilylbenzene-1-boronic acid (**8**) were dissolved in toluene and the solution degassed with N₂. 1M aq Na₂CO₃ solution was added and the solution was degassed again (Scheme 3.12). Pd was added and the mixture refluxed for 24 h.



Scheme 3.12: Synthesis of 1,3,5,7-tetrakis(4''-trimethylsilyl-1,4'-biphenyl)adamantane

After work up, the product was purified by chromatographic separation, first with hexane as eluents, later changing to a mixture of hexane/chloroform (4/1) and finally recrystallized in toluene to give 1,3,5,7-tetrakis(4''-trimethylsilyl-1,4'-biphenyl)adamantane (**31**) as white crystals with 74% yield. 1,3,5,7-Tetrakis(4''-trimethylsilyl-2'',5''-di-*n*-hexyl-1,4'-biphenyl)-adamantane (**32**) (Scheme 3.13) was prepared via similar procedures in which Ba(OH)₂ was used instead of Na₂CO₃. In contradiction with 1,3,5,7-tetrakis(4''-trimethylsilyl-1,4'-biphenyl)adamantane (**31**), 1,3,5,7-tetrakis(4''-trimethylsilyl-2'',5''-di-*n*-hexyl-1,4'-biphenyl)-adamantane (**32**) could not be recrystallized. The yield was approximately 20% lower, possibly due to the steric hindrance of the hexyl side chains.

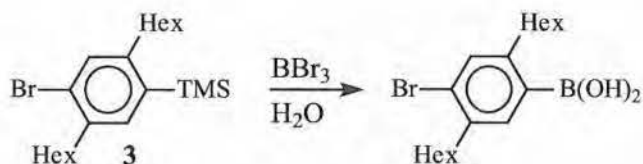


Scheme 3.13: Synthesis of 1,3,5,7-tetrakis(4''-trimethylsilyl-2'',5''-di-*n*-hexyl-1,4'-biphenyl)-adamantane

Both (**31**) and (**32**) were synthesized to investigate the effect of their structure on their solubility. This solubility often causes problems when molecules with higher molar masses are prepared, but both of these reaction products these (**31**) and (**32**) were very soluble in most common organic solvents.

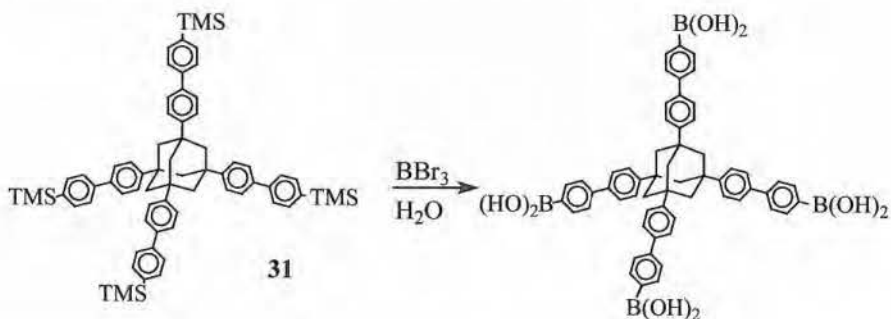
These reactions were not only executed to investigate the coupling properties of the aryliodide present on (**29**). The reaction product e.g. 1,3,5,7-tetrakis(4''-trimethylsilyl-1,4'-biphenyl)adamantane (**31**) can also be used for the synthesis of another tetra-functionalized molecular knot.

It is known that an aryltrimethylsilane can be transformed in one step into an arylboronic acid by treatment with BBr_3 ⁴⁴ followed by hydrolysis. *Schluter et al* describes the synthesis⁴⁵ of 2,5-di-*n*-hexyl-4-bromobenzene-1-boronic acid (Scheme 3.14). This compound was obtained (in high yield) by desilylation of 1-bromo-2,5-di-*n*-hexyl-4-trimethylsilylbenzene (**3**) using boron tribromide.



Scheme 3.14: Synthesis of 2,5-di-*n*-hexyl-4-bromobenzene-1-boronic acid

We tried a similar and slightly modified reaction procedure for the synthesis of the tetra-boronic acid out of 1,3,5,7-tetrakis(4''-trimethylsilyl-1,4'-biphenyl)adamantane (**31**) (Scheme 3.15). This tetra-boronic acid would be ideal for the coupling of aryl bromides, iodines and triflates via palladium-catalyzed reactions.



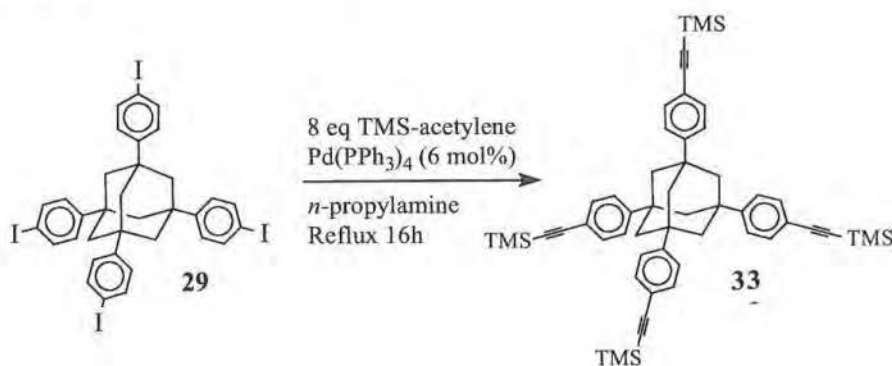
Scheme 3.15: Conversion TMS into boronic acid

Organoboronic acids probably offer the most versatile functionality in organometallic coupling reactions due to their easy work-up, low toxicity and environmental impact, compatibility with electrophilic substituents, air stability and the limited number of side reactions under the coupling conditions.

The palladium-catalyzed cross-coupling reaction of arylboronic acids with aryl halides or triflates to give biaryls can be achieved in high yields and is compatible with various functional groups on either coupling partner. The relative reactivity of the leaving group typically being: $I > OTf > Br > Cl$.

All attempts to synthesize this tetra-substituted boronic acid failed up to now. The reasons must be sought in the occurrence of deboronation reactions and because boronic acids tend to form cyclic anhydrides (boroxines). Depending upon solvent polarity and water content, they exist as mixtures of the monomeric and trimeric forms. The reaction mixture was a clear solution and once water was added a white product precipitated out of the solution. The $^1\text{H-NMR}$ of this slightly soluble product still showed TMS peaks present, this indicates that not all TMS functions are replaced. For this reason this reaction procedure was not suitable to create a pure tetra-substituted boronic acid.

The second derivatization of 1,3,5,7-tetrakis(4-iodophenyl)adamantane (**29**) was investigated by coupling it with commercially available trimethylsilylacetylene.

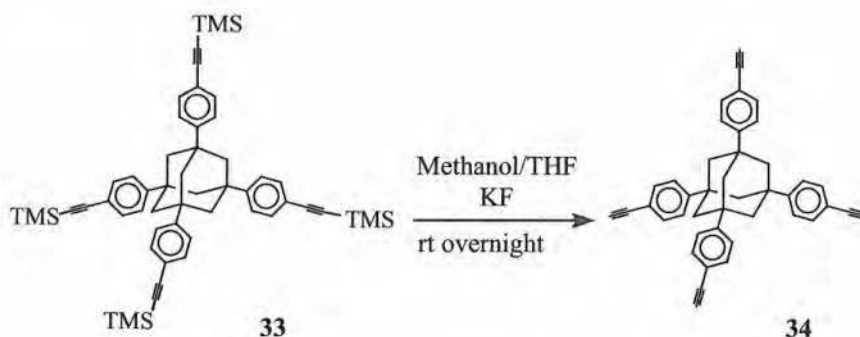


Scheme 3.16: Synthesis of 1,3,5,7-tetrakis(4-{2-trimethylsilyl}-1-ethynyl}phenyl)adamantane

To a stirred solution of 1,3,5,7-tetrakis(4-iodophenyl)adamantane and eight equivalents of trimethylsilylacetylene in *n*-propylamine, a solution of $\text{Pd}[\text{P}(\text{Ph})_3]_4$ in *n*-propylamine was added. This mixture was refluxed overnight and the solvent evaporated.

Purification via chromatographic separation through silica gel with hexane/ CHCl_3 (3/1) as eluents and recrystallization in a mixture of chloroform and hexane gave 1,3,5,7-tetrakis(4-{2-trimethylsilyl}-1-ethynyl}-phenyl)adamantane (**33**) as white crystals with 87% yield. The trimethylsilyl groups act as protection groups for the acetylene and can easily be removed by a number of bases.

Deprotection of 1,3,5,7-tetrakis(4-{2-trimethylsilyl}-1-ethynyl)-phenyladamantane (**33**) was performed in a mixture of methanol and tetrahydrofuran with KF as base (Scheme 3.17). The reaction mixture was stirred (at room temperature) overnight. The crude product was dissolved in chloroform to precipitate the K-salts and recrystallized in a mixture of chloroform and hexane. 1,3,5,7-tetrakis(4-ethynyl)-phenyladamantane (**34**) was obtained as white powder with 92% yield.

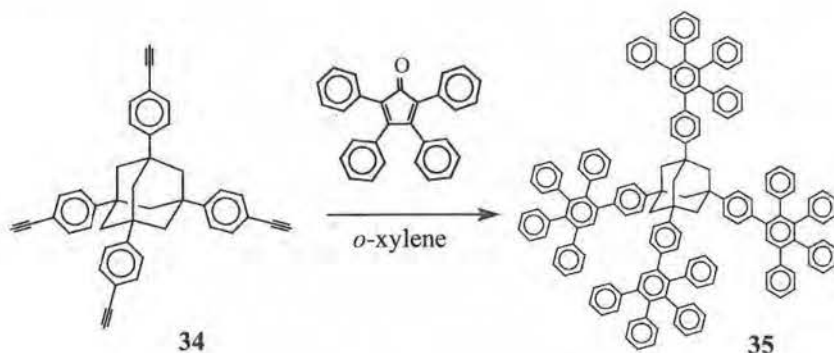


Scheme 3.17: Synthesis of 1,3,5,7-tetrakis(4-ethynyl)-phenyladamantane

1,3,5,7-Tetrakis(4-ethynyl)-phenyladamantane (**34**) can be used for Diels Alder reactions with different kinds of dienophiles for the formation of (for example) fluorescent materials. We tried one reaction with tetraphenylpentacyclodienone for the synthesis of compound (**35**). This was to investigate whether 1,3,5,7-tetrakis(4-ethynyl)-phenyladamantane (**34**) would be a potential molecular knot for the synthesis of three-dimensional networks via Diels Alder reactions.

1,3,5,7-Tetrakis(4-ethynyl)-phenyladamantane (**34**) and an excess of tetraphenylpentacyclodienone were refluxed in *o*-xylene (Scheme 3.18).

The reaction product was purified by precipitation in ethanol, this to remove the tetraphenylcyclopentadienone, and recrystallized in a mixture of chloroform and ethanol. Yields of more than 90% could be achieved. This indicates the efficient coupling properties of this system via Diels Alder reactions.



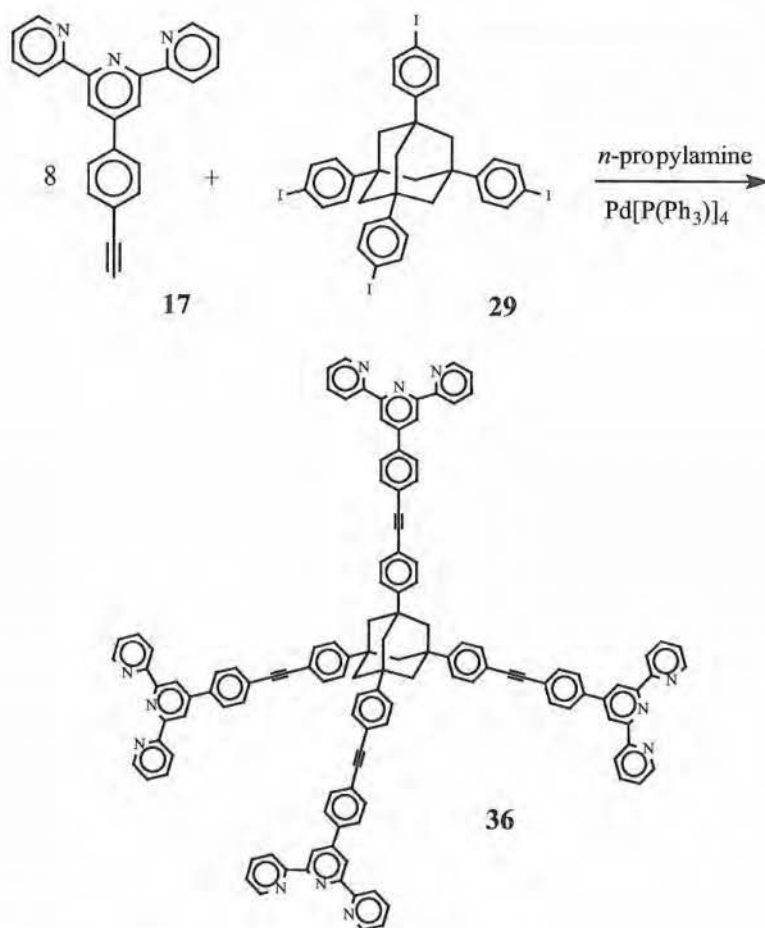
Scheme 3.18: Investigation of coupling properties via Diels Alder reaction.

The excess of the cyclopentadienone could be removed very easily by precipitating the product in ethanol. The synthesis is based on [2+4] Diels-Alder cycloaddition of tetraphenylcyclopentadienone to the ethynyl compound (**34**), followed by the elimination of carbon monoxide. This reaction concept originally presented by *Dilthey et al*^{46,47}, and studied in detail by *Ogliaruso*⁴⁸⁻⁵⁰ and *Ried*⁵¹⁻⁵⁴, involves the addition of tetraphenylcyclopentadienone to a phenylacetylene unit to obtain a pentaphenylbenzene unit. The advantages of this cycloaddition are that it is practically free of side reactions and that the equilibrium is shifted toward the product due to the irreversible loss of CO and the formation of a benzene ring. A retro-Diels-Alder reaction, therefore, cannot occur.

1,3,5,7-Tetrakis(4-ethynyl)-phenyladamantane (**34**) can also be used for coupling reactions with different kinds of aryl halogenides. A coupling reaction with 4'-(4'''-bromophenyl)-2,2':6',2''-terpyridine (**15**) and 1,3,5,7-tetrakis(4-ethynyl)-phenyladamantane (**34**) would give the same molecular knot (**36**) (Scheme 3.19) as with the coupling of 1,3,5,7-tetrakis(4-iodophenyl)-adamantane (**29**) and 4'-(4-ethynylphenyl)-2,2':6',2''-terpyridine (**17**).

This will be explained in the next paragraph. A possible way to create networks with 1,3,5,7-tetrakis(4-ethynyl)-phenyladamantane (**34**) is to couple it with e.g. 1,4-dibromobenzene.

Finally the last derivatization of 1,3,5,7-tetrakis(4-iodophenyl)-adamantane (**29**) with 4'--(4-ethynylphenyl)-2,2':6',2''-terpyridine (**17**) gave 1,3,5,7-tetrakis[[4'-[4-{2-(phenyl)-1-ethynyl}phenyl]-2,2':6',2''-terpyridine]-adamantane (**36**), (Scheme 3.19) a tetra-functionalized molecular rod.



Scheme 3.19: Synthesis of 1,3,5,7-tetrakis[[4'-[4-{2-(phenyl)-1-ethynyl}phenyl]-2,2':6',2''-terpyridine]adamantane

1,3,5,7-Tetrakis(4-iodophenyl)-adamantane (**29**) and 4'-(4-ethynyl-phenyl)-2,2':6',2''-terpyridine (**17**) were refluxed overnight under palladium catalysis during which a yellow precipitate was formed. The precipitate was separated by filtration and purified by chromatographic separation with chloroform as eluents, and finally recrystallized twice in chloroform to give 1,3,5,7-tetrakis[[4'-[4-{2-(phenyl)-1-ethynyl}phenyl]-2,2':6',2''-terpyridine]-adamantane (**36**) as a pure white powder with 60% yield. MALDITOF as well as electron spray experiments showed the correct ion peak at 1766 m/z. The melting point was 361°C as indicated by DSC experiments (Figure 3.21).

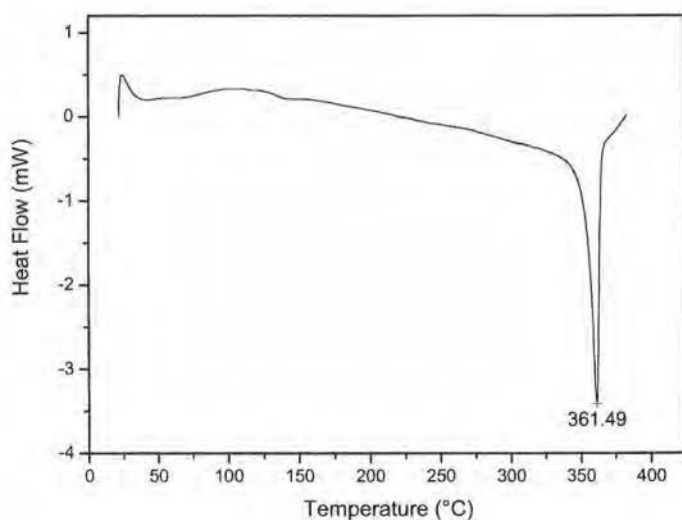


Figure 3.21: DSC of 1,3,5,7-tetrakis[[4'-[4-{2-(phenyl)-1-ethynyl}phenyl]-2,2':6',2''-terpyridine]adamantane (**36**)

This knot is a highly stable solid, TGA under oxygen showed degradation at 521°C (Figure 3.22).

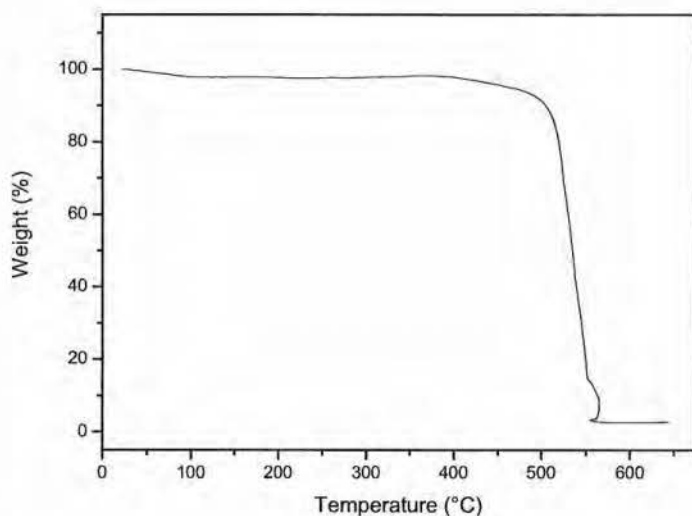


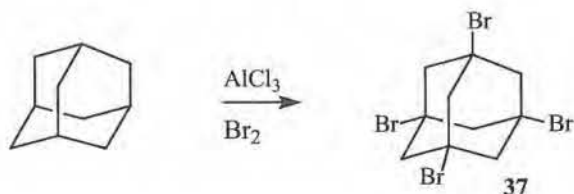
Figure 3.22: TGA of 1,3,5,7-tetrakis[[4'-[4-{2-(phenyl)-1-ethynyl}phenyl]-2,2':6',2''-terpyridine]adamantane (**36**)

This molecular knot (**36**) can couple with our bisterpyridines via metal complexation reactions, this will be explained later in chapter four. Because (**36**) has only a functionality of four, and knots with a higher functionality are thought to be necessary to create very strong networks, synthesis was started of 1,3,5,7-tetrakis(1,3-dibromophenyl)adamantane (**38**) (See Scheme 3.21), which comprises a molecular knot with an eight-functionality.

3.3.2.2 Synthesis of 1,3,5,7-tetrakis(1,3-dibromophenyl)adamantane

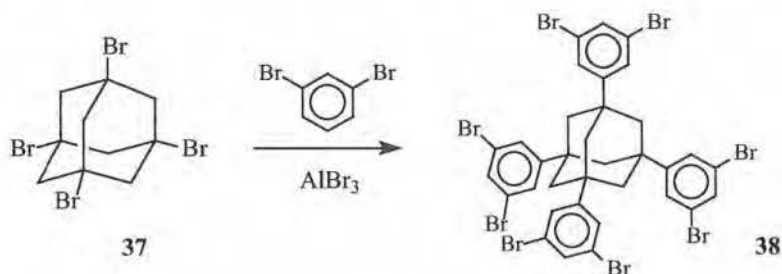
1,3,5,7-Tetrabromoadamantane (**37**) was prepared via several literature procedures^{19,20} of which the method of *Menger and Migulin*^{20a} was the most convenient one. Adamantane was added in small portions to a stirred mixture of bromine and anhydrous AlCl_3 at 0°C (Scheme 3.20). The mixture was heated till 70°C and refluxed at that temperature for 24 hours. Hydrogen bromide evolved vigorously during the addition and heating. The reaction mixture was treated subsequently with aqueous sodium sulfite, to remove the excess bromine, and hydrochloric acid to dissolve the aluminium salts.

The resulting solid was filtered and recrystallized in acetonitrile to give 1,3,5,7-tetrabromoadamantane (**37**) as light brown crystals with 48% yield.



Scheme 3.20: Synthesis of 1,3,5,7-tetrabromoadamantane

This 1,3,5,7-tetrabromoadamantane (**37**) is a tetra-functionalized molecular knot, which can be transformed into an octa-functionalized molecular knot (Scheme 3.21). 1,3,5,7-Tetrabromoadamantane (**37**), 1,3-dibromobenzene and AlBr_3 were stirred in a chilled flask (0°C) for 4 hours, allowed to warm to room temperature (stirred overnight) and finally heated at



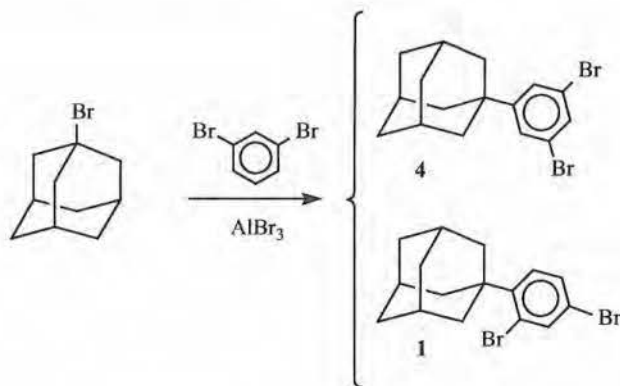
60°C for 5 hours.

Scheme 3.21: Synthesis of 1,3,5,7-tetrakis(1,3-dibromophenyl)adamantane

The reaction mixture was poured onto acidic ice. After the ice was molten the layers were separated and the organic layer was washed with water and a saturated NaCl solution. The product was isolated by precipitation into methanol. Then it was purified by chromatographic separation, first in a chloroform/hexane mixture (1/15), secondly in a chloroform/hexane mixture (1/1) and finally by recrystallization from chloroform to give 1,3,5,7-tetrakis(1,3-dibromophenyl)-adamantane (**38**) with 32% yield.

A lack of regioselectivity for this reaction (isolated mixtures of meta/para isomers) was observed in literature²². 1,3,5,7-Tetrakis(1,3-dibromophenyl)-adamantane (**38**) was isolated in good yields, but the slightly-chloroform-soluble product showed evidence of “ortho” as well as “meta” isomer formation by ¹³C-NMR. If we compare our results with literature, where 13 different carbon atoms were found at 41.4, 46.6, 123.6, 125.4, 126.8, 127.3, 128.3, 130.2, 130.6, 131.7, 132.4, 133.7 and 150.8 ppm, we only found six different carbon atoms with $\delta = 39.3, 46.0, 123.3, 127.0, 132.3,$ and 151.5 ppm. Also ¹H-NMR gave other results in literature, $\delta = 2.04$ (br, s, 12H) and 7.45 (br, apparent t, 12 H) in contradiction with our results were $\delta = 2.01$ (s, 12H); 7.49 (t, 8H) and 7.56 (m, 4H).

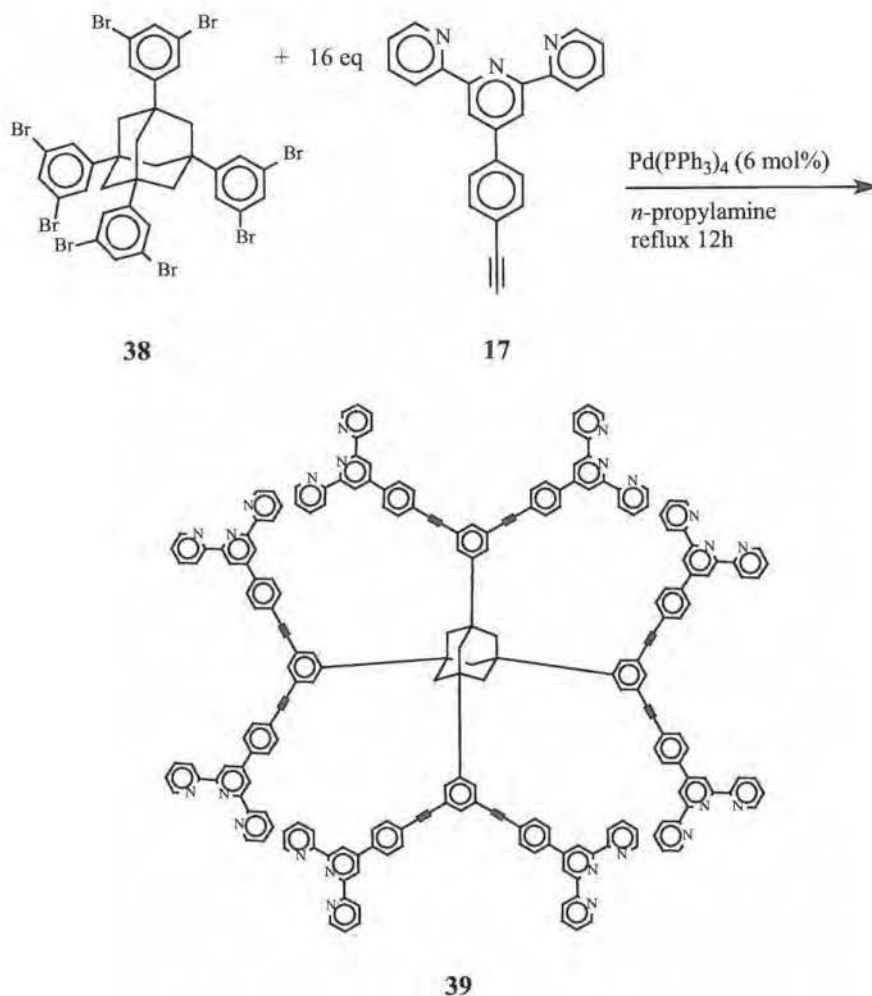
In literature²² a model reaction of 1-bromoadamantane with 1,3-dibromobenzene gave a 1:4 ratio of ortho to meta isomers of 1,3-dibromo-4/5-(1-adamantyl)benzene (Scheme 3.22) consistent with the formation of isomer mixtures in the tetrasubstituted case.



Scheme 3.22: Model reaction

Presumably the column chromatographic separation or the recrystallization separated both isomers to give 1,3,5,7-tetrakis(1,3-dibromophenyl)adamantane (**38**) as a pure white solid. This 1,3,5,7-tetrakis(1,3-dibromophenyl)adamantane (**38**) is a suitable octa-functionalized molecular knot for coupling with e.g. diboronic acids in order to create three dimensional networks.

Out of this knot another octa-functionalized molecular knot was synthesized (Scheme 3.23).



Scheme 3.23: Synthesis of 1,3,5,7-tetrakis[1,3-di-(4'-phenyl-1-ethynyl)-2,2':6',2''-terpyridine]phenyl]adamantane

1,3,5,7-Tetrakis(1,3-dibromophenyl)adamantane (**38**) and 4-(4-ethynylphenyl)-2,2':6',2''-terpyridine (**17**) were refluxed in *n*-propylamine under palladium catalysis. The mixture was stirred overnight during which a yellow precipitate was formed.

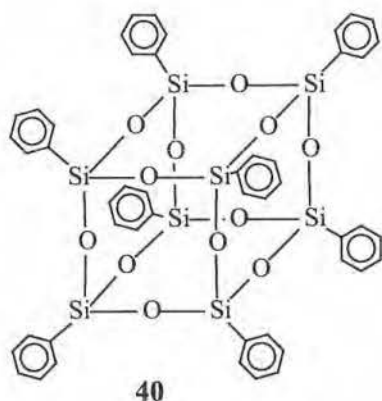
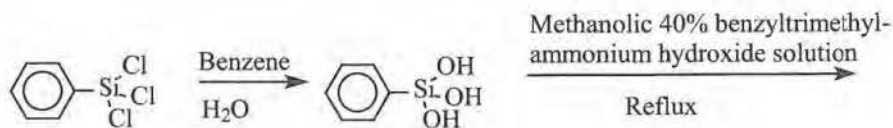
The solid was filtered off and chromatographic separation on silicagel gave 1,3,5,7-tetrakis[1,3-di-(4'-phenyl-1-ethynyl-2,2':6',2''-terpyridine)-phenyl]adamantane (**39**) as a slightly soluble yellow solid with a yield of 50%. Mass spectral analysis showed that not only the octa-functionalized but also hexa- and hepta-functionalized species were present in the reaction mixture. Separation of these very similar molecules was not possible.

3.3.3 Synthesis Of Silsesquioxanes

Knots with an adamantane core as well as silsesquioxanes were investigated as rigid molecular knots. Octaphenylpentacyclo[9.5.1.1^{3,9}.1^{5,17}.1^{7,13}]octasiloxane (**40**) (phenyl-T₈) is the most heat-resistant oligosilsesquioxane known. It does not change when heated in the air to its melting point (500°C)³⁷. This organic-inorganic hybrid is a potential highly functionalized molecular knot if it is possible to functionalize the phenyl rings present on the silicon-oxygen cage.

3.3.3.1 Synthesis of octaphenylpentacyclo[9.5.1.1^{3,9}.1^{5,17}.1^{7,13}]octasiloxane

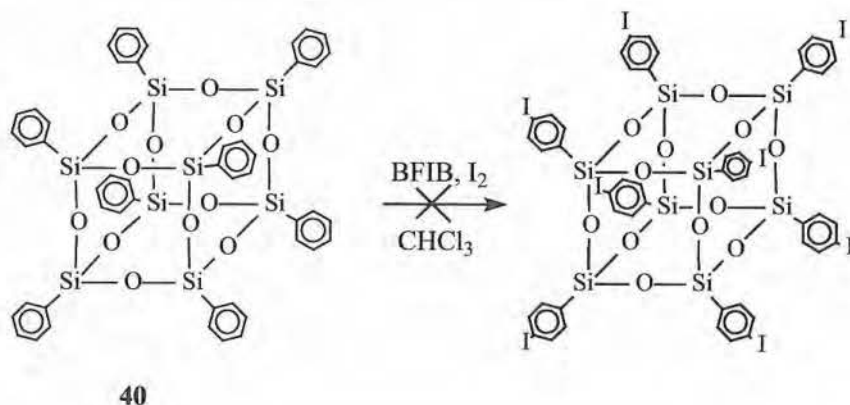
Octaphenylpentacyclo[9.5.1.1^{3,9}.1^{5,17}.1^{7,13}]octasiloxane (**40**) (phenyl-T₈) was prepared following literature procedures³⁶. Commercially available phenyltrichlorosilane was dissolved in benzene and shaken with water until hydrolysis was complete (Scheme 3.24). After removing the acid layer and washing with water, commercially available 40% benzyltrimethylammonium hydroxide solution was added.



Scheme 3.24: Synthesis of octaphenylpentacyclo[9.5.1.1^{3,9}.1^{5,17}.1^{7,13}]-octasiloxane

The mixture was refluxed for 4 hours, allowed to stand for 4 days, refluxed another 48 hours, and then cooled and filtered to give phenyl-T₈. Purification could be effected by sublimation under vacuum or recrystallization from hot o-chlorobenzene and gave octaphenylpentacyclo[9.5.1.1^{3,9}.1^{5,17}.1^{7,13}]-octasiloxane (**40**) with 57% yield. In literature³⁶ yields up to 88% and even 98% (on longer refluxing) are reported.

Via the same literature procedures as used for the functionalization of 1,3,5,7-tetraphenyladamantane, octa-functionalization of octaphenylpentacyclo[9.5.1.1^{3,9}.1^{5,17}.1^{7,13}]octasiloxane (**40**) was tried (Scheme 3.25).



Scheme 3.25: Synthesis of octa(*p*-iodophenyl)pentacyclo[9.5.1.1^{3,9}.1^{5,15}.1^{7,13}]-octasiloxane

Octaphenylpentacyclo[9.5.1.1^{3,9}.1^{5,17}.1^{7,13}]octasiloxane (**40**), iodine, and [bis-(trifluoroacetoxy)iodo]benzene were stirred under nitrogen at room temperature overnight. After work up and chromatographic purification, mass spectral analysis showed that the octa-iodinated cage was formed but ¹H-NMR as well as HPLC measurements showed always a mixture of many inseparable products. These HPLC measurements were recorded for different eluents combinations with a diode array detector (190-367 nm). Furthermore the HPLC analysis was evaluated for two column systems (Ultrapack UL 215 and Chrompack inertsil 5Si). Because the reaction product was always a mixture of inseparable products and the yield decreases dramatically with the number of iodine substituents present, no further functionalization reactions on phenyl-T₈ were executed. A possible solution for this issue was to start the condensation reaction, (for the formation of a fully condensed octa-functionalized phenylsilsesquioxane) with a *p*-halogenated phenyltrichlorosilane (Figure 3.23).

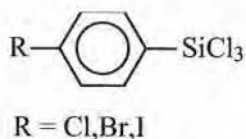
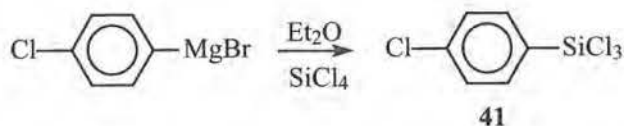


Figure 3.23: *p*-Halogenated phenyltrichlorosilane

This would directly give an octa-functionalized *p*-substituted silsesquioxane cage. Despite the statement in literature³⁷ that the introduction of a halogen atom, or a methyl substituent into the phenyl group of C₆H₅SiCl₃ would make the formation of the corresponding fully condensed phenylsilsesquioxanes much more difficult, synthesis was started from the monomer *p*-chlorophenyltrichlorosilane.

3.3.3.2 Synthesis of octa(*p*-chlorophenyl)pentacyclo[9.5.1.1^{3,9}.1^{5,15}.1^{7,13}]octa-siloxane

Under continuous stirring 1-bromo-4-chlorobenzene (mixed in dry diethyl ether) was added drop by drop to magnesium flakes (covered in dry diethyl ether) in accordance with literature procedures^{55,56}. Stirring was continued while the reaction mixture was refluxed for two hours. This Grignard mixture was added drop by drop with stirring to silicontetrachloride diluted with dry diethyl ether during which insoluble magnesium salts were formed (Scheme 3.26).



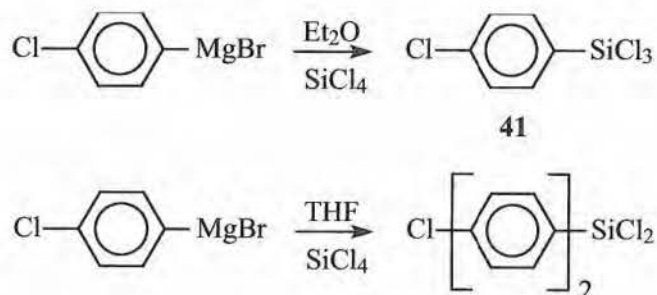
Scheme 3.26: Synthesis of 4-chlorophenyltrichlorosilane

Stirring was continued while the mixture was refluxed for another 5 hours. The ethereal solution was decanted from the insoluble magnesium salts and the residue extracted several times with boiling ether. The combined ethereal solutions were evaporated. Purification was performed by distillation giving 4-chlorophenyl-trichlorosilane (**41**) as a highly water, air sensitive, colourless and fuming liquid with a yield of 52%.

The synthesis of 4-chlorophenyltrichlorosilane (**41**) gave however a lot of problems. The general inability to accomplish clean, integral, partial substitution leading to organosilanes is the primary, but not the only, restriction of the Grignard process. The difficult separation of the corrosive, hydrolytical sensitive halosilanes from the reaction mixture gave also significant problems.

Another general problem for the formation of organosilanes by Grignard methods is that substitution of the chlorine on siliciumtetrachloride is rarely stepwise. Multiple substitution is usually slightly favoured, presumably owing to the complex “dimeric” nature of the Grignard reagent. Furthermore, the activation energy for sequential substitution varies over only a narrow range as evidenced by the 18.2-21.2 kcal/mol range reported for methylchlorosilanes⁵⁷.

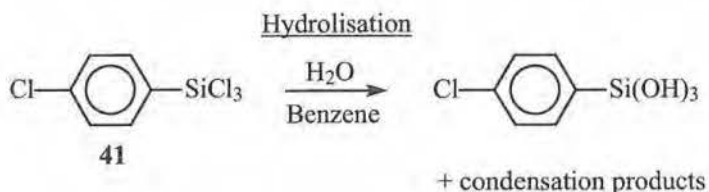
Of the two most common solvents for Grignard reagents, substitution on siliciumtetrachloride is easier with tetrahydrofuran than diethyl ether (Scheme 3.27). The ability to run reactions at more elevated temperatures owing to the higher boiling point of tetrahydrofuran allows the reaction to proceed further. The use of tetrahydrofuran as a solvent has a distinct operational difference when compared with diethyl ether. Magnesium halides are relatively soluble in tetrahydrofuran, requiring a concentration or second-solvent precipitation to remove the salts. For this reason synthesis of 4-chlorophenyltrichlorosilane (**41**) always failed when using tetrahydrofuran as the solvent.



Scheme 3.27: Synthesis of 4-chlorophenyltrichlorosilane

Mass spectral analysis showed that the reaction resulted in the formation of di-substituted silane (Scheme 3.27) while no 4-chlorophenyltrichlorosilane could be detected.

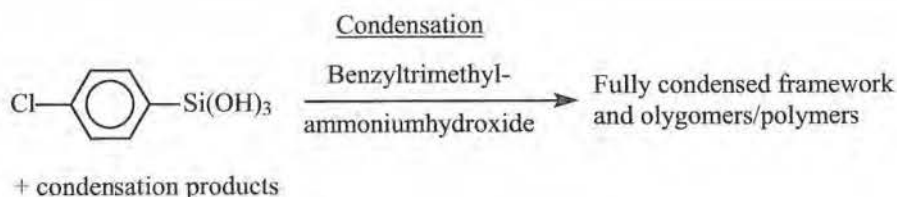
Subsequently 4-chlorophenyltrichlorosilane (**41**) was dissolved in benzene and shaken with brine until hydrolysis was complete (Scheme 3.28). Brine was used instead of water to get a better separation between the water and benzene layer.



Scheme 3.28: Hydrolyzation of 4-chlorophenyltrichlorosilane

During the hydrolyzation the benzene layer became turbid and warm due to HCl formation. The formed HCl act as an in situ catalyst for the condensation of the trifunctional organosilicon monomer. Therefore purification and separation of the hydroxide was not possible. The silanol species resulting from hydrolysis of *p*-ClC₆H₅-SiCl₃ undergoes condensation to form Si-O-Si bonds. This process takes place almost simultaneously with hydrolysis, especially when chlorosilanes are used as starting materials. Since it is not practical to try to isolate silanol species as intermediates, the hydrolysis and condensation are carried out in a one-pot process.

When the hydrolysis was complete (pH of the water layer was 7) the layer was washed once again, the layers separated and the benzene layer refluxed with a methanolic 40% benzyltrimethylammonium hydroxide solution (Scheme 3.29).



Scheme 3.29: Condensation

The result of this condensation reaction highly depended on:

- the nature of the solvent used,
- type of catalyst,
- addition of water,

- concentration of the initial monomer in solution,
- character of substituent X in the initial monomer ($XSiY_3$) (X was in our case $p\text{-ClC}_6\text{H}_5\text{-}$),
- nature of the functional groups Y in the initial monomer ($Y = \text{Cl}$ in our case),
- solubility of the polyhedral oligomers formed,
- temperature
- and reaction time.

Because of structural similarities between $[\text{C}_6\text{H}_5\text{SiO}_{3/2}]_8$ and $[\text{ClC}_6\text{H}_4\text{SiO}_{3/2}]_8$, we used similar conditions for the formation of $[\text{ClC}_6\text{H}_4\text{SiO}_{3/2}]_8$ (Figure 3.24) as we used for the formation of $[\text{C}_6\text{H}_5\text{SiO}_{3/2}]_8$ (40).

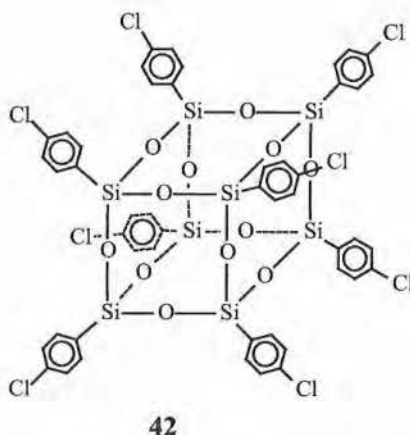


Figure 3.24: Octa(p -chlorophenyl)pentacyclo[9.5.1.1^{3,9}.1^{5,15}.1^{7,13}]octasiloxane

After 4 hours of reflux, 24 hours at room temperature and again 24 hours of reflux no discrete molecular clusters could be indicated in contradiction with previous results for octaphenylpentacyclo[9.5.1.1^{3,9}.1^{5,17}.1^{7,13}]octasiloxane (40). Therefore various reaction times and different concentrations were tested (Table 1) to check whether it is possible to obtain discrete molecular clusters.

Entry	Solvent (ml)	Reflux time (h)	Yield (%)
1	15	4	13
2		24	3
3		48	2
4	30	4	11
5		24	14
6		98	1
7	45	4	8
8		24	7
9		24+3(w) ^a	39
10		48	6
11		48+3(w) ^a	27
12		72	6
13		72+3(w) ^a	21
14	60	4	1
15		6+72(h) ^a	61
16		24	3
17		24+3(w) ^a	57
18		48	3
19		48+3(w) ^a	48
20		72	5

0.4 ml of a methanolic 40% benzyltrimethylammonium hydroxide solution was used for all reactions. ^a Reactions were allowed to stand at RT for 72 (h)ours or 3 (w)eeks after reflux.

Table 3.1: Reaction conditions for the synthesis of $[\text{ClC}_6\text{H}_4\text{SiO}_{3/2}]_8$

The solvent in each experiment was benzene. The yield indicates the yield of fully condensed frameworks. When comparing entries 9,11,13 and 15,17,19 it can be concluded that prolonged reflux is not favourable for the formation of the cages. In addition, very long reaction times with high base concentration (Entry 6) are also unfavourable.

Under basic conditions the formation of POSS frameworks is thermodynamically controlled⁵⁸. The formation and cleavage of Si-O-Si linkages are facile, thus in most cases complex product mixtures result from the base-catalyzed hydrolytic condensation of RSiX_3 or from possible redistribution reactions of $[\text{RSiO}_{3/2}]$. Normally the driving force for cage forming reactions with high yield is precipitation of a very poorly soluble (i.e. insoluble) product. In our case $[\text{ClC}_6\text{H}_4\text{SiO}_{3/2}]_8$ (**42**) was precipitated out of the reaction mixture when standing at room temperature (after reflux). On the other hand the low solubility of $[\text{C}_6\text{H}_5\text{SiO}_{3/2}]_8$ (**40**) resulted in an insoluble product even at reflux. If the reaction mixture was not refluxed prior to standing at room temperature no discrete molecular clusters could be indicated. Best results were obtained (Entry 15) when the mixture was refluxed for 6 hours and allowed to stand for 3 days at room temperature. During that time the cage was precipitating out of the solution. This octa(*p*-chlorophenyl)pentacyclo[9.5.1.1^{3,9}.1^{5,15}.1^{7,13}]octasiloxane (**42**) was a white chloroform soluble powder and could be obtained with 61% yield. The product was stable until 472 °C under oxygen (Figure 3.25) and until 487 °C under nitrogen (Figure 3.26) as indicated via TGA analysis.

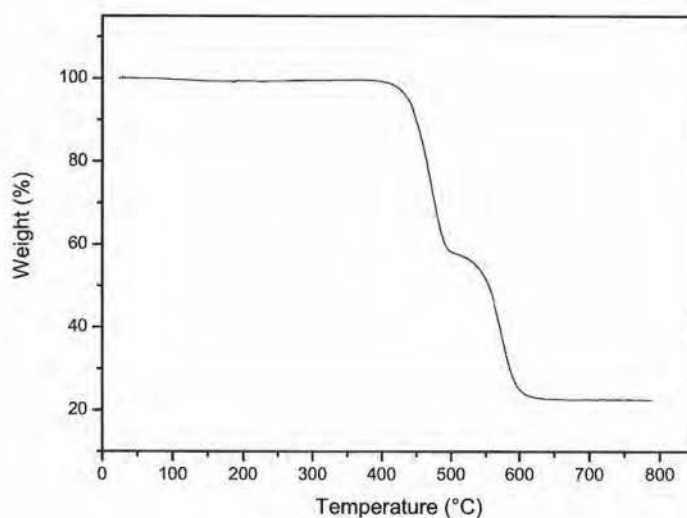


Figure 3.25: TGA of octa(*p*-chlorophenyl)pentacyclo[9.5.1.1^{3,9}.1^{5,15}.1^{7,13}]-octasiloxane (**42**) under oxygen

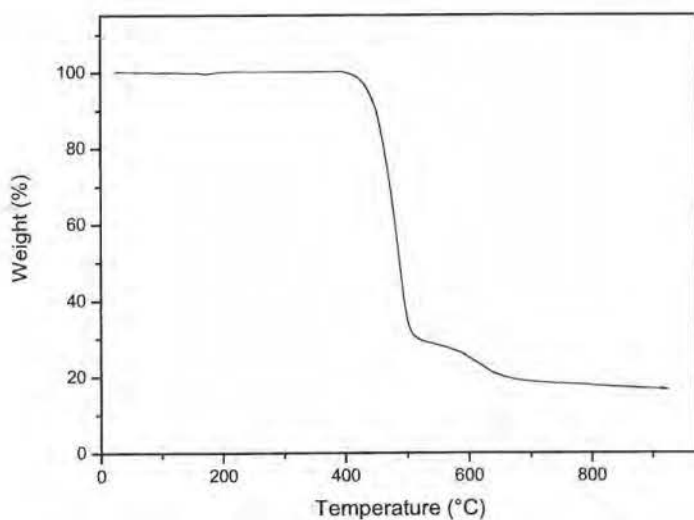


Figure 3.26: TGA of octa(*p*-chlorophenyl)pentacyclo[9.5.1.1^{3,9}.1^{5,15}.1^{7,13}]-octasiloxane (**42**) under nitrogen

¹H-NMR, ¹³C-NMR and ²⁹Si-NMR measurements, of the discrete molecular cluster, were not sufficient to decide whether T₈ exclusively was formed because higher completely condensed cages (for example T₁₀, T₁₂) could also be formed. Therefore the T₈ structure was confirmed by single crystal X-ray diffraction (Figure 3.27).

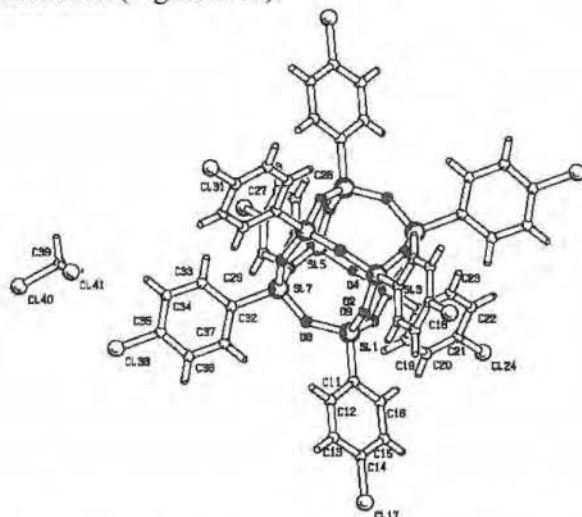


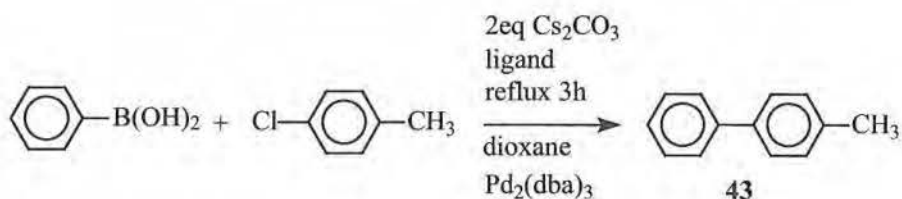
Figure 3.27: Crystal structure of octa(*p*-chlorophenyl)pentacyclo[9.5.1.1^{3,9}.1^{5,15}.1^{7,13}]-octasiloxane. Only the asymmetric unit is labeled (half a molecule plus CH₂Cl₂ solvent molecule).

At room temperature the crystals were not stable in the X-ray beam. Therefore the crystal was immersed in mineral oil, mounted in a nylon loop and cryo-cooling techniques were applied during the data collection. The crystal packing contains large voids in between the molecules of about 115 \AA^3 each, which, according to the different electron density maps, are occupied by disordered solvent molecules.

Previous to these base catalyzed reactions, many acid catalyzed reactions were tried but none of them were successful, all of them lead to intractable resins rather than discrete molecular clusters.

Because theoretical measurements (See Chapter One) showed enhanced properties of the networks formed with fully condensed octasilsesquioxane cubes linked by four phenyl rings, we investigated the coupling properties of aryl chlorides with boronic acids. A few test reactions were performed with toluene and phenylboronic acid (Scheme 3.30).

Different solvents, bases, Pd-catalysts and ligands were tried. Best results were obtained if phenylboronic acid and 4-chlorotoluene were refluxed for 3 hours in dry dioxane. Cs_2CO_3 was used as base. It was ground with a mortar and pestle and dried thoroughly prior to use. Tris(dibenzylideneacetone)-dipalladium (0) ($\text{Pd}_2(\text{dba})_3$) was used as Pd-catalyst with 1,3-bis(2,4,6-trimethylphenyl)imidazolium chloride as ligand in a Pd:ligand ratio 1:2. The coupling product 4-methyl-biphenyl (**43**) could be obtained with yields of more than 90%.



Scheme 3.30: Testreaction

These Suzuki cross coupling reactions⁵⁹ were performed in the presence of highly active palladium catalysts⁶⁰⁻⁷¹.

The highest yields were obtained when 1,3-bis(2,4,6-trimethylphenyl)imidazolium chloride (Figure 3.28) was used as ligand^{72,73}.

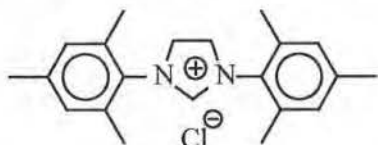
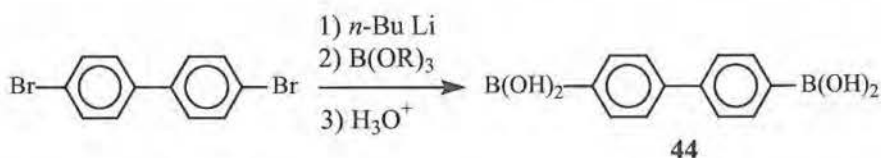


Figure 3.28: 1,3-Bis(2,4,6-trimethylphenyl)imidazolium chloride

The efficiency of this catalyst is most likely due to the combination of a number of factors. The electronic properties of the ligand are certainly of importance because sufficiently electron-rich ligands promote the oxidative addition of the aryl chloride. However, previous studies^{74,75} have shown that electron-rich trialkylphosphines such as PCy_3 are rather inefficient ligands for the Suzuki coupling. Although these electron rich ligands facilitate oxidative addition, they also decrease the rate of the reductive elimination processes. This reflects that a combination of both steric bulk and electronic properties of the ligand is important. Not only the nature of the ligand but also the P/Pd ratio is an important parameter for catalyst productivity⁶².

Because the coupling of arylchlorides with aryl boronic acids was possible in high yields, synthesis was started of 4,4'-biphenylene diboronic acid (**44**) (Scheme 3.31).

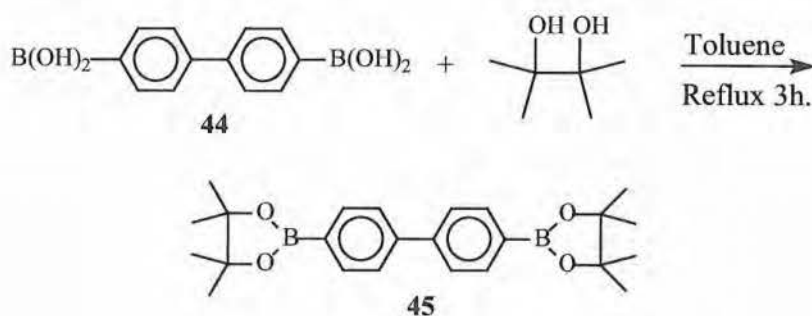


Scheme 3.31: Synthesis of 4,4'-biphenylene diboronic acid

To a solution of 4,4'-dibromobiphenyl in tetrahydrofuran at -78°C , was added dropwise 3 eq *n*-butyllithium. The mixture was allowed to warm up to room temperature and stirred for one hour. Then the solution was cooled once again and 5 eq triisopropylborate was added.

After this, the reaction was warmed up to room temperature, stirred overnight, diluted with diethylether, and added to a stirred mixture of crushed ice and concentrated sulphuric acid. The addition of ether and water facilitated the separation of the layers. The layers were separated and the aqueous layer washed with diethylether. The combined organic layers were dried over MgSO_4 and evaporated. The solid was washed twice with cold diethylether and dried in vacuo to give 4,4'-biphenyldiboronic acid (**44**) as a pure white solid with 62% yield.

This diboronic acid (**44**) was used as linker between the molecular knot (**42**) using the same reaction conditions as used for the Suzuki cross coupling reaction of chlorotoluene with phenylboronic acid. The reaction gave however no coupling products. This is possible due to the limited solubility of the diboronic acid (**44**). For this reason the pinacol ester (**45**) (Scheme 3.32) was prepared which is expected to be much more soluble than the diboronic acid.



Scheme 3.32: Synthesis of 4,4'-biphenyldiboronic acid pinacol ester

4,4'-Biphenyldiboronic acid (**44**) and pinacol were refluxed in toluene under a Dean-Stark head. Toluene was evaporated after completion of the reaction and chromatographic separation through silica gel with chloroform as eluents and recrystallization in hexane gave 4,4'-biphenyldiboronic acid pinacol ester (**45**) as white crystals with 95% yield.

4,4'-Biphenyldiboronic acid pinacol ester (**45**) was used under the same reaction conditions as it was used for the coupling of phenylboronic acid and 4-chlorotoluene, but again no coupling products were formed.

The pinacol ester (**45**) probably needs water to hydrolyze before it can be used in coupling reactions. Because the disadvantages in all these reactions is the decreased reactivity of the aryl chlorides in Pd-catalyzed reactions, synthesis of a silsesquioxane cage with a bromine or iodine, (instead of the chlorine) was necessary. Unfortunately, synthesis of the monomers 4-bromo-trichlorophenylsilane or 4-iodo-trichlorophenylsilane were not successful till now.

3.4 CONCLUSIONS

1,3,5,7-Tetrakis(4-iodophenyl)adamantane (**29**) and 1,3,5,7-tetrakis(4-ethynyl)-phenyladamantane (**34**), both tetra-functionalized molecular knots, were prepared in gram quantities. They can both be used in Pd-catalyzed coupling reactions with e.g. diarylhalogenides.

1,3,5,7-Tetrakis(1,3-dibromophenyl)adamantane (**38**) was, in contradiction with literature, obtained as pure product and not as a mixture of isomers. This octa-functionalized knot can be extended with 4'-(4-ethynylphenyl)-2,2':6',2''-terpyridine (**17**), a previous synthesized molecular rod (See pg 42 Chapter Two) to give 1,3,5,7-tetrakis[1,3-di-(4'-phenyl-1-ethynyl-2,2':6',2''-terpyridine)phenyl]adamantane (**38**) as an octa-functionalized molecular knot. This octadentate ligand still needs to be purified because traces of the hexa- and hepta-substituted form were present in the reaction mixture.

1,3,5,7-Tetrakis[[4'-[4-{2-(phenyl)-1-ethynyl}phenyl]-2,2':6',2''-terpyridine]adamantane (**36**) was obtained as a pure tetra-functionalized molecular knot and is used in coupling reactions via complexation reactions as will be explained in chapter four.

Finally octa(*p*-chlorophenyl)pentacyclo-[9.5.1.1^{3,9}.1^{5,15}.1^{7,13}]octasiloxane (**42**) was synthesized in reasonable yields although it was mentioned in the literature as "never having been synthesized" and "difficult to prepare", but it was possible to synthesize it in reasonable yields. A disadvantage for our purposes is the decreased reactivity of the arylchlorides. Therefore synthesis of monomers 4-bromo-trichlorophenylsilane or 4-iodo-trichlorophenylsilane are necessary to prepare fully condensed silsesquioxane knots with better coupling properties.

3.5 REFERENCES

1. Tamara M. Gund, Eiji Osawa, Van Zandt Williams, Jr., P. v. R. Schleyer, *J. Org. Chem.*, **1974**, 39, 2979-2994.
2. W. D. Graham, P. v. R. Schleyer, *Tetrahedron letters*, **1972**, 12, 1179-1180.
3. W. David Graham, Paul von R. Schleyer, *J. Am. Chem. Soc.*, **1973**, 94, 5785-5786.
4. G. A. Olah, G. K. S. Prakash, J. G. Shih, V. V. Krishnamurthy, G. D. Mateescu, G. Liang, G. Sipos, V. Buss, T. M. Gund, P. v; R. Schleyer, *J. Am. Chem. Soc.*, **1985**, 107, 2764-2772.
5. I. L. Karle, J. Karle, *J. Am. Chem. Soc.*, **1965**, 84, 917-920.
6. *Organic synthesis*, Vol 53 pg 30-34.
7. Tamara M. Gund, V. Z. Williams, Eiji Osawa, P. v; R. Schleyer, *Tetrahedron letters*, **1970**, 44, 3877-3880.
8. Tamara M. Gund, P. v. R. Schleyer, Gerald D. Unruh, Gerald J. Gleicher, *J. Org. Chem.*, **1974**, 39, 2995-3003.
9. Tamara M. Gund, M. Nomura, V. Z. Williams, Jr., P. v. R. Schleyer, *Tetrahedron letters*, **1970**, 56, 4875-4878.
10. D. Faulker, R. A. Glendinning, D. E. Johnston, M. A. McKervey, *Tetrahedron letters*, **1971**, 20, 1671-1674.
11. T. Courtney, D. E. Johnston, M. A. McKervey, J. J. Rooney, *J. C. S. Perkin I*, **1972**, 2691-2696.
12. L. Vodicka, J. Janku, J. Burkhard, *Collection Czechoslovak Chem. Commun.*, **1983**, 48, 1162-1172.
13. G. A. Olah, P. Ramaiah, C. B. Rao, G. Sandford, R. Golam, N. J. Trivedi, J. A. Olah, *J. Am. Chem. Soc.*, **1993**, 115, 7246-7249.
14. Tamara M. Gund, P. V. R. Schleyer, *Tetrahedron letters*, **1971**, 19, 1583-1586.
15. George A. Olah, An-hsiang Wu, Omar Farooq, G. K. Surya Prakash, *J. Org. Chem.*, **1989**, 54, 1450-1451.
16. S. Landa, S. Hala, *Chem. Listy*, **1957**, 51, 2325.
17. H. F. Reinhardt, *J. Am. Chem. Soc.*, **1962**, 26, 3258-3261.
18. Dan Farcasiu, Anca Ghenciu, Jing Qi Li, *Journal of Catalysis*, **1996**, 158, 116-127.

19. Gilbert P. Sollott, Everett E. Gilbert, *J. Org. Chem.*, **1980**, 45, 5405-5408.
20. (a) Frederic M. Menger, Vasily A. Migulin *J. Org. Chem.*, **1999**, 64, 8916-8921. (b) Stetter, Wulff, *Chemische Berichte*, **1960**, 93, 1366-1371. (c) Peter R. Schreiner, Oliver Lauenstein, Igor V. Kolomitsyn, Suad Nadi, Andrey A. Fokin, *Angew. Chem. Int Ed.*, **1998**, 37, 1895-1897. (d) W. Heitz, C. Meckel-Jonas, M. D. Roth, J. H. Wendorff, *Acta Polymer.*, 49, 35-44. (e) Matthias Bremer, Peter S. Gregory, Paul von R. Schleyer, *J. Org. Chem.*, **1989**, 54, 3796-3799. (f) Matthias Bremer, Peter S. Gregory, Paul von R. Schleyer, *New J. Chem.*, **1989**, 13, 767-769.
21. Robert D. Bach, Robert C. Badger, *Synthesis*, **1979**, 529.
22. Veronica R. Reichert, Lon J. Mathias *Macromolecules*, **1994**, 27, 7015-7023.
23. E. B. Merkushev, N. D. Simakhina, G. M. Koveshnikova, *Synthesis*, **1980**, 486-487.
24. Raymond C. Ford, JR., Paul Von R. Schleyer, **1964**, 277-300.
25. Paul Von R. Schleyer, *J. Am. Chem. Soc.*, **1957**, 79, 3292.
26. Paul Von R. Schleyer, M. M. Donaldson, *J. Am. Chem. Soc.*, **1960**, 82, 4645.
27. Fort, R. T. In *Adamantane: The Chemistry of Diamond Molecules*; Gassman, P. G., Ed.; Studies in Organic Chemistry; Marcel Dekker: New York, **1976**, 5.
28. Chunye, H.; Yan, Q.; Changyou, Y. *Chinese Science bulletin* **1999**, 44, 2044-2047.
29. Chavalovsky, V.; Bazant, V. *Collection Czechoslov. Chem. Commun.* **1951**, 16, 581-590.
30. Gruttner, G.; Krause, E. *Berichte* **1917**, 50, 1559-1568.
31. Unno, M.; Alias, B. S.; Arai, M.; Takada, K.; Tanaka, R.; Matsumoto, H. *appl. organometal. Chem.* **1999**, 13, 303-310.
32. Ladenburg, A., *Annalen*, **1875**, 179, 143.
33. Meads, J.A.; Kipping, F.S. *J. Chem. Soc.*, **1915**, 107, 459.
34. John F. Brown, Lester H. Vogt, *J. Am. Chem. Soc.* **1965**, 87(19), 4313.
35. John F. Brown, *J. Am. Chem. Soc.* **1965**, 87(19), 4317.

36. John F. Brown, Lester H. Vogt, Paul I. Prescott, *J. Am. Chem. Soc.* **1964**, 86(19), 1120.
37. Mikhail G. Voronkov, Vladimir I. Lavrent'yev, *Topics in Current Chemistry*, **1982**, 102, 199-237.
38. Frank J. Feher, Theodore A. Budzichowski. *Journal of Organometallic Chemistry*, **1989** 379, 33-40.
39. Rikowski, E.; Marsmann, H. C., *Polyhedron*, **1997**, 16, 3357-61.
40. G. Nuding, F. Vogtle, K. Danielmeier, E. Steckhan, *Synthesis*, **1996**, 1, 71-76.
41. Gary J. Edwards, Stephen R. Jones, John M. Mellor, *J. Chem. Soc. Perkin Trans II*, **1977**, 4, 505-510.
42. J. H. Wieringa, J. Strating, Hans Wynberg, *Synthetic Communications*, **1972**, 2(4), 191-195.
- 42b. David S. Seager and Roger K. Murray Jr., *J. Org. Chem.*, **1993**, 58, 5560-5561.
43. Koch, H. Haaf, W., *Angew. Chem.*, **1960**, 72, 628.
44. a) W. Haubold, J. Herdtle, W. Gollinger W. Enholz, *Journal of Organometallic Chemistry*, **1986** 315, 1. b) Wolfgang Schacht, Dieter Kaufmann, *Journal of Organometallic Chemistry*, **1987** 331, 139-152.
45. Volker Hensel, A.-Dieter Schlüter, *Liebigs Ann. Recueil*, **1997**, 303-309.
46. Dilthey W., Schommer W., Dierichs H., Trösken O., *Ber. Dtsch. Chem. Ges.*, **1933**, 66, 1627.
47. Dilthey W., W. Hurtig, *Ber. Dtsch. Chem. Ges.*, **1934**, 67, 2004.
48. Oligaruso, M. A., Schadoff L. A., Becker E. I., *J. Org. Chem.*, **1963**, 28, 2725.
49. Oligaruso M. A., Becker E. I., *J. Org. Chem.*, **1965**, 30, 3354.
50. Oligaruso M. A., Romanelli M., Becker, E. I. *Chem. Rev.*, **1965**, 65, 261.
51. Ried W., Bönninghausen K. H. *Chem. Ber.*, **1960**, 93, 1769.
52. Ried W., Saxena V. B. *Angew. Chem. Int. Ed.*, **1968**, 7, 378.
53. Ried W., Freitag D. *Angew. Chem. Int. Ed.*, **1968**, 7, 835.
54. Ried W., Saxena V. B., *Liebigs Ann. Chem.*, **1970**, 739, 159.

55. V. Chvalovsky, V. Bazant, *Collection Czechoslov. Chem. Commun.* **1951**, 16, 580.
56. A. Ya. Yakubovich, G. V. Motsarev, *Journal of general chemistry of the USSR*, **1953**, 23, 421-425.
57. A. F. Reid, C. J. Wilkins, *J. Chem. Soc.*, **1955**, 4029.
58. Feher, F. J. Book Gelest: Silanes, silicones and metal organics 2000 **1998**, 43.
59. Norio Miyaura, Akira Suzuki, *Chem. Rev.*, **1995**, 95, 2457-2483.
60. Chunming Zhang, Mark L. Trudell, *Tetrahedron Letters*, **2000**, 41, 595-598.
61. Harald Gröger, *J. Prakt. Chem.*, **2000**, 342, No. 4, 334-339.
62. John P. Wolfe, Robert A. Singer, Bryant H. Yang, Stephen L. Buchwald, *J. Am. Chem. Soc.* **1999**, 121, 9550-9561.
63. Alexander Zapf, Matthias Beller, *Chem. Eur. J.*, **2000**, 6, No. 10, 1830-1833.
64. Xiaohong Bei, Thomas Crevier, Anil S. Guram, Bernd Jandeleit, Timothy S. Powers, Howard W. Turner, Tetsuo Uno, W. Henry Weinberg, *Tetrahedron Letters*, **1999**, 40, 3855-3858.
65. Alexander Zapf, Andreas Ehrentraut, Matthias Beller, *Angew. Chem. Int. Ed.*, **2000**, 39, No. 22, 4153-4155.
66. Adam F. Littke, Gregory C. Fu, *Angew. Chem. Int. Ed.*, **1998**, 37, No. 24, 3387-3388.
67. Adam F. Littke, Chaoyang Dai, Gregory C. Fu, *J. Am. Chem. Soc.* **2000**, 122, 4020-4028.
68. John P. Wolfe, Stephen L. Buchwald, *Angew. Chem.*, **1999**, 111, No. 16, 2570-2573.
69. Xiaohong Bei, Howard W. Turner, W. Henry Weinberg, Anil S. Guram, *J. Org. Chem.*, **1999**, 64, 6797-6803.
70. John P. Wolfe, Stephen L. Buchwald, *Angew. Chem. Int. Ed.*, **1999**, 38 No. 16, 2413-2416.
71. David W. Old, John P. Wolfe, Stephen L. Buchwald, *J. Am. Chem. Soc.* **1998**, 120, 9722-9723.
72. Chunming Zhang, Jinkun Huang, Mark L. Trudell, Steven P. Nolan, *J. Org. Chem.*, **1999**, 64, 3804-3805.

73. Volker P. W. Böhm, Christian W. K. Gstöttmayr, Thomas Weskamp, Wolfgang A. Herrmann, *Journal of Organometallic Chemistry*, **2000**, 595, 186-190.
74. Shen W., *Tetrahedron Lett.*, **1997**, 38, 5575-5578.
75. Firooznia F., Gude C., Chan K., Satoh Y., *Tetrahedron Lett.*, **1998**, 39, 3387-3388.

IV

CHAPTER FOUR: COMPLEXATION AND NETWORK FORMATION

4.1 INTRODUCTION

In our second approach we wanted to use complexation as a coupling method for the synthesis of highly rigid networks. The use of terpyridine derivatives offers here the possibility to use complexation reactions for coupling of terpyridines to one another. The terdentate ligand 2,2':6',2''-terpyridine (Figure 4.1) was first isolated in the thirties by *Morgan and Burstall*¹, as one of the many products from the reaction of pyridine with iron(III) chloride²⁻⁵.

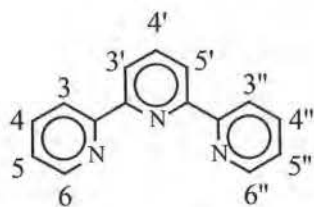


Figure 4.1: 2,2':6',2''-Terpyridine

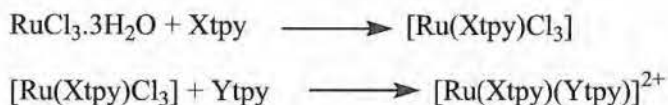
Since the time they described the synthesis, there have been many investigations of this metal-complexing ligand and its complexes. In the last years this moiety has also become a key building block in supramolecular science for the construction of ordered architectures⁶.

2,2':6',2''-Terpyridine contains three nitrogen atoms and can therefore act as a tridentate ligand and form stable complexes by chelating a broad variety of transition metal ions⁷ such as cobalt(II), copper(II), nickel(II), ruthenium(II), etc...

A great number of terpyridine derivatives have been used to prepare Ru(II) complexes⁸. For this reason, and because ruthenium offers the possibility to synthesize large constructs, with little equilibration (metal-ligand exchange) under mild physicochemical conditions due to the unique strength of the terpyridine-Ru coordination⁹, Ru was chosen as transition metal for complex formation.

Compared to "classical" covalent polymers, metallo-supramolecular polymers offer many advantages. Besides the formation via self-organization processes, the reversibility of the supramolecular bond allows the construction of "smart" materials with tuneable properties. Moreover, the electrical and photochemical properties of the utilized complexes can be engineered by choosing the appropriate metal and counterion^{7b,8a,9}. Most of the time counterions such as Cl⁻, BF₄⁻ or PF₆⁻ are used, only *Newkome et al.* introduced a neutral metallodendrimer where eight internal carboxylate groups balance the charge of the Ru^{II} centers¹⁰.

In each case, the complexes we have prepared were obtained by a simple synthetic route (Scheme 4.1), in which one equivalent of a suitable 4'-substituted 2,2':6',2''-terpyridine ligand (Xtpy) reacted with commercial RuCl₃·3H₂O in boiling methanol or ethanol to give the ruthenium(III) complex [Ru(Xtpy)Cl₃] as a dark brown, insoluble paramagnetic solid.

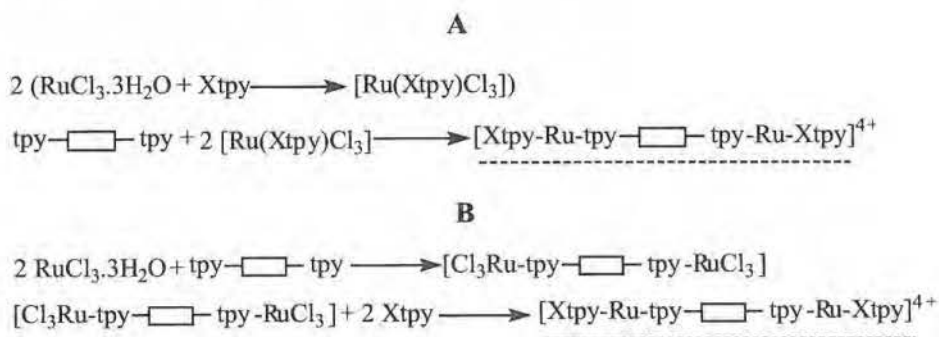


Scheme 4.1: Reaction course complex formation with Ru

The RuCl₃-complexes are insoluble and were used without further purification for the next step. The ruthenium(III) complex [Ru(Xtpy)Cl₃] was then treated with one equivalent of a second 4'-substituted 2,2':6',2''-terpyridine ligand, Ytpy, (which might be the same or different from Xtpy) in boiling methanol (or mixture with chloroform) in the presence of the reducing

agent N-ethylmorpholine. After a period of reflux red-brown solutions were obtained, which were filtered hot and treated with an excess of $[\text{NH}_4][\text{PF}_6]$. In each case a red-brown precipitate was obtained. In the case of the homoleptic complexes (Xtpy = Ytpy) the compound $[\text{Ru}(\text{Xtpy})_2][\text{PF}_6]_2$ was obtained $^1\text{H-NMR}$ spectroscopically pure. The heteroleptic complexes $[\text{Ru}(\text{Xtpy})(\text{Ytpy})][\text{PF}_6]_2$ were found by $^1\text{H NMR}$ spectroscopy to contain small amounts of the corresponding homoleptic species $[\text{Ru}(\text{Xtpy})_2][\text{PF}_6]_2$ and $[\text{Ru}(\text{Ytpy})_2][\text{PF}_6]_2$. In general, a given heteroleptic cation $[\text{Ru}(\text{Xtpy})(\text{Ytpy})]^{2+}$ could be obtained either by the reaction of $[\text{Ru}(\text{Xtpy})\text{Cl}_3]$ with Ytpy or of $[\text{Ru}(\text{Ytpy})\text{Cl}_3]$ with Xtpy.

Apart from these homoleptic and heteroleptic monocomplexes, di- and tetracomplexes were also prepared to study the chemistry of this complexation reactions. Dicomplexes e.g. can be prepared either by reacting bis-functionalized ligands with $[\text{Ru}(\text{Xtpy})\text{Cl}_3]$ or with a bis-terpyridine connected by a spacer (rectangle) (Scheme 4.2).



Scheme 4.2: Synthesis of dicomplexes via two different routes

These bi-functionalized ligands are of special interest due to their ability to serve as bridging ligands in metal-containing polymers, possibly allowing materials with tailored physical properties¹¹. By connecting two terpyridine units via a rigid spacer attached to their 4'-position, bridging ligands displaying axial symmetry can be obtained (Figure 4.2).

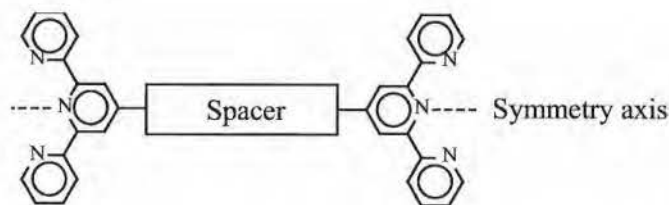


Figure 4.2: Bis-functionalized ligand

The spacers play a 2-fold role: They (i) control the supramolecular structure (in particular of the intercomponent distances and angles); (ii) They control the electronic communication between components. This latter was of no importance for our purposes. Three different bis-terpyridines; 1,4-di[4'-(4-ethynylphenyl)-2,2':6',2''-terpyridine]-2-(3,7-dimethyloctyl)-5-methoxybenzene (**22**), 1,4-bis-(2,2':6',2''-terpyridin-4'-yl)benzene (**20**) and bis[(2,2':6',2''-terpyridin-4'-yl)-phenyl]ethyne (**18**) were prepared. The corresponding spacers of these bis-terpyridines derivatives are represented in Figure 4.3.

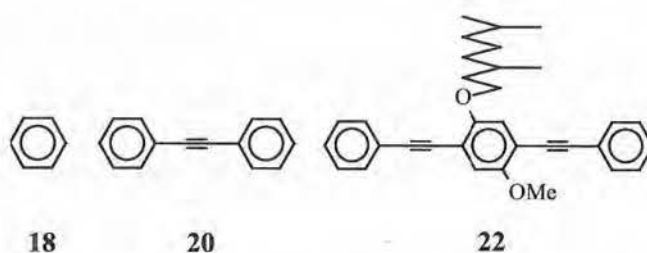


Figure 4.3: Spacers of 4'-substituted bis[2,2':6',2''-terpyridines] **18**, **20** and **22**

These bis-terpyridines can be treated with commercial $\text{RuCl}_3 \cdot 3\text{H}_2\text{O}$ (See Scheme 4.2 B) to create rigid linkers which can be used to form linkages between terpyridine substituted knots (such as 1,3,5,7-tetrakis[[4'-(4-{2-(phenyl)-1-ethynyl}phenyl)-2,2':6',2''-terpyridine]adamantane](**36**), and in this way create molecular networks.

4.2 SYNTHESIS OF COMPLEXES

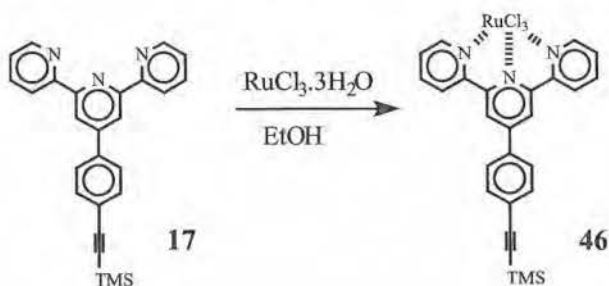
4.2.1 SYNTHESIS OF MONOCOMPLEXES

4.2.1.1 Synthesis of homoleptic complexes

To obtain a better insight into the chemistry involved in these complexation reactions, we first started with the synthesis of some homoleptic complexes.

These homoleptic complexes are complexes with the same 2,2':6',2''-terpyridine ligand on both sides of the metal atom. Ruthenium, zinc and cobalt homoleptic complexes were synthesized. The Ru-complexes were synthesized in a 'stepwise manner' (as explained in the introduction), the Zn- and Co-complexes were generated in situ by adding an excess of solid $\text{Zn}(\text{CH}_3\text{COO})_2$ or $\text{Co}(\text{CH}_3\text{COO})_2$.

The synthesis of these ruthenium homoleptic complexes consists of two steps. In the first step the RuCl_3 -terpyridine complex was formed by refluxing a solution of commercial $\text{RuCl}_3 \cdot 3\text{H}_2\text{O}$ and 4'-[4-{2-(trimethylsilyl)-1-ethynyl}phenyl]-2,2':6',2''-terpyridine (**16**) in EtOH for 3 hours (Scheme 4.3) during which a brown precipitate was formed.



Scheme 4.3: Synthesis of RuCl_3 -Complex (**46**)

After cooling the brown precipitate was filtered and washed sequentially with EtOH, H_2O and diethylether. The brown minimally soluble solid (**46**) was obtained with 95% yield and was used later without further purification. Due to the low solubility of (**46**) it was not possible to get a NMR spectrum.

The UV-Vis signal of around 390 nm indicated the formation of the RuCl₃-terpyridine complex (Figure 4.4). This signal is typical for all RuCl₃-terpyridine complexes.

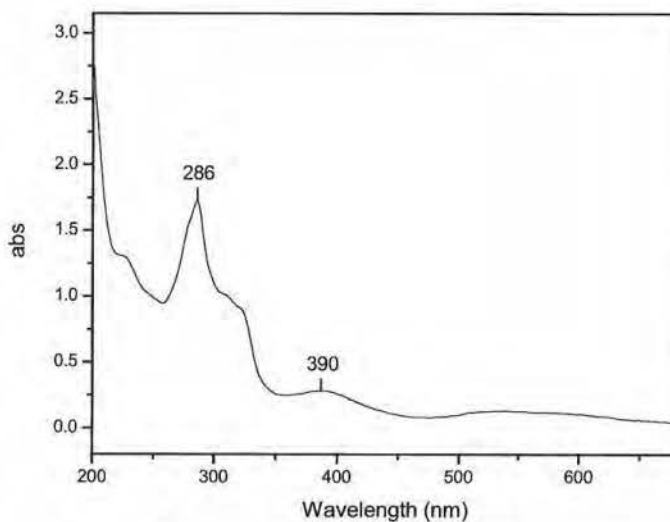
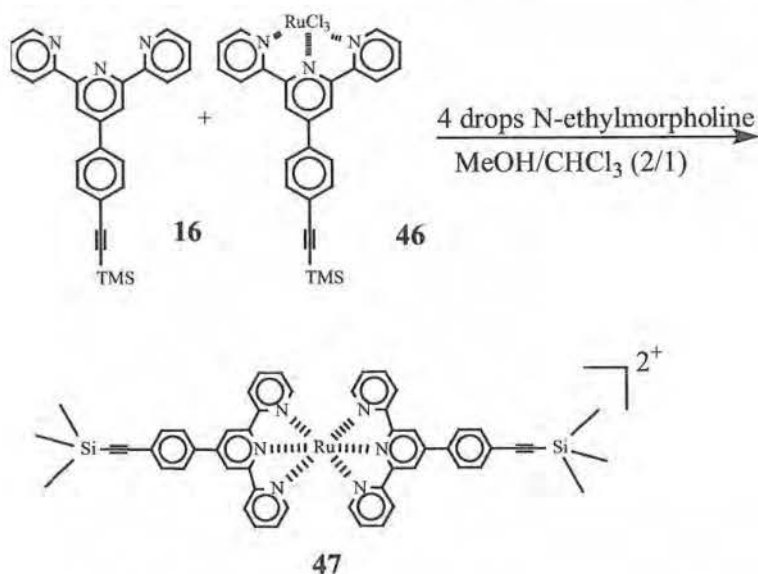


Figure 4.4: UV-Vis of RuCl₃-terpyridine complexes

In the next step this RuCl₃-terpyridine complex (**46**) was treated with one equivalent of 4'-[4-{2-(trimethylsilyl)-1-ethynyl}phenyl]-2,2':6',2''-terpyridine (**16**) in a mixture methanol/chloroform (2/1) under reducing conditions (N-ethylmorpholine). The mixture was refluxed for 6 hours until it turned into a clear red solution (Scheme 4.4). This color transformation indicated that the Ru-terpyridine complex was formed.



Scheme 4.4: Synthesis of bis[4-[4-{2-(trimethylsilyl)-1-ethynyl}phenyl]-2,2':6',2''-terpyridyl]-ruthenium(II) hexafluorophosphate

After cooling to room temperature excess $[\text{NH}_4][\text{PF}_6]$ was added to precipitate the homoleptic complex (47) out of the solution. The red precipitate was filtered off and washed sequentially with H_2O and diethylether to give complex (47) as a red solid with 87% yield. UV-Vis showed a signal at 490 nm indicating the formation of the homoleptic complex (Figure 4.5). The relatively intense and broad absorption band in the visible region, which is responsible for the deep red colour, is due to a spin-allowed $d \rightarrow \pi^*$ metal-to-ligand charge transfer transition¹² (MLCT band) where an electron promotion from metal-centered d orbitals to unfilled ligand centered π^* orbitals occur. No signal around 390 nm was observed which indicated that no RuCl_3 -terpyridine complex (46) was left.

The UV-Vis spectra of the ruthenium complexes in acetonitrile or methanol solution to exhibit characteristic MLCT transitions (Figure 4.5) in the visible region in the wavelength range 475-498 nm in addition to intense ligand centred (LC) transitions to higher energy.

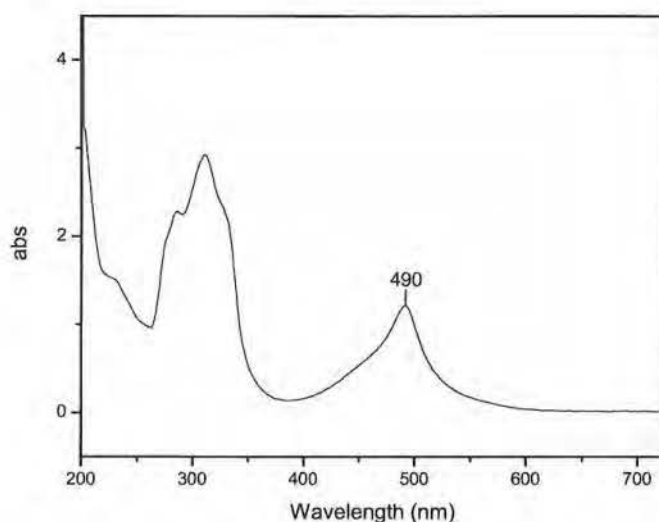
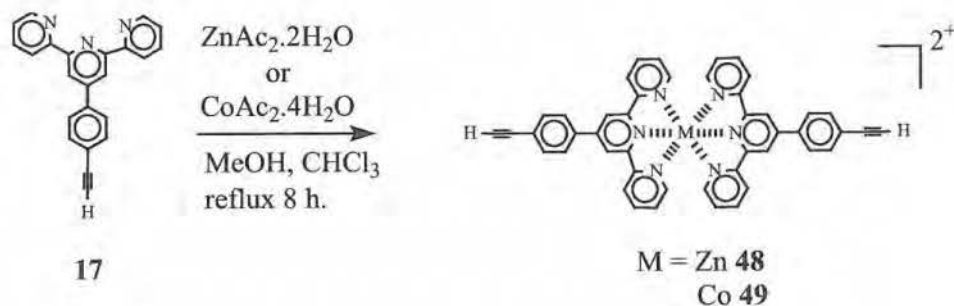


Figure 4.5: UV-Vis of Ru-terpyridine complexes

Satisfactory F.A.B. mass spectra were obtained for Ru-terpyridine complex (47) and all the other monocomplexes that were synthesized. All of them showed clusters of peaks which indicate the correct isotopomer distributions assigned to the complex which lost one or both counter ions $[\text{PF}_6^-]$ which was at m/z 1057 ($\text{M}-\text{PF}_6^-$)⁺ and 912 ($\text{M}-2\text{PF}_6^-$)²⁺ in the case of complex (47).

Apart from these ruthenium complexes, zinc and cobalt complexes were also synthesized. These complexes were in contradistinction with the ruthenium complexes generated in situ. The metal atom directly forms a complex with two 2,2':6',2''-terpyridine ligands. To create the complexes, a suspension of 4'-ethynylphenyl-2,2':6',2''-terpyridine (17) in a mixture of MeOH and CHCl_3 was refluxed for 8 hours in the presence of Zn(II)acetate or Co(II)acetate (Scheme 4.5).



Scheme 4.5: Synthesis of bis[4'-(4-ethynylphenyl)-2,2':6',2''-terpyridyl]zinc(II) hexafluorophosphate (**48**) and bis[4'-(4-ethynylphenyl)-2,2':6',2''-terpyridyl]cobalt(II) hexafluorophosphate (**49**)

After cooling to room temperature excess of [NH₄][PF₆] was added to precipitate the complexes. This precipitate was filtered off and washed sequentially with H₂O and Et₂O to give the Zn-complex (**48**) as a white solid with 92% yield and the Co-complex (**49**) as a deep maroon solid with 79% yield. Both of these complexation reactions with Zn(II)acetate and Co(II)acetate were also tried with 4'-(4-{2-(trimethylsilyl)-1-ethynyl}phenyl)-2,2':6',2''-terpyridine (**16**). These reactions gave similar results. The trimethylsilyl group of 4'-(4-{2-(trimethylsilyl)-1-ethynyl}phenyl)-2,2':6',2''-terpyridine (**16**) is apparently sensitive towards the acetate and deprotection occurs. ¹H-NMR showed a signal at 3.70 ppm, which indicated the deprotection. No traces of trimethylsilyl could be detected.

The absorption spectrum of Zn and Co terpyridine complex (Figure 4.6) in acetonitrile solution at room temperature showed no MLCT band like the Ru terpyridine complexes.

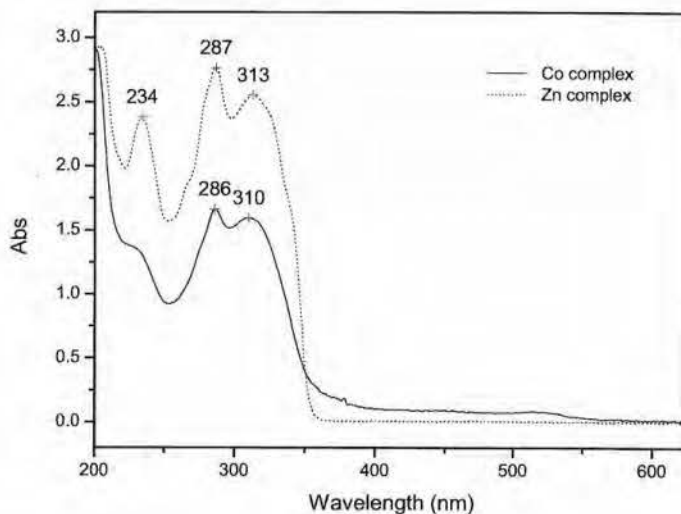


Figure 4.6: UV-Vis of Zn (**48**) and Co (**49**) terpyridine complex

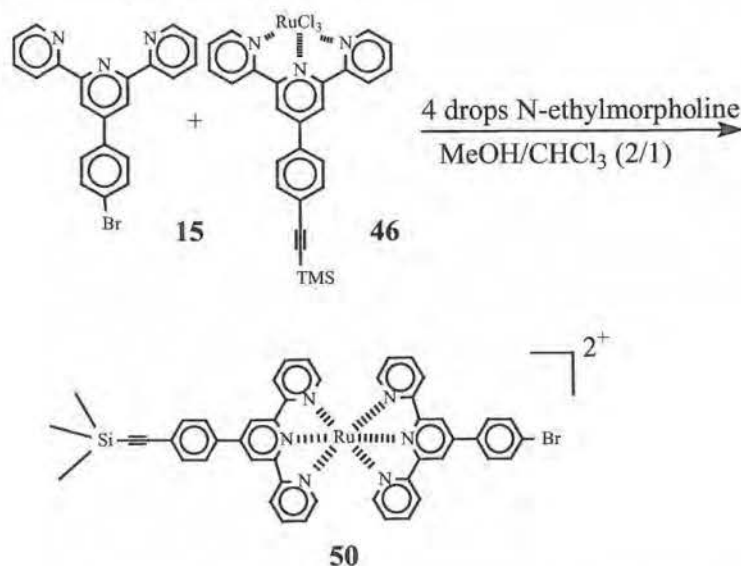
The d^{10} zinc(II) ion is difficult to oxidize or to reduce, and as a consequence no metal-to-ligand (MLCT) or ligand-to-metal (LMCT) charge-transfer excited states are expected. The red-brown coloration of the solution in the case of the Co complex is associated with unresolved metal centered d-d transitions in the range from 450 to 550 nm.¹³

The synthesis of Co or Zn heteroleptic complexes was not possible via this reaction path since there is no selectivity towards the two different terpyridine units, consequently a mixture of heteroleptic and homoleptic complexes is formed.

4.2.1.2 Synthesis of heteroleptic complexes

To check whether ligand scrambling occurs and in which amount, the heteroleptic complex of 4'-(4'''-bromophenyl)-2,2':6',2''-terpyridine (**15**) and 4'-[4-{2-(trimethylsilyl)-1-ethynyl}phenyl]-2,2':6',2''-terpyridine (**16**) was synthesized. These heteroleptic complexes are complexes with a different 2,2':6',2''-terpyridine ligand on both side of the metal.

Synthesis occurs via the same reaction path as for the preparation of the homoleptic complexes; to a suspension of RuCl_3 -terpyridine complex (**46**) and 4'- $(4''')$ -bromophenyl)-2,2':6',2''-terpyridine (**15**) in methanol was added N-ethylmorpholine and the mixture was refluxed for 4 hours until it turned into a clear red solution (Scheme 4.6).



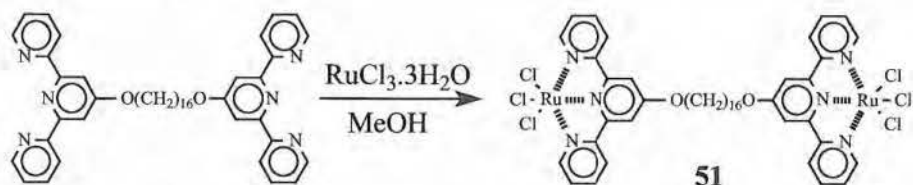
Scheme 4.6: Synthesis of heteroleptic complex (**50**)

After cooling to room temperature an excess of $[\text{NH}_4][\text{PF}_6]$ was added and the red precipitate was filtered off and washed sequentially with H_2O and Et_2O to give the heteroleptic complex (**50**) as a red solid with 78% yield. $^1\text{H-NMR}$ spectroscopy indicated small amounts ($\pm 5\%$) of the corresponding homoleptic species, which indicated ligand scrambling had occurred. The red color and as a consequence the UV signal at 490 nm and FAB signals at m/z 1039 (M-PF_6^+) and 894 (M-2PF_6^{2+}) indicated the heteroleptic complex (**50**) was formed.

4.2.2 SYNTHESIS OF DICOMPLEXES

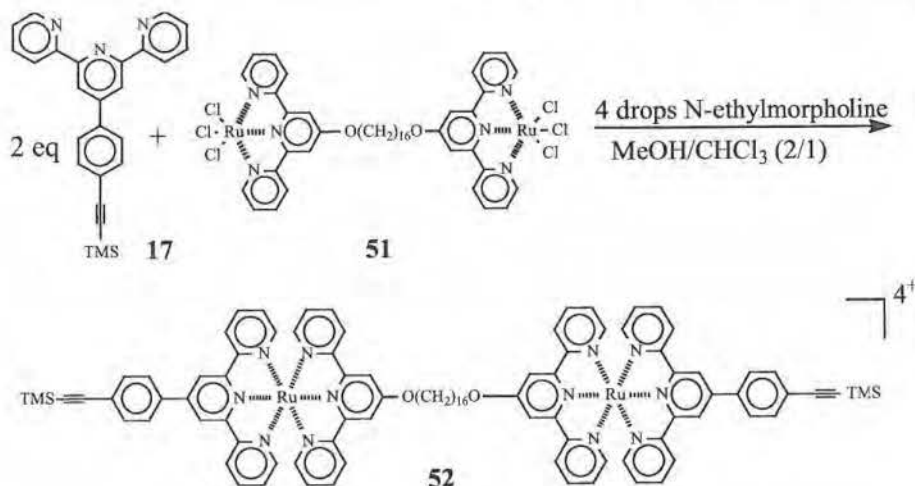
Not only mono but also di- and tetra-complexes were prepared for two reasons; firstly to investigate whether yields for the synthesis of the di- and tetra-complexes were as high as for the monocomplexes and secondly (more importantly) because these dicomplexes are useful to get an idea about the spectroscopic properties since these bisterpyridines were used later as rigid linkers to create molecular networks. Flexible as well as rigid dicomplexes were synthesized with 1,4-di[4'-(4-ethynylphenyl)-2,2':6',2''-terpyridine]-2-(3,7-dimethyloctyl)-5-methoxy-benzene (**22**) which was prepared in our lab and 1,16-bis(2,2':6',2''-terpyridin-4'-yloxy)-hexadecane which was provided by the TU/e.

For the preparation of the flexible dicomplex a solution of 1,16-bis(2,2':6',2''-terpyridin-4'-yloxy)-hexadecane in chloroform was added dropwise to a solution of $\text{RuCl}_3 \cdot 3\text{H}_2\text{O}$ in methanol and the mixture refluxed for 5 hours (Scheme 4.7).



Scheme 4.7: Synthesis of RuCl_3 -Complex (**51**)

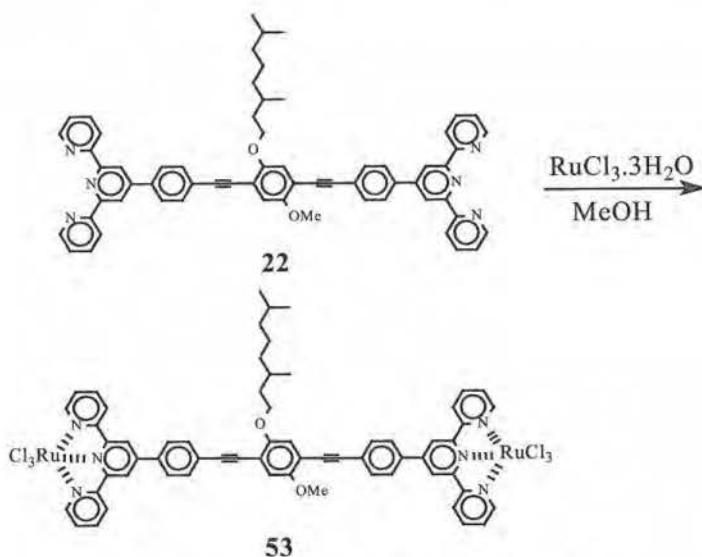
After cooling to room temperature the brown precipitate was filtered, washed sequentially with CHCl_3 , H_2O and Et_2O then dried in vacuo, yielding the RuCl_3 -complex (**51**) as a brown solid with 89% yield. UV-Vis spectra showed a signal at 394 nm indicating the ruthenium trichloride complex was formed. In the next step, the RuCl_3 -complex (**51**) was treated without further purification with two equivalents 4'-[4-{2-(trimethylsilyl)-1-ethynyl}phenyl]-2,2':6',2''-terpyridine (**16**), under reducing conditions (N-ethylmorpholine) and refluxed in a mixture methanol/chloroform for 5 hours (Scheme 4.8).



Scheme 4.8: Synthesis of bi-complex (**52**)

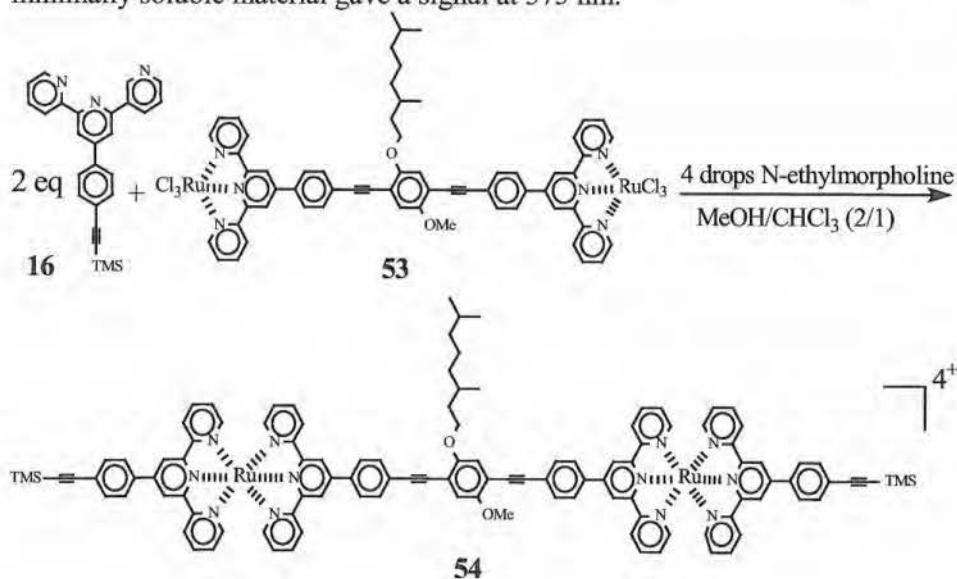
After cooling to room temperature an excess of $[\text{NH}_4][\text{PF}_6]$ was added and the precipitate was filtered off and washed sequentially with H_2O and Et_2O to give complex (**52**) as a red solid with 83% yield. UV-Vis measurements showed a signal at 492 nm and no signal at 394 nm was present, this indicated the formation of the bi-complex (**52**).

For the preparation of the rigid bi-complex (**54**) (Scheme 4.10), the same reaction procedure was followed as for the synthesis of the flexible bi-complex (**52**).



Scheme 4.9: Synthesis of RuCl_3 -complex (**53**)

The RuCl₃-complex (**53**) was obtained with 84% yield and was coloured brown like all the other RuCl₃-complexes. UV-Vis measurements of this minimally soluble material gave a signal at 375 nm.



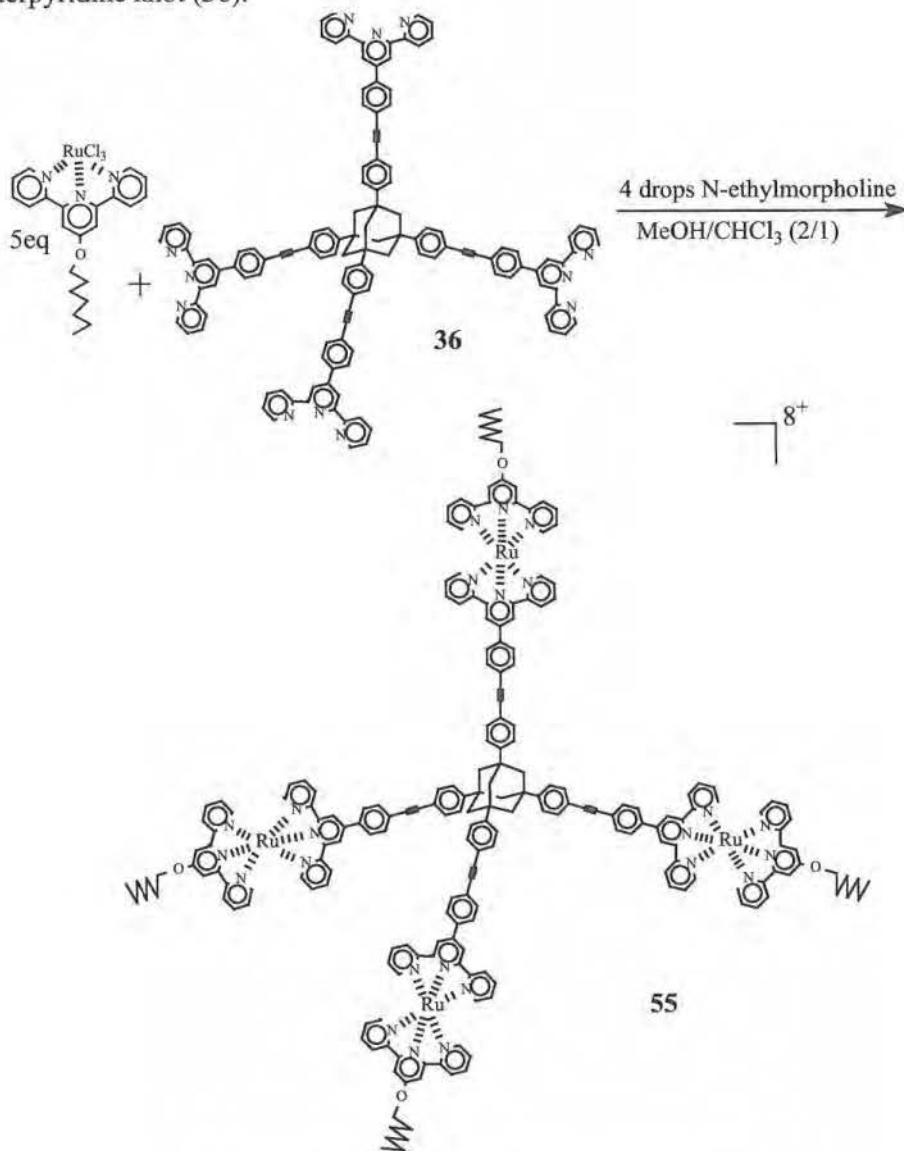
Scheme 4.10: Synthesis of bi-complex (**54**)

Starting from the RuCl₃-complex (**53**), the rigid terpyridine bi-complex (**54**) was obtained with 85% yield. UV-Vis measurements showed the MLCT signal at 496 nm.

4.2.3 SYNTHESIS OF TETRACOMPLEXES

Finally the synthesis of the tetra-complex (**55**) was started because 1,3,5,7-tetrakis[[4'-[4-{2-(phenyl)-1-ethynyl}phenyl]-2,2':6',2''-terpyridine]-adamantane (**36**) was synthesized before to be used later as a molecular knot in the synthesis of the molecular networks. Consequently, this tetra-complex could provide us with useful spectroscopic information for later analysis of the corresponding networks.

Molecular knot 1,3,5,7-tetrakis[[4'-[4-{2-(phenyl)-1-ethynyl}phenyl]-2,2':6',2''-terpyridine]-adamantane (**36**) was first dissolved in chloroform because it was insoluble in methanol. This solution was added dropwise to a refluxing suspension of the RuCl₃-complex in methanol under reducing conditions (N-ethylmorpholine) and refluxed overnight (Scheme 4.11). A small excess of the RuCl₃-complex was used to ensure full substitution of the tetra-terpyridine knot (**36**).



Scheme 4.11: Synthesis of tetra-complex (**55**)

After cooling to room temperature the mixture was filtered and the filtrate treated with an excess of $[\text{NH}_4][\text{PF}_6]$. The red precipitate was filtered off and washed sequentially with H_2O and Et_2O to give tetra-complex (**55**) as a red solid with 58% yield. The product was purified via chromatographic separation with bio-beads SX-1 and DMF as eluents. MALDI-TOF measurements indicated the correct molecular ion which has lost one, two, three and four $[\text{PF}_6]^-$ counter ions at m/z : 4568 ($\text{M}-\text{PF}_6^-$)⁺; 4424 ($\text{M}-2\text{PF}_6^-$)⁺, 4280 ($\text{M}-3\text{PF}_6^-$)⁺ and 4136 ($\text{M}-4\text{PF}_6^-$)⁺ (Figure 4.7) respectively.

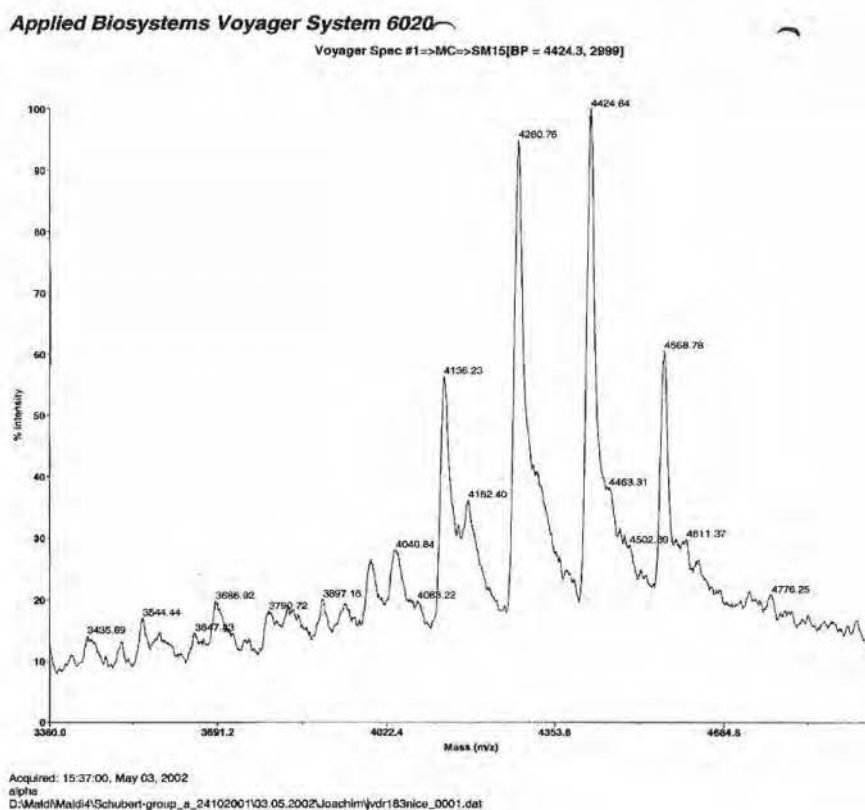


Figure 4.7: MALDI-TOF of tetra-complex (**55**)

UV-Vis measurements in acetonitrile solution indicated the MLCT signal at 493 nm (Figure 4.8).

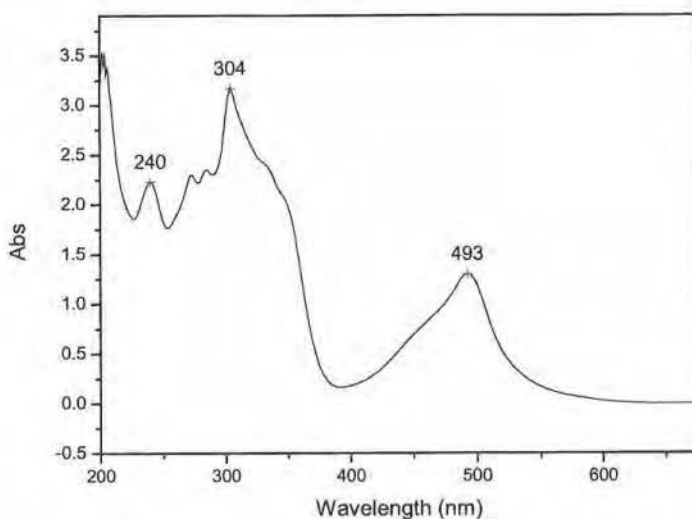
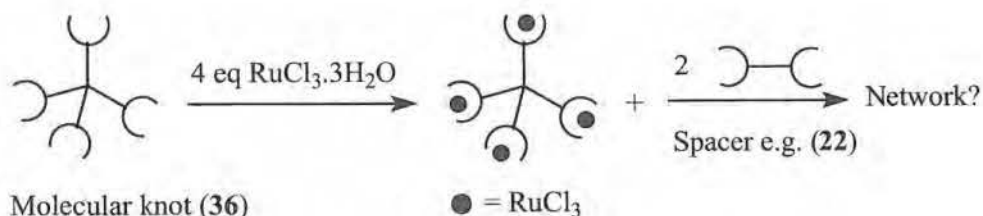


Figure 4.8: UV-Vis of tetra-complex (55)

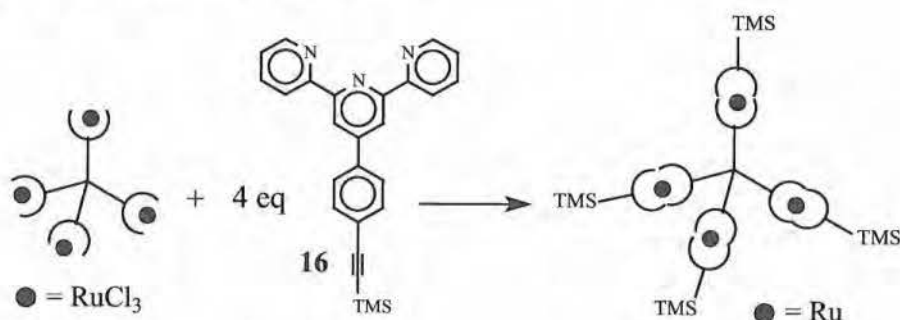
4.3 SYNTHESIS OF NETWORKS

For the creation of the molecular networks with molecular knot (36), two synthetic paths were investigated. The first synthetic path involves the synthesis of a tetra-substituted RuCl_3 -terpyridine complex (Scheme 4.12) which can react with two equivalents of a molecular spacer (one of our previously synthesized bis-terpyridines 18, 20, and 22) to form molecular networks. Molecular knot 1,3,5,7-tetrakis[[4'-[4-{2-(phenyl)-1-ethynyl}phenyl]-2,2':6',2''-terpyridine]-adamantane (36) is represented as depicted below and will be used so hereafter.



Scheme 4.12: First synthetic pathway towards molecular networks.

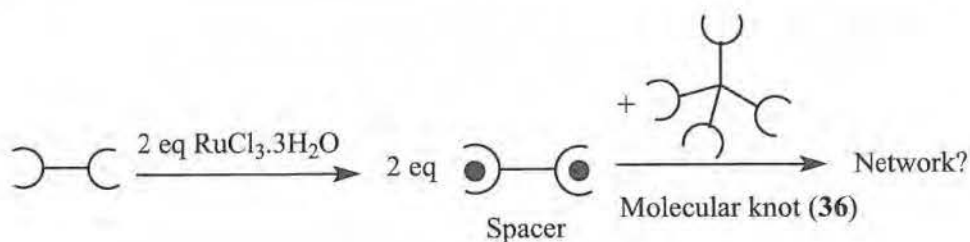
The synthesis of the tetra-substituted RuCl_3 -terpyridine complex from molecular knot (**36**) was performed in two different solvents. In the first reaction molecular knot (**36**) was dissolved in chloroform and added dropwise to a solution of 4 eq $\text{RuCl}_3 \cdot 3\text{H}_2\text{O}$ in methanol. In the second reaction DMF was used as the solvent. Both mixtures were refluxed overnight and the precipitate filtered off and washed sequentially with chloroform, water and diethyl ether. Since the RuCl_3 -complex of molecular knot (**36**) was insoluble at room temperature in common organic solvents, no spectroscopic data could be obtained. To check whether the molecular knot was tetra-substituted a test reaction was executed with 4'-[4-{2-(trimethylsilyl)-1-ethynyl}phenyl]-2,2':6',2''-terpyridine (**16**) (Scheme 4.13).



Scheme 4.13: Testreaction

The presumed tetra-substituted RuCl_3 -terpyridine complex was refluxed overnight with a small excess of 4'-[4-{2-(trimethylsilyl)-1-ethynyl}phenyl]-2,2':6',2''-terpyridine (**16**) and N-ethylmorpholine in a mixture of chloroform and methanol. Work up was performed in the same way as all previous reactions but however gave no results. The RuCl_3 -complex of molecular knot (**36**) is probably insoluble, consequently it had not reacted with terpyridine (**16**). For this reason it is useless as a molecular building block.

Since the solubility of the tetra-substituted RuCl_3 -terpyridine complex was much too low, another synthetic path was followed. Not the knot was converted to its corresponding RuCl_3 -terpyridine complex but the better soluble molecular rods were converted to their corresponding RuCl_3 -terpyridine complex (Scheme 4.14).



Scheme 4.14: Second synthetic pathway towards molecular networks.

To circumvent solubility problems and to check whether it was possible to obtain a molecular network without precipitation of some low molecular weight particles, network formation was first investigated by reacting molecular knot 1,3,5,7-tetrakis[[4'-[4-{2-(phenyl)-1-ethynyl}phenyl]-2,2':6',2''-terpyridine]-adamantane (36) with the long flexible, highly soluble bis RuCl₃-terpyridine complex (Figure 4.9).

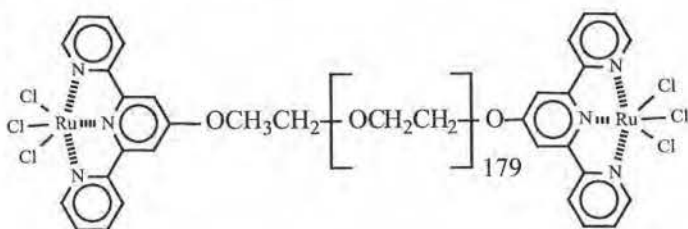
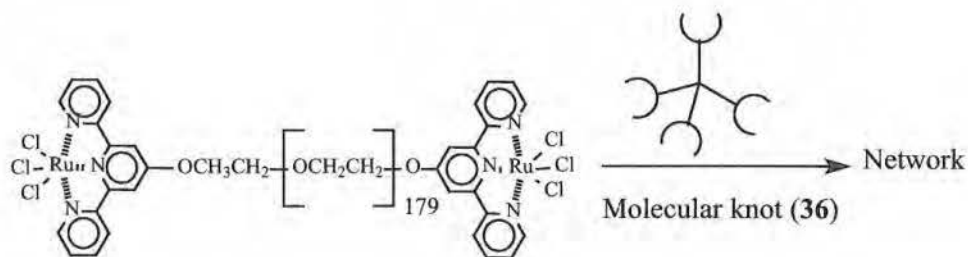


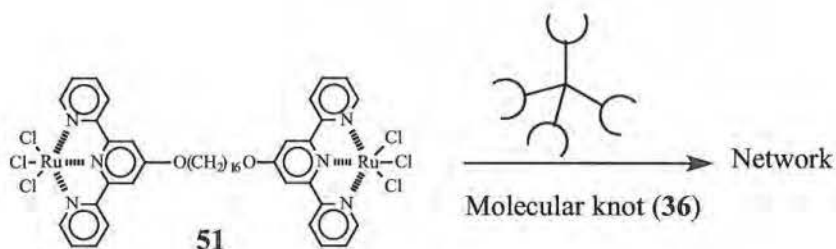
Figure 4.9: Bis RuCl₃-terpyridine complex

Molecular knot (36) and bis RuCl₃-terpyridine complex (Figure 4.9) were refluxed in a methanol/chloroform mixture with N-ethylmorpholine as the reducing agent. Initially a white precipitate was still present in the reaction mixture at reflux temperature, this indicated that the molecular knot was only partially dissolved. After one day of reflux no white precipitation was left in the reaction mixture. This indicated the slightly soluble molecular knot (36) had reacted with the highly soluble molecular spacer and was consequently dissolved. This coupling of the molecular knot with the spacer was also indicated by the red colour of the reaction mixture which had initially a brown color.



Scheme 4.15: Synthesis of molecular network with long flexible spacers

The same reaction procedure was used for the formation of networks with molecular knot (36) and bis RuCl_3 -terpyridine complex (51) (Scheme 4.16)



Scheme 4.16: Synthesis of molecular network with shorter flexible spacers

In contradiction with the previous reaction, precipitation of the network with $[\text{NH}_4][\text{PF}_6]$ was possible. The $^1\text{H-NMR}$ spectra of the product showed broad peaks. These broad peaks indicated that a polymer or network was formed. The values of the signals correspond to the $^1\text{H-NMR}$ signals of the tetra-complex (55) and bi-complex (52). No signals of the free molecular knot (36) could be detected. This network is currently under investigation at the TU/e.

4.4 REFERENCES

1. Morgan, G. T., Burstall F. H., *J. Chem. Soc.* **1931**, 20.
2. Morgan, G. T., Burstall F. H., *J. Indian Chem. Soc., Ray Commem.*, **1933**, 1.
3. Morgan, G. T., Burstall F. H., *J. Chem. Soc.* **1934**, 1499.
4. Morgan, G. T., Burstall F. H., *J. Chem. Soc.* **1932**, 20.
5. Morgan, G. T., Burstall F. H., *J. Chem. Soc.* **1938**, 1672.
6. (a) U.S. Schubert, C. Eschbaumer, P. Andres, H. Hofmeier, C.H. Weidl, E. Herdtweck, E. Dulkeith, A. Morteani, N.E. Hecker, J. Feldman. *Synthetic Metals*, **1999**, 121, 1249-1252. (b) Bernold Hasenkopf, Jean-Marie Lehn, *Helvetica Chimica Acta*, **1996**, 79, 1643-1650. (c) George R. Newkome, Enfei He, Charles N. Moorefield, *Chem. Rev.*, **1999**, 99, 1689-1746.
7. (a) W. R. McWinnie, J. D. Miller, *Adv. Inorg. Chem. Radiochem.*, **1969**, 12, 135-215. (b) Edwin C. Constable, *Adv. Inorg. Chem. Radiochem.*, **1986**, 30, 69.
8. (a) Edwin C. Constable, Alexander M. W. Cargill Thompson, *New J. Chem.*, **1992**, 16, 855-867. (b) Kirchhoff J.R., McMillin D.R., Marnot P.A., Sauvage J.P., *J. Am. Chem. Soc.*, **1985**, 107, 1138. (c) Winkler J.R., Netzel T.L., Okumura M., Sutin N., *J. Am. Chem. Soc.*, **1987**, 109, 2381. (d) Jean-Paul Collin, Stephane Guillerez, Jean-Pierre Sauvage, Francesco Barigelletti, Luisa De Cola, Lucia Flamigni, Vincenzo Balzani, *Inorg. Chem.*, **1991**, 30, 4230-4238. (e) Constable E.C., Cargill Thompson A.M.W., Armaroli N., Balzani V., Maestri M., *Polyhedron*, **1992**, 20, 2707-2709. (f) Edwin C. Constable, Alexander M. W. Cargill Thompson, *J. Chem. Soc. Dalton Trans.*, **1994**, 1409-1418. (g) Edwin C. Constable, Alexander M. W. Cargill Thompson, *J. Chem. Soc. Chem. Commun.*, **1992**, 617-619. (h) George R. Newkome, Francesca Cardullo, Edwin C. Constable, Charles N. Moorefield, Alexander M. W. Cargill Thompson, *J. Chem. Soc. Chem. Commun.*, **1993**, 925-927. (i) Mauro Maestri, Nicola Armaroli, Vincenzo Balzani, Edwin C. Constable, Alexander M. W. Cargill Thompson, *Inorg. Chem.*, **1995**, 24, 2759-2767. (j)

- Edwin C. Constable, Alexander M. W. Cargill Thompson, *J. Chem. Soc. Dalton Trans.*, **1995**, 1615-1627. (k) Francesco Barigelletti, Lucia Flamigni, Vincenzo Balzani, Jean-Paul Collin, Jean-Pierre Sauvage, Edwin C. Constable, Alexander M. W. Cargill Thompson, *J. Chem. Soc. Chem. Commun.*, **1993**, 942. (l) Jean-Paul Collin, Stephane Guillerez, Jean-Pierre Sauvage, Francesco Barigelletti, Luisa De Cola, Lucia Flamigni, Vincenzo Balzani, *Inorg. Chem.*, **1992**, 31, 4112.
9. Jean-Francois Gohy, Bas G. G. Lohmeijer, Sunil K. Varshney, Ulrich S. Schubert, *Macromolecules*, **2002**, 35, 7427-7435.
10. G. R. Newkome, E. He, *J. Mater. Chem.*, **1997**, 7, 1237-1244.
11. (a) Constable E. C. *Macromol. Symp.* **1995**, 98, 503. (b) Kelch S, Rehahn M., *Macromolecules*, **1999**, 32, 5818. (c) Schütte M., Kurth D. G., Linford M. R., Cölfen H., Möhwald H., *Angew. Chem.*, **1998**, 110, 3058 and *Angew. Chem. Int. Ed. Engl.*, **1998**, 37, 2891. (d) Schubert U. S., Eschbaumer C., *Polym. Prepr.* **1999**, 40, 1070. (e) Schubert U. S., Hien O., Eschbaumer C., *Macromol. Rapid Commun.* **2000**, 21, 1156. (f) Schwab P. F. H., Levin M. D., Michl J., *Chem. Rev.*, **1999**, 99, 1863.
12. (a) Jean-Pierre Sauvage, Jean-Paul Collin, Jean-claude Chambron, Stephane Guillerez, Christophe Coudret, *Chem. Rev.*, **1994**, 94, 993-1019. (b) Stone M.L., Crosby G.A., *Chem. Phys. Lett.*, **1981**, 79, 169.
13. Dirk G. Kurth, Markus Schütte, Jin Wen, *Colloids and Surfaces*, **2001**, 8, 200, 633-644.

V

CHAPTER FIVE: CONCLUSIONS AND FUTURE PERSPECTIVES

5.1 INTRODUCTION

In this last chapter a short overview is given of the problems that occurred during the course of this work. Not only problems concerning the synthesis of the building blocks but also problems that can occur at a later stage of the project will be discussed in summary. This chapter furthermore includes possible solutions, adaptations or suggestions concerning the synthesis of the rods as well as the knots and perspectives for their later use in the formation of three-dimensional networks.

5.2 MOLECULAR RODS

5.2.1 MOLECULAR RODS: OLIGOPHENYLENES

4-Bromo-2,5,2'',5''-tetra-*n*-hexyl-4'''-trimethylsilyltetraphenyl (12) (Figure 5.1) was synthesized in excellent yields following literature procedures¹⁻³. All synthesis and results were in accordance with these published procedures.

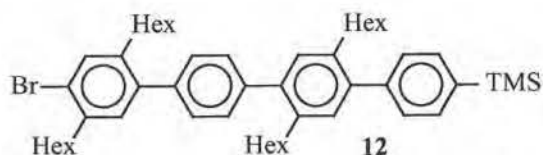


Figure 5.1: 4-Bromo-2,5,2'',5''-tetra-*n*-hexyl-4'''-trimethylsilyltetraphenyl

This tetraphenyl (**12**) can be used as a rigid rod as well as a half-rod depending on the functional groups at the termini. Changing these groups is easy and can be achieved with high yields. It is possible to synthesize longer oligomers via the same repetitive strategies. *Schluter et al*^{1,2} reported the synthesis of a series of monodisperse rigid-rods with up to 16 phenylene rings and with defined functional groups at both termini (Figure 5.2).

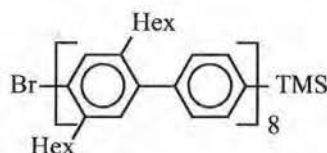


Figure 5.2: Hexadecaphenylene

The solubility, which was often a major drawback, is enhanced by the introduction of flexible side chains (hexyl). It can be enhanced even more by starting with monomers bearing longer side chains or poly-ether chains. Using this hexadecaphenylene instead of the 4-bromo-2,5,2'',5''-tetra-*n*-hexyl-4'''-trimethylsilyltetraphenyl (**12**) as a rigid rod between the molecular knots, decreases the density of the three dimensional network because of the strong increase in length going from tetraphenyl (**12**) to hexadecaphenyl derivatives.

It is possible that these oligophenylenes will be too flexible to be used as rigid linkers between the molecular knots. If the final network collapses too quickly when put under pressure, as an alternative fluorene rods can be used. The planes of the rings of adjacent phenylene moieties in *p*-oligophenylenes form an angle of 20-40° because of the steric repulsion between the ortho hydrogens^{4,5}. Substitution of the ring leads to an increase in twist angles. The twisted geometry and the reduced conjugation enhance the flexibility of the backbone. The repulsion, however, is not strong enough to prevent rapid rotation around a single bond between the units, and an average planar structure of the parent oligomer is the result. Planarization may be achieved by introduction of suitable ring-forming substituents as in for example oligofluorenes (Figure 5.3).

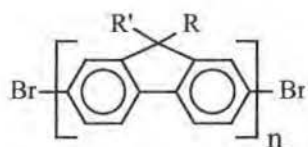


Figure 5.3: Oligofluorene

R and R' are e.g. long alkyl chains which maintain the solubility of the molecular rod. The "bridge" they form between the two adjacent phenylene units prevents the rotation and planarization is achieved.

5.2.2 MOLECULAR RODS: TERPYRIDINES

The poor solubility of the bis-terpyridine rods (Figure 5.4) bis[(2,2':6',2''-terpyridin-4'-yl)phenyl]ethyne (**18**), 1,4-bis(2,2':6',2''-terpyridin-4'-yl)benzene (**20**) and even 1,4-di[4-(4-ethynylphenyl)-2,2':6',2''-terpyridine]-2-(3,7-dimethyloctyl)-5-methoxybenzene (**22**) was a major drawback for processability at a later stage, therefore synthesis of better soluble bis-terpyridines was started.

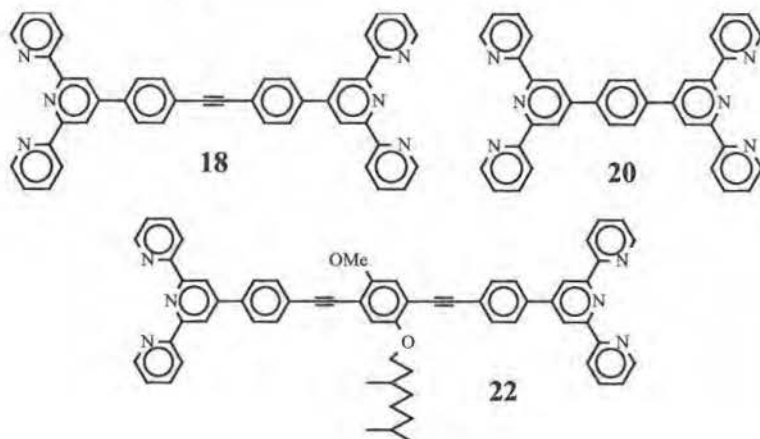
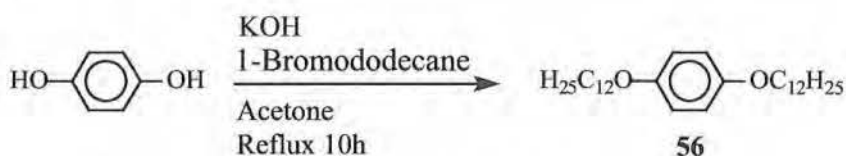


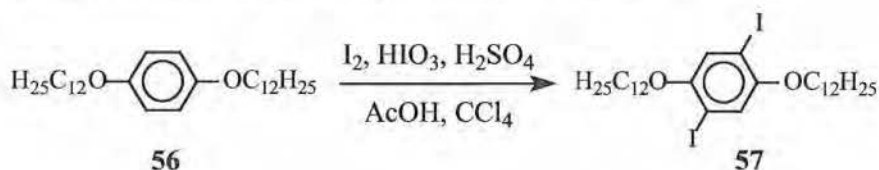
Figure 5.4: Bis-terpyridines

The synthesis of phenylene units bearing long flexible side chains such as e.g. 1,4-didodecanoxybenzene (**56**) were presumed to circumvent this problem (Scheme 5.1). To synthesize 1,4-didodecanoxybenzene (**56**) hydroquinone, 1-bromododecane and KOH were refluxed ten hours in acetone. Then water was added, the layers separated and the water layer extracted with diethyl ether. The combined organic phases were washed successively with 10% aqueous NaOH and brine, dried with MgSO_4 and the solvent evaporated. Recrystallization from diethyl ether gave 1,4-didodecanoxybenzene (**56**) as white crystals with 64% yield.



Scheme 5.1: Synthesis of 1,4-didodecanoxybenzene

This 1,4-didodecanoxybenzene (**56**) was iodinated with iodine, HIO_3 , 30% H_2SO_4 and CCl_4 in AcOH (Scheme 5.2) as described in literature⁶. It was heated for three hours at 75°C after which the mixture was cooled to room temperature. The crystals were filtered out and washed with a large amount of methanol and then recrystallized twice with ethanol to give 1,4-didodecanoxy-2,5-diiodobenzene (**57**) as a white powder with 82% yield.



Scheme 5.2: Synthesis of 1,4-didodecanoxy-2,5-diiodobenzene

This 1,4-didodecanoxy-2,5-diiodobenzene (**57**) is a precursor for the synthesis of soluble bisterpyridines (Figure 5.5) as described in literature⁷.

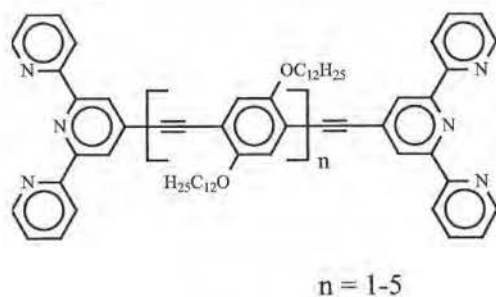
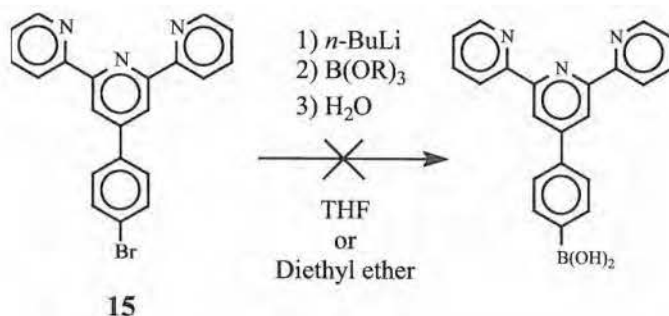


Figure 5.5: Soluble bis-terpyridine

These soluble and rigid terpyridine based ditopic ligands, bearing one to five ($n = 1$ to 5) phenylene/ethynylene modules, have been synthesized in literature via a stepwise procedure. A plausible way to extend the molecular length of these molecular rods without introducing undue solubility problems is to make use of 1,4-disubstituted phenylene fragments bearing solubilizing dodecyloxy groups in the 2,5-positions (**57**)⁸⁻¹⁰.

Another problem we were dealing with was the introduction of a boronic acid functionality into terpyridine ligand (**15**) (Scheme 5.3). The synthesis of this terpyridine ligand, provided with a boronic acid functionality, would be very useful for the creation of multi terpyridine-substituted molecular knots, since boronic acids couple easily with different kinds of aryl halides. The conventional route to aryl boronic acids involves the intermediary of the analogous aryllithium which is usually obtained by lithiation of the parent aryl bromide with *n*-butyllithium (See e.g. pg 36 Chapter Two). This reacts rapidly with electrophilic triisopropyl borate to generate the ester of the boronic acid, which is readily hydrolysed to the acid during work-up. However, attempts to prepare the boronic acid from 4'-(4-bromophenyl)-2,2'-6',2''-terpyridine (**15**) consistently failed (Scheme 5.3).



Scheme 5.3: Synthesis of boronic acid substituted terpyridine

Reactions were performed in THF as well as diethyl ether using equimolar or excesses of *n*-butyllithium, but none of them proved to be useful. In literature¹¹ the use of *n*-butyllithium or *tert*-butyllithium also proved equally unsuccessful. Therefore they used an alternative method for the preparation of arylboronates, namely the Miyaura¹² cross-coupling procedure. This method involves the palladium catalyzed coupling of the aryl halide with e.g. bis(pinacolato) diboron ($\text{Me}_4\text{C}_2\text{O}_2$) $_2$ B-B($\text{Me}_4\text{C}_2\text{O}_2$) (A) or pinacolborane^{13,14} (B) (Figure 5.6).

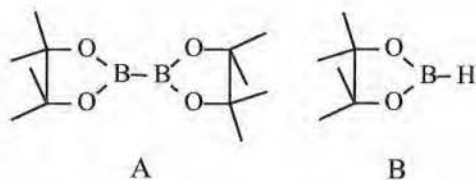
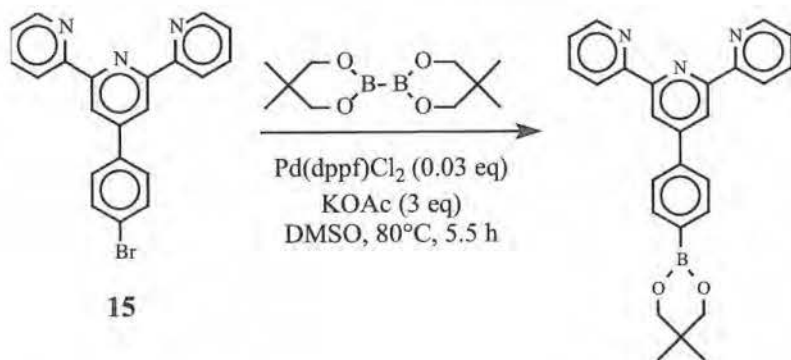


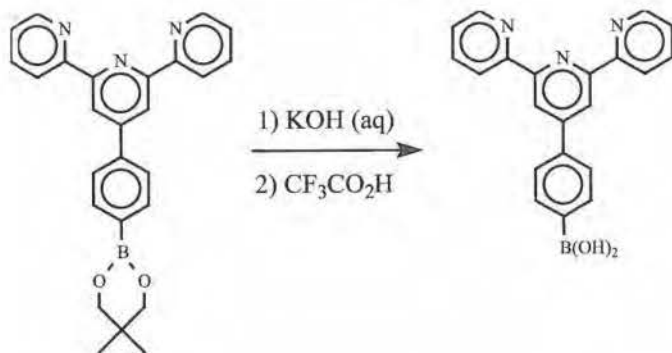
Figure 5.6: Bis(pinacolato) diboron (A) and pinacolborane (B)

Because the pinacolate ester is especially resistant to hydrolysis, bis(neopentyl glycolato)diboron (Scheme 5.4) was used instead of bis(pinacolato) diboron (A) or pinacolborane (B)



Scheme 5.4: Synthesis of 4'-{4-(neopentyl glycolatoboron)phenyl}-2,2':6',2''-terpyridine

This neopentyl glycolatoboron hydrolysed readily to the boronic acid (Scheme 5.5).



Scheme 5.5: Synthesis of phenylboronic acid appended 2,2':6',2''-terpyridine

This boronic acid can be used for coupling with e.g. 1,3,5,7-tetrakis(4-iodophenyl)adamantane (**29**) and 1,3,5,7-tetrakis(1,3-dibromophenyl)-adamantane (**38**) to create other similar highly functionalized molecular knots (Figure 5.7).

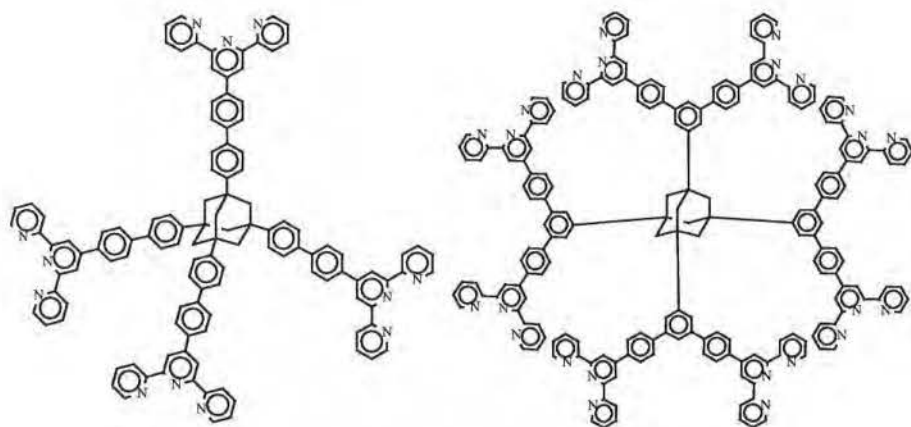
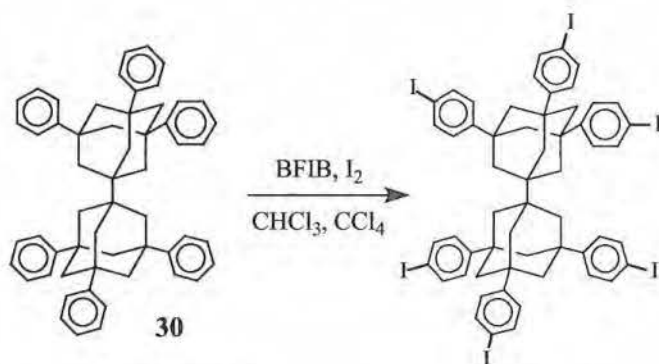


Figure 5.7: Terpyridine substituted molecular knots

5.3 MOLECULAR KNOTS

5.3.1 MOLECULAR KNOTS: ADAMANTANES AND DERIVATIVES

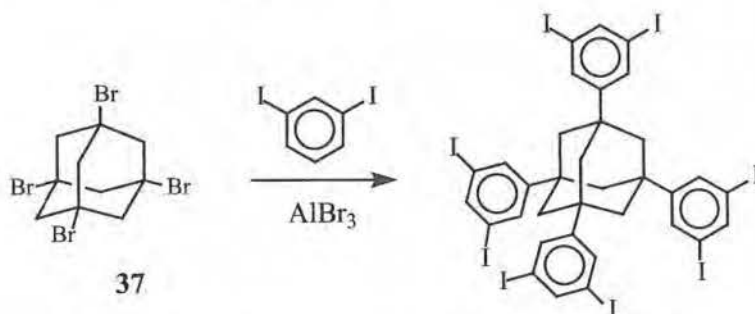
Because iodination of 1,3,5,7-tetraphenyladamantane (**28**) was possible with BFIB and I₂ in chloroform to give 1,3,5,7-tetrakis(4-iodophenyl)adamantane¹⁵ (**29**), similar reaction procedures could be repeated for iodination of 3,3',5,5',7,7'-hexaphenyl-1,1'-biadamantane (**30**) (Scheme 5.6).



Scheme 5.6: Synthesis of 3,3',5,5',7,7'-hexa-*p*-iodophenyl-1,1'-biadamantane

This 3,3',5,5',7,7'-hexa-*p*-iodophenyl-1,1'-biadamantane (**30**) is a rigid molecular knot which can couple at high yields with e.g. arylhalides and unprotected acetylenes via Pd catalyzed reactions since the aryl iodine is highly reactive towards these Pd catalyzed reactions.

Another reaction which is maybe a possibility to create a multifunctional molecular knot is the coupling of 1,3,5,7-tetrabromoadamantane (**37**) with 1,3-diiodobenzene and AlBr₃ as catalyst. Because the synthesis of 1,3,5,7-tetrakis(1,3-dibromophenyl)adamantane (**38**) from 1,3,5,7-tetrabromoadamantane (**37**) showed a lack of regioselectivity (NMR spectra showed evidence of "ortho" as well as "meta" isomer formation) (This was also observed in literature¹⁵), the same reaction procedure can be repeated with 1,3-diiodobenzene instead of 1,3-dibromobenzene (Scheme 5.7).



Scheme 5.7: Synthesis of 1,3,5,7-tetrakis(1,3-diiodophenyl)adamantane

It is possible that due to the more sterical hindrances of the iodine in comparison with the bromine (because the iodine is bigger than bromine) a higher selectivity is achieved.

5.3.2 MOLECULAR KNOTS: SILSESQUIOXANES

Despite the statement in literature¹⁶ that introduction of a halogen atom or a methyl substituent into the phenyl group of C₆H₅SiCl₃ would make the formation of the corresponding fully condensed phenylsilsesquioxanes much more difficult, we succeeded in the synthesis of octa(*p*-chlorophenyl)pentacyclo-[9.5.1.1^{3,9}.1^{5,15}.1^{7,13}]-octasiloxane (**42**) (Figure 5.8).

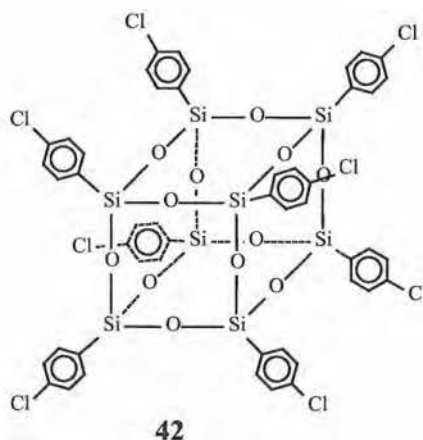


Figure 5.8: Octa(*p*-chlorophenyl)pentacyclo[9.5.1.1^{3,9}.1^{5,15}.1^{7,13}]-octasiloxane

Although recently high yield coupling reactions with chlorine are well-known¹⁷, the synthesis of monomers 4-bromophenyltrichlorosilane or 4-iodophenyltrichlorosilane (Figure 5.9) would be very interesting.



Figure 5.9: 4-Bromo/Iodophenyltrichlorosilane

If it is possible to synthesize octa(*p*-bromophenyl)pentacyclo[9.5.1.1^{3,9}.1^{5,15}.1^{7,13}]octasiloxane or octa(*p*-iodophenyl)pentacyclo[9.5.1.1^{3,9}.1^{5,15}.1^{7,13}]octasiloxane (Figure 5.10) via similar procedures as we have used for the synthesis of octa(*p*-chlorophenyl)pentacyclo[9.5.1.1^{3,9}.1^{5,15}.1^{7,13}]-octasiloxane (**42**), coupling reactions in milder conditions with the molecular rods can be performed.

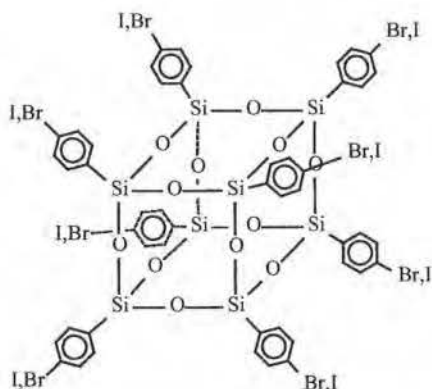


Figure 5.10: Octa(*p*-bromo/iodophenyl)pentacyclo[9.5.1.1.^{3,9}.1^{5,15}.1^{7,13}]-octasiloxane

Another advantage is the relative reactivity of the leaving group being iodine > bromine >> chlorine. Thus iodine and bromine have much better coupling properties with e.g. arylboronic acids and acetylenes in contradiction with chlorine. Therefore coupling reactions with iodine proceeds at much higher yields as with chlorine and consequently coupling with the molecular rods would perform more efficiently.

5.4 GENERAL CONCLUSIONS

During the course of this work, not only the unreliability of some of the published literature procedures caused problems, but also the poor solubility of some molecular knots and rods was cumbersome. To succeed in the creation of a soluble rigid network the two building blocks, the knot as well as the rods have to be soluble enough. It is possible that the rods have to be provided with polyether side chains in order to keep the network in solution. The solvation effect of the hydrogen bondings will give a better interaction with the solvent. For this reason it will keep the rods in solution while simple alkyl chains will not. The problems involving the solubility of the two building blocks were underestimated and have to be kept in mind for the synthesis of rigid knots and rods in the future.

For the synthesis of the three dimensional networks three different reaction types were proposed; two through formation of covalent bonds and one via complexation reactions.

The first covalent bonding type involves the palladium catalyzed coupling reaction of aryl halogenides with boronic acids. For this type of reaction molecular rods such as e.g. 4-bromo-2,5,2'',5''-tetra-*n*-hexyl-4'''-trimethylsilyl-tetraphenyl (**12**) and molecular knots as e.g. 1,3,5,7-tetrakis(4-iodophenyl)-adamantane (**29**) and 1,3,5,7-tetrakis(1,3-dibromophenyl)-adamantane (**38**) can be used.

The second reaction type involves a Diels-Alder reaction where coupling can be accomplished between a dienophile and an ethynyl compound. The test reaction with molecular knot 1,3,5,7-tetrakis(4-ethynyl)-phenyladamantane (**34**) and tetraphenylpentacyclodienone looked promising. Yields of more than 90% could be reached indicating the efficient coupling properties of these systems via Diels-Alder reactions. The advantages of this cycloaddition are that it is practically free of side reactions and that the equilibrium is shifted toward the products due to the irreversible loss of CO and the formation of a benzene ring. A retro-Diels-Alder reaction, therefore, cannot occur. Tetra-functionalized molecular knot 1,3,5,7-tetrakis(4-ethynyl)-phenyladamantane (**34**) can possibly couple with rigid bis-dienophyles e.g. 3.3'-(4,4'-biphenyl)-bis-(2.4.5-triphenyl-cyclopentadienon) to form rigid networks.

The third reaction type for the formation of three dimensional networks investigated was via complexation reactions. This method is a more 'elegant' method than the method based on covalent bond formation since the reversibility of the complexes offers the possibility for a systematic building up of the networks. Two reactions between the molecular knot 1,3,5,7-tetrakis[[4'-[4-{2-(phenyl)-1-ethynyl}phenyl]-2,2':6',2''-terpyridine]adamantane (**36**) and two flexible bisterpyridines were executed and are currently under investigation. The synthesis of the networks via complexation reactions was first investigated with these flexible bisterpyridines to examine whether it was possible to create soluble networks. In the future, shorter, rigid, highly soluble bisterpyridines will be needed to be used as a linker between multiple terpyridine substituted molecular knots to create rigid networks. In this way the goals set out at the beginning of this work may be achieved.

5.5 REFERENCES

1. Volker Hensel, A.-Dieter Schlüter, *Liebigs Ann. Recueil*, **1997**, 303-309.
2. Petra Liess, Volker Hensel, A.-Dieter Schlüter, *Liebigs Ann.*, **1996**, 1037-1040.
3. Matthias Rehahn, Arnulf-Dieter Schlüter, W. James Feast, *Synthesis*, **1988**, 386-388.
4. Peter F. H. Schwab, Michael D. Levin, Josef Michl, *Chem. Rev.*, **1999**, 99, 1863-1933.
5. James M. Tour, Jaydeep J. S. Lamba, *J. Am. Chem. Soc.*, **1993**, 115, 4935-4936.
6. Zhenan Bao, Yongming Chen, Rubing Cai, Luping Yu, *Macromolecules*, **1993**, 26, 5281-5286.
7. Abderrahim Khatyr and Raymond Ziessel, *J. Org. Chem.*, **2000**, 65, 3126-3134.
8. Shenlin Huang and James M. Tour, *J. Am. Chem. Soc.*, **1999**, 121, 4908-4909.
9. Schlicke B., Belzel P., De Cola L., Sabbioni E., Balzani P., *J. Am. Chem. Soc.*, **1999**, 121, 4207.
10. Khatyr A., Ziessel R., *Tetrahedron Lett.*, **1999**, 40, 5515-5518.
11. Catherine J. Aspley, J. A. Gareth Williams, *New J. Chem.*, **2001**, 25, 1136-1147.
12. Tatsuo Ishiyama, Miki Murata and Norio Miyaura, *J. Org. Chem.*, **1995**, 60, 7508-7510.
13. Miki Murata, Shinji Watanabe, and Yuzuru Masuda, *J. Org. Chem.*, **1997**, 62, 6458-6459.
14. Miki Murata, Tatsuo Ishiyama, Shinji Watanabe, and Yuzuru Masuda, *J. Org. Chem.*, **2000**, 65, 164-168.
15. Veronica R. Reichert, Lon J. Mathias *Macromolecules*, **1994**, 27, 7015-7023.
16. Mikhail G. Voronkov, Vladimir I. Lavrent'yev, *Topics in Current Chemistry*, **1982**, 102, 199-237.

17. (a) Chunming Zhang, Mark L. Trudell, *Tetrahedron Letters*, **2000**, 41, 595-598. (b) Harald Gröger, *J. Prakt. Chem.*, **2000**, 342, No. 4, 334-339. (c) John P. Wolfe, Robert A. Singer, Bryant H. Yang, Stephen L. Buchwald, *J. Am. Chem. Soc.* **1999**, 121, 9550-9561. (d) Alexander Zapf, Matthias Beller, *Chem. Eur. J.*, **2000**, 6, No. 10, 1830-1833. (e) Xiaohong Bei, Thomas Crevier, Anil S. Guram, Bernd Jandeleit, Timothy S. Powers, Howard W. Turner, Tetsuo Uno, W. Henry Weinberg, *Tetrahedron Letters*, **1999**, 40, 3855-3858. (f) Alexander Zapf, Andreas Ehrentraut, Matthias Beller, *Angew. Chem. Int. Ed.*, **2000**, 39, No. 22, 4153-4155. (g) Adam F. Littke, Gregory C. Fu, *Angew. Chem. Int. Ed.*, **1998**, 37, No. 24, 3387-3388. (h) Adam F. Littke, Chaoyang Dai, Gregory C. Fu, *J. Am. Chem. Soc.* **2000**, 122, 4020-4028. (i) John P. Wolfe, Stephen L. Buchwald, *Angew. Chem.*, **1999**, 111, No. 16, 2570-2573. (j) Xiaohong Bei, Howard W. Turner, W. Henry Weinberg, Anil S. Guram, *J. Org. Chem.*, **1999**, 64, 6797-6803. (k) John P. Wolfe, Stephen L. Buchwald, *Angew. Chem. Int. Ed.*, **1999**, 38 No. 16, 2413-2416. (l) David W. Old, John P. Wolfe, Stephen L. Buchwald, *J. Am. Chem. Soc.* **1998**, 120, 9722-9723. (m) Chunming Zhang, Jinkun Huang, Mark L. Trudell, Steven P. Nolan, *J. Org. Chem.*, **1999**, 64, 3804-3805. (n) Volker P. W. Böhm, Christian W. K. Gstöttmayr, Thomas Weskamp, Wolfgang A. Herrmann, *Journal of Organometallic Chemistry*, **2000**, 595, 186-190.

VI

CHAPTER SIX: EXPERIMENTAL PART

6.1 GENERAL REMARKS AND INSTRUMENTATION

Materials. All starting materials were obtained from commercial suppliers (Aldrich, Acros, Fluka, Strem, Riedel de Haen) and were used without purification. Solvents were used in HPLC grade purity as purchased. Diethylether and tetrahydrofuran were distilled under nitrogen from molten sodium benzophenone ketyl. All atmosphere-sensitive reactions were performed under argon or nitrogen. Analytical thin-layer chromatography (TLC) was performed on commercial Merck plates coated with silica gel. Visualization was accomplished with UV light. Flash chromatography was carried out with silica gel 60 (230-400 mesh) from Merck.

NMR analyses. ^1H -, ^{13}C -, and ^{29}Si -NMR analyses were performed in CDCl_3 and recorded on a Varian Inova 300 and 400 spectrometer. ^1H -NMR spectra were collected at 300 MHz using a 4395 Hz spectral width, a relaxation delay of 8 s, a pulse width of 40 μs , 65 K data points and CHCl_3 (7.241 ppm) as internal reference. ^{13}C -NMR spectra were obtained at 75 MHz using a 16000 Hz spectral width, a relaxation delay of 60 s to obtain fully quantitative spectra, a pulse width of 6.8 μs , 32 K data points and CDCl_3 (77.2 ppm) as internal reference. ^{29}Si -NMR spectra were collected at 79.6 MHz using a 70000 Hz spectral width, a pulse width of 7 μs , a relaxation delay of 60 s, 32 K data points and TMS as external reference.

Attached proton test (APT) spectra were acquired to discriminate between protonated and non-protonated aromatic carbon resonances.

Mass spectral analysis. Analyses were conducted on a Finningan TSQ-70 mass spectrometer (70 eV). Spectra were recorded by DCI-probe analysis (+ CI mode) with isobutane as reagent gas. MALDI-TOF mass spectra were measured using *o*-cyano-4-hydroxycinnamic acid as matrix.

Fourier Transform Infrared Spectra. Spectra were recorded on a Perkin Elmer spectrum one FT-IR spectrometer. KBr was used to prepare solid samples and liquid samples were recorded between salt plates.

Ultraviolet Visible Spectroscopy (UV-VIS). Spectra were recorded on a CARY 500 UV-VIS-NIR spectrophotometer (interval: 1nm, scan rate 600 nm/min, continuous run from 200 to 700 nm).

6.2 SYNTHESIS OF OLIGOPHENYLENES

1,4-Dihexylbenzene (1)

The hexylmagnesium bromide (378g, 2.0 mol, 2.5 eq) was added dropwise, over 15 min, to an ice cooled and stirred mixture of 1,4-dichlorobenzene (118g, 0.80 mol) and (dppp)Cl₂Ni (0.5g, 0.9 mmol) in diethylether (600 ml). The cooling bath was removed and the ether began to boil after an induction period of about 30 min. The mixture was then refluxed for 24 hours, cooled to 0 °C and carefully quenched with water (50 ml), followed by 2N HCl (500 ml). After separation of the layers, the aqueous layer was extracted with ether (2 x 200 ml), the combined organic layers were washed with H₂O (100 ml) and dried with MgSO₄. The solvent was removed in vacuo and the crude product was distilled through a Vigreux column to give 1,4-dihexylbenzene (1) as a viscous oil (156.9g, 0.631 mol, 80%). ¹H-NMR (CDCl₃): δ 0.89 (t, J = 6.9 Hz, 6H, CH₃); 1.26-1.38 (m, 12H, CH₂); 1.56-1.68 (m, 4H, CH₂); 2.58 (t, J = 7.8 Hz, 4H, α-CH₂); 7.10 (s, 4H, ph). MS (EI, m/e) = 246 (M⁺); 175 (M⁺ - C₅H₁₁).

2,5-Dibromo-1,4-dihexylbenzene (2)

Bromine (120.7g, 0.75 mol, 2.05 eq) was added dropwise, over 45 min, to a stirred and ice-cooled solution of 1,4-dihexylbenzene (1) (90.7g, 0.37 mol) and iodine (0.46g, 3.2 mmol), in dark. After 24 hours at room temperature, 20% aq. KOH solution (230 ml) was added and the mixture was shaken under slight warming until the color disappears. The mixture was cooled to room temperature, the aqueous solution decanted, and the remaining residue was recrystallized twice from EtOH to give 2,5-dibromo-1,4-dihexylbenzene (2) as white crystals (98g, 0.246 mol, 76%). ¹H-NMR (CDCl₃): δ 0.88 (t, J = 6.9 Hz, 6H, CH₃); 1.24-1.40 (m, 12H, CH₂); 1.51-1.60 (m, 4H, CH₂); 2.62 (t, J = 7.8 Hz, 4H, α-CH₂); 7.34 (s, 2H, ph). MS (EI, m/e) = 404 (M⁺); 333 (M⁺ - C₅H₁₁); 253 (M⁺ - C₅H₁₁Br).

1-Bromo-2,5-di-*n*-hexyl-4-trimethylsilylbenzene (3)

To a suspension of 2,5-dibromo-1,4-dihexylbenzene (2) (75g, 185.5 mmol) in diethyl ether (1000 ml) at -78 °C, *n*-butyllithium (96.5 ml, 241 mmol, 2.5M solution in hexane) was added over a period of an hour. The reaction mixture was allowed to warm up to 0 °C. The colourless solution was then cooled once again to -78 °C and trimethylchlorosilane (40.3g, 371 mmol) was added over a period of 30 min. The reaction mixture was allowed to warm to room temperature over 12 h and H₂O (500 ml) was added. The layers were separated, the aqueous layer was washed with diethyl ether (2 x 200 ml) and the combined organic layers were washed with H₂O (2 x 200 ml). The organic phase was dried over MgSO₄. Vacuum distillation gave 1-bromo-2,5-di-*n*-hexyl-4-trimethylsilylbenzene (3) as a colourless oil (67.5g, 169 mmol, 92%). ¹H-NMR (CDCl₃): δ 0.34 (s, 9H, TMS); 0.93 (m, 6H, CH₃); 1.33-1.40 (m, 12H, CH₂); 1.55-1.62 (m, 4H, CH₂); 2.68 (m, 4H, α-CH₂); 7.27 (s, 1H, ph); 7.40 (s, 1H, ph). MS (EI, m/e) = 398 (M⁺); 383 (M⁺ - CH₃); 325 (M⁺ - TMS).

4-Bromo-2,5-di-*n*-hexyl-1-iodobenzene (4)

To a solution of 1-bromo-2,5-di-*n*-hexyl-4-trimethylsilylbenzene (3) (30.0g, 75.5 mmol) in CCl₄ (150 ml) at 0 °C, a solution of ICl (13.4g, 82.7 mmol) in CCl₄ (50 ml) was added over 20 min. The reaction mixture was allowed to warm to room temperature over a period of 30 min. An aqueous solution of sodium disulfite (100 ml, 1M) was then added. The layers were

separated, the aqueous layer was washed with CCl_4 (2 x 50 ml) and the combined organic layers were washed with water (2 x 50 ml). The organic phase was dried over MgSO_4 . Chromatographic separation on silica gel with hexane gave 4-bromo-2,5-di-*n*-hexyl-1-iodobenzene (**4**) as colourless crystals. (32.2g, 71.55 mmol, 95%). $^1\text{H-NMR}$ (CDCl_3): δ 0.88 (t, $J = 6.3$ Hz, 6H, CH_3); 1.30-1.40 (m, 12H, CH_2); 1.48-1.56 (m, 4H, CH_2); 2.59 (t, $J = 7.8$ Hz, 4H, $\alpha\text{-CH}_2$); 7.31 (s, 1H, ph); 7.60 (s, 1H, ph). MS (EI, m/e) = 450 (M^+); 379 ($\text{M}^+ - \text{C}_5\text{H}_{11}$); 253 ($\text{M}^+ - \text{C}_5\text{H}_{11}\text{I}$).

2,5-Di-*n*-hexyl-4-trimethylsilylbenzene-1-boronic acid (**5**)

To a solution of 1-bromo-2,5-di-*n*-hexyl-4-trimethylsilylbenzene (**3**) (27.4g, 69.0 mmol) in a mixture of diethyl ether (500 ml) and tetrahydrofuran (500 ml) at -78°C a solution of *n*-butyllithium (82.8 ml, 207 mmol, 2.5M in hexane) was added over a period of 30 min. and the reaction mixture was allowed to warm to -10°C . The solution was then cooled once again to -78°C and triisopropyl borate (51.9g, 276 mmol) was added over a period of 60 min. The reaction was allowed to warm to room temperature and stirred overnight. Water (400 ml) was added and the layers were separated. The aqueous layer was washed with diethylether (2 x 200 ml) and the combined organic layers were washed with water (2 x 200 ml). The organic phase was dried over MgSO_4 . Chromatographic separation on silica gel with (a) hexane and (b) hexane/ethyl acetate (3/1) gave 2,5-di-*n*-hexyl-4-trimethylsilylbenzene-1-boronic acid (**5**) (18.6g, 51.5 mmol, 78%) as a colourless oil. $^1\text{H-NMR}$ (CDCl_3): δ 0.34 (s, 9H, TMS); 0.75-0.89 (m, 6H, CH_3); 1.20-1.65 (m, 16H, CH_2); 2.71 (t, $J = 8.1$ Hz, 2H, $\alpha\text{-CH}_2$); 3.14 (t, $J = 7.8$ Hz, 2H, $\alpha\text{-CH}_2$); 7.35 (s, 1H, ph); 7.98 (s, 1H, ph). $^1\text{H-NMR}$ (DMSO): δ 0.24 (s, 9H, TMS); 0.82-0.88 (m, 6H, Me); 1.24-1.50 (m, 16H, CH_2); 2.56 (t, $J = 8$ Hz, 2H, $\alpha\text{-CH}_2$); 2.64 (t, $J = 8$ Hz, 2H, $\alpha\text{-CH}_2$); 7.11 (s, 1H, ph); 7.19 (s, 1H, ph); 7.96 (s, 2H, $\text{B}(\text{OH})_2$). MS (EI, m/e) = 1036 (trimer, M^+).

4-Biphenylboronic acid (**6**)

n-Butyllithium (12.3ml, 15.4 mmol, 2.5 M solution in hexane) was added to a solution of 4-bromobiphenyl (4.6g, 20 mmol) in dry diethylether (100 ml) at -78°C . The mixture was allowed to warm up to room temperature and stirred at 25°C for 1h. The resulting solution was added dropwise to a cooled

(-78 °C) solution of trimethyl borate (9.2 ml, 40.8 mmol) in Et₂O (120 ml). After complete addition, the mixture was allowed to warm up to room temperature, and stirred for a further 12 h at 25 °C. Subsequently, 3M HCl (120 ml) was added. The organic layer was separated, washed with H₂O (2 x 150 ml) and dried over MgSO₄. The crude product was dissolved in hot toluene ((100 ml (depending of quantity of the product))) and the resulting solution was filtered through a column of silica gel with toluene as the eluent to remove all the impurities. Pure product was eluted with acetone as the mobile phase. The solvent was removed in vacuo and the residue was dissolved in hot toluene (100 ml). After cooling to room temperature, diluted HCl (200 ml) was added, and the mixture was stirred for a further 12 h. Finally, the white solid was filtered and dried in vacuo to give 4-biphenylboronic acid (**6**) (1.34g, 6.6 mmol, 33%) as a white solid. ¹H-NMR (CDCl₃): δ 7.44 (m, 3H); 7.64 (m, 3H); 7.77 (m, 2H); 8.33 (d, J = 8 Hz, 1H). MS (EI, m/e) = 198 (M⁺), 180 (M⁺-H₂O); 153 (M⁺-B(OH)₂).

1-Bromo-4-trimethylsilylbenzene (**7**)

A 1-L 3-necked flask, equipped with a mechanical stirrer, thermometer, addition funnel, nitrogen inlet and cooling bath, was charged with 1,4-dibromobenzene (66.7g, 0.283 mol) and *t*-butyl methyl ether (285 ml). The solution was cooled to 0-5°C and *n*-butyllithium (113.06 ml, 0.283 mol, 2.5M in hexane) was added over a period of 30 minutes while maintaining an internal temperature of 5-10°C. The reaction was stirred for 15 minutes. Chlorotrimethylsilane (36 ml, 0.283 mol) was added over a period of 20 minutes while maintaining an internal temperature of 15-18°C. The mixture was warmed to 20-22°C and allowed to stir for 1.5 hours. A solution of saturated aqueous ammonium chloride in water (70 ml) was added over a period of 15 minutes while maintaining an internal temperature of 22-23°C. The solution was stirred for 15 minutes and the layers were separated. The organic layer was filtered by suction through Celite (50g). The filtrate was concentrated under reduced pressure. Distillation (105-115°C 25-30mm) gave 1-bromo-4-trimethylsilylbenzene (**7**) (58.9g, 257 mmol, 91%) as a colourless oil. ¹H-NMR (CDCl₃): δ 0.24 (s, 9H, TMS); 7.35 (d, J = 7.8 Hz, 2H, ph); 7.47 (d, J = 7.8Hz, 2H, ph). MS (EI, m/e) = 231 (M⁺); 215 (M⁺-CH₃).

4-Trimethylsilylbenzene-1-boronic acid (8)

To a solution of 1-bromo-4-trimethylsilylbenzene (7) (30.0g, 131 mmol) in a mixture of diethylether (600 ml) and tetrahydrofuran (600 ml) at -78°C , *n*-butyllithium (68 ml, 170 mmol, 2.5 M solution in hexane) was added dropwise. The reaction was stirred for 1 hour at -78°C . Triisopropyl borate (49.25g, 60.8 ml, 262 mmol) in diethylether (50 ml) was added dropwise and the reaction mixture was allowed to warm to room temperature overnight. Water (500 ml) was added and the layers were separated. The aqueous layer was washed with diethylether (2 x 250 ml) and the combined organic layers were washed with water (2 x 250 ml). The organic phase was dried over MgSO_4 . Chromatographic separation on silicagel with (a) CHCl_3 and (b) $\text{CHCl}_3/\text{MeOH}$ (20:1) gave 4-trimethylsilylbenzene-1-boronic acid (8) (19.0g, 98 mmol, 75%). $^1\text{H-NMR}$ (CDCl_3): δ 0.33 (s, 9H, TMS); 7.68 (d, $J = 7.8$ Hz, 2H, ph); 8.20 (d, $J = 7.8$ Hz, 2H, ph). $^1\text{H-NMR}$ (DMSO): δ 0.23 (s, 9H, TMS); 7.47 (d, $J = 7.2$ Hz, 2H, ph); 7.75 (d, $J = 7.2$ Hz, 2H, ph); 8.06 (s, 2H, $\text{B}(\text{OH})_2$). MS (EI, m/e) = 585 (trimer, M^+).

4-Bromo-2,5-di-*n*-hexyl-4'-trimethylsilylbiphenyl (9)

4-Trimethylsilylbenzene-1-boronic acid (8) (15g, 92.78 mmol) and 4-bromo-2,5-di-*n*-hexyl-1-iodobenzene (4) (34.8g, 92.78 mmol) were dissolved in toluene (230 ml). The solution was degassed and flushed with N_2 . An aqueous 1 M solution of Na_2CO_3 (175 ml) was added and the solution degassed again. Tetrakis(triphenylphosphine)-palladium(0) (525mg) was added and the mixture was refluxed for 48 hours. The mixture was allowed to cool to room temperature and the layers were separated. The aqueous layer was washed with toluene (2 x 50 ml) and the combined organic layers with water (50 ml). The organic layer was dried over MgSO_4 . Chromatographic separation on silicagel with hexane as eluents gave 4-bromo-2,5-di-*n*-hexyl-4'-trimethylsilylbiphenyl (9) as a colourless oil. (39.47g, 83.4 mmol, 90%). $^1\text{H-NMR}$ (CDCl_3): δ 0.3 (s, 9H, TMS); 0.83 (t, $J = 7.2$ Hz, 3H, CH_3); 0.87 (t, $J = 7.2$ Hz, 3H, CH_3); 1.12-1.62 (m, 16H, CH_2); 2.49 (t, $J = 8.1$ Hz, 2H, $\alpha\text{-CH}_2$); 2.68 (t, $J = 7.8$ Hz, 2H, $\alpha\text{-CH}_2$); 7.03 (s, 1H, ph); 7.25 (d, $J = 7.8$ Hz, 2H, ph); 7.43 (s, 1H, ph); 7.54 (d, $J = 7.8$ Hz, 2H, ph). MS (EI, m/e) = 474 (M^+); 401 ($\text{M}^+ - \text{TMS}$).

4-Bromo-2,5-di-*n*-hexyl-4'-iodobiphenyl (10)

To a stirred and ice-cooled solution of 4-bromo-2,5-di-*n*-hexyl-4'-trimethylsilylbiphenyl (**9**) (6.6g, 14.01 mmol) in CCl₄ (50 ml), a solution of iodine monochloride (2.4g, 15 mmol) in CCl₄ (25 ml) was slowly added. After stirring for 12 h at room temperature, an aqueous solution of sodium disulfite (1M, 25ml) was added. The layers were separated, the aqueous layer washed with CCl₄ (2 x 10 ml) and the combined organic layers were washed with water (10 ml). The organic layer was dried over MgSO₄. Chromatographic separation on silica gel with hexane/acetic acid ethyl ester (9:1) gave 4-bromo-2,5-di-*n*-hexyl-4'-iodobiphenyl (**10**) (6.21g, 11.82 mmol, 85%) as a colourless oil. ¹H-NMR (CDCl₃): δ 0.84 (m, 6H); 1.15-1.60 (m, 16H); 2.45 (t, J = 8.1 Hz, 2H); 2.67 (t, J = 8.1 Hz, 2H); 6.97 (s, 1H); 7.01 (d, J = 8.4 Hz, 2H); 7.42 (s, 1H); 7.71 (d, J = 8.4 Hz, 2H). MS (EI, m/e) = 526 (M⁺).

2,5-Di-*n*-hexyl-4'-trimethylsilylbiphenyl-4-boronic acid (11)

To a solution of 4-bromo-2,5-di-*n*-hexyl-4'-trimethylsilylbiphenyl (**9**) (14g, 30 mmol) in diethylether (50 ml) at -78 °C, *n*-butyllithium (14 ml, 36 mmol, 2.5M in hexane) was added. After 2 hours the solution was slowly added to triisopropylborate (21 ml, 90 mmol). The reaction mixture was allowed to come to room temperature overnight. Water (50 ml) was added and the layers were separated. The aqueous layer was washed with diethylether (2 x 30 ml) and the combined organic layers with water (2 x 30 ml). The organic layer was dried over MgSO₄. Chromatographic separation through silica gel with (a) hexane and (b) diethylether gave 2,5-di-*n*-hexyl-4'-trimethylsilylbiphenyl-4-boronic acid (**11**) (8.6g, 19.6 mmol, 65%) as a white powder. ¹H-NMR (acetone): δ 0.31 (s, 9H, TMS); 0.77-0.86 (m, 6H, CH₃); 1.15-1.80 (m, 16H, CH₂); 2.55 (t, J = 8.1 Hz, 2H, α-CH₂); 2.70 (t, J = 8.1 Hz, 2H, α-CH₂); 6.96 (s, 1H, ph); 7.30 (d, J = 8.4 Hz, 2H, ph); 7.51 (s, 1H, ph); 7.60 (d, J = 8.4 Hz, 2H, ph); 8.21 (s, 2H, B(OH)₂). MS (EI, m/e) = 1260 (trimer, M⁺).

4-Bromo-2,5,2'',5''-tetra-*n*-hexyl-4''''-trimethylsilyltetraphenyl (12)

2,5-Di-*n*-hexyl-4'-trimethylsilylbiphenyl-4-boronic acid (**11**) (3g, 6.85 mmol) and 4-bromo-2,5-di-*n*-hexyl-4'-iodobiphenyl (**10**) (3.6g, 6.85 mmol) were dissolved in toluene (55 ml) the solution was degassed and purged

with N₂ repeatedly. An aqueous solution of Na₂CO₃ (1M, 21 ml) was added. The system was degassed again and tetrakis(triphenylphosphine)palladium(0) (50 mg) was added. The mixture was refluxed for 48 hours with vigorous stirring. The mixture was allowed to cool to room temperature and the layers were separated. The aqueous layer washed with toluene (2 x 30 ml) and the combined organic layers with water (30 ml). The organic layer was dried over MgSO₄. Chromatographic separation through silica gel with hexane gave 4-bromo-2,5,2'',5''-tetra-*n*-hexyl-4''''-trimethylsilyltetraphenyl (**12**) (3.58g, 4.51 mmol, 66%) as a white powder. ¹H-NMR (CDCl₃): δ 0.30 (s, 9H, TMS); 0.78-0.90 (m, 12H, CH₃); 1.17-1.62 (m, 32H); 2.56 (m, 6H); 2.70 (m, 2H); 7.10 (s, 1H); 7.13 (s, 1H); 7.17 (s, 1H); 7.31 (d, J = 8.1 Hz, 2H); 7.35 (d, J = 8.1 Hz, 2H); 7.38 (d, J = 8.1 Hz, 2H); 7.44 (s, 1H); 7.56 (d, J = 8.1 Hz, 2H). MS (EI, m/e) = 794 (M⁺); 714 (M⁺-Br).

6.3 SYNTHESIS OF TERPYRIDINES

E)-3-(4''-Bromophenyl)-1-(pyrid-2'-yl)prop-2-enone (**13**)

4-Bromobenzaldehyde (37.0g, 200 mmol) was dissolved in MeOH (500 ml). 1M NaOH (150 ml) and 2-acetylpyridine (25.6g, 211 mmol) was added and the reaction mixture was stirred for 30 min. The resulting precipitate was filtered off, dissolved in CH₂Cl₂ and washed with water (100 ml). The organic phase was dried over MgSO₄, filtered, and evaporated. The residue was recrystallized twice from methanol to give E)-3-(4''-bromophenyl)-1-(pyrid-2'-yl)prop-2-enone (**13**) as a light yellow solid (38g, 132 mmol, 66%). ¹H-NMR (CDCl₃): δ 7.49 (m, 1H, H₃Py); 7.51 (d, J = 8.8 Hz, 2H, ph); 7.53 (d, J = 8.8 Hz, 2H, ph); 7.82 (d, J = 16.0 Hz, 1H, CH); 7.87 (td, J = 1.6, 7.6 Hz, 1H, H₄Py); 8.15 (d, J = 7.6 Hz, 1H, H₃Py); 8.25 (d, J = 16.0 Hz, 1H, CH); 8.71 (ddd, J = 0.8, 1.6, 7.6 Hz, 1H, H₅Py). MS (EI, m/e) = 287 (M⁺); 260 (M⁺-NCH₂); 180 (M⁺-NCH₂Br).

N-[2-(pyrid-2'-yl)-2-oxoethyl]pyridinium iodide (**14**)

To a solution of 2-acetylpyridine (24.2g, 200 mmol) in dry pyridine (50 ml) was added a solution of I₂ (51g, 200 mmol) in dry pyridine (150 ml). The reaction mixture was refluxed for 3 h and allowed to stand still overnight.

The crystals were filtered and washed with pyridine. The crystals were recrystallized twice from ethanol/water (1/5) to give N-[2-(pyrid-2'-yl)-2-oxoethyl]pyridinium iodide (**14**) as glittering light brown crystals (48.5g, 148 mmol, 75%). ¹H-NMR (DMSO): δ 6.51 (s, 2H, CH₂); 7.83 (ddd, J = 1.2, 4.8, 7.6 Hz, 1H); 8.07 (dd, J = 1.2, 7.6 Hz, 1H); 8.14 (td, J = 1.6, 7.6 Hz, 1H); 8.28 (dd, J = 6.0, 7.6 Hz, 2H); 8.73 (t, J = 7.6 Hz, 1H); 8.88 (ddd, J = 0.8, 1.6, 4.8 Hz, 1H); 9.01 (d, J = 6.0 Hz, 2H). MS (+FAB) = 369 (M⁺); 199 (M⁺ - I).

4'-(4'''-Bromophenyl)-2,2':6',2''-terpyridine (**15**)

E)-3-(4''-Bromophenyl)-1-(pyrid-2'-yl)prop-2-enone (**13**) (5.8g, 20.0 mmol), N-[2-(pyrid-2'-yl)-2-oxoethyl]pyridinium iodide (**14**) (6.2g, 20.0 mmol), and ammonium acetate (40.0g, 510 mmol) were dissolved in glacial acetic acid (40 ml) and refluxed for 7 hours. The reaction mixture was kept at room temperature overnight and was then made alkaline by addition of NaOH (10M, 70 ml). The reaction mixture was extracted with CH₂Cl₂ (5 x 100 ml). The combined organic phases were dried with MgSO₄ and evaporated. The crude product was recrystallized with acetonitrile to give 4'-(4'''-bromophenyl)-2,2':6',2''-terpyridine (**15**) (5.4g, 13.65 mmol, 68%) as white needles. ¹H-NMR (CDCl₃): δ 7.39 (ddd, J = 1.2, 4.8, 7.6 Hz, 2H, H_{5,5'}-Py); 7.62 (d, J = 8.8 Hz, 2H, ph); 7.79 (d, J = 8.8 Hz, 2H, ph); 7.91 (td, J = 1.6, 7.6 Hz, 2H, H_{4,4'}-Py); 8.69 (d, J = 7.6 Hz, 2H, H_{3,3'}-Py); 8.72-8.73 (m, 2H, H_{6,6'}-Py); 8.74 (s, 2H, H_{3,3'}-Py). MS (EI, m/e) = 389 (M⁺); 308 (M⁺ - Br); 229 (M⁺ - PyBr); 154 (M⁺ - PphBr).

4'-[4-{2-(Trimethylsilyl)-1-ethynyl}phenyl]-2,2':6',2''-terpyridine (**16**)

To a stirred solution of 4'-(4'''-bromophenyl)-2,2':6',2''-terpyridine (**15**) (2g, 5.15 mmol) and trimethylsilylacetylene (1.49 ml, 10.5 mmol) in *n*-propylamine (180 ml) was added dropwise a solution of [Pd(PPh₃)₄] (0.36g, 0.312 mmol, 6 mol%) in *n*-propylamine (150 ml). The mixture was refluxed at 60 °C overnight. The solvent was evaporated and chromatographic separation on silicagel, with chloroform as eluents, gave 4'-[4-{2-(trimethylsilyl)-1-ethynyl}phenyl]-2,2':6',2''-terpyridine as a yellow powder. The product was recrystallized in acetonitrile to give 4'-[4-{2-(trimethylsilyl)-1-ethynyl}phenyl]-2,2':6',2''-terpyridine (**16**) (1.9g, 4.96 mmol, 91%) as white needles. ¹H-NMR (300 MHz, CDCl₃, 25° C): δ 0.26 (s, 9H, TMS); 7.34 (ddd, J

= 1.2, 4.8, 7.6 Hz, 2H, H_{5,5'}Py); 7.59 (d, J = 8.4 Hz, 2H, ph); 7.84 (d, J = 8.4 Hz, 2H, ph); 7.86 (td, J = 1.6, 7.6 Hz, 2H, H_{4,4'}Py); 8.65 (d, J = 7.6 Hz, 2H, H_{3,3'}Py); 8.69-8.72 (m, 2H, H_{6,6'}Py); 8.70 (s, 2H, H_{3',5'}Py). ¹³C-NMR (75 MHz, CDCl₃, 25° C) δ 0.70 (3C, CH₃); 96.47 (1C, C≡C-TMS); 105.43 (1C, C≡C-TMS); 119.14 (2C, C_{3',5'}Py); 121.95 (2C, C_{3,3'}Py); 124.49 (3C, C₁ph, C_{5,5'}Py); 127.71 (2C, C_{3,5}ph); 133.14 (2C, C_{2,6}ph); 137.47 (2C, C_{4,4'}Py); 138.88 (1C, C₄ph); 149.67 (3C, C_{4',6,6'}Py); 156.49 (2C, C_{2,2',2'',6'}Py); 156.58 (2C, C_{2,2',2'',6'}Py). MS (EI, m/e) = 405 (M⁺); 390 (M⁺-CH₃); 308 (M⁺-C≡C-TMS).

4'-(4-Ethynylphenyl)-2,2':6',2''-terpyridine (17)

To a stirred solution of 4'-[4-{2-(trimethylsilyl)-1-ethynyl}phenyl]-2,2':6',2''-terpyridine (16) (2.3g, 5.66 mmol) in a mixture of THF (96 ml) and methanol (60 ml) was added KF (0.36g, 6.2 mmol, 1.2 eq). The mixture was stirred overnight and the solution was concentrated by rotary evaporation. The crude product was purified by flash chromatography with CHCl₃ as eluents to give 4'-(4-ethynylphenyl)-2,2':6',2''-terpyridine (17) (1.7g, 5.11 mmol, 90%) as a white powder. ¹H-NMR (CDCl₃): δ 3.17 (s, 1H, acetylene); 7.39 (ddd, J = 1.2, 4.8, 7.6 Hz, 2H, H_{5,5'}Py); 7.61 (d, J = 8.4 Hz, 2H, ph); 7.89 (d, J = 8.4 Hz, 2H, ph); 7.92 (td, J = 1.6, 7.6 Hz, 2H, H_{4,4'}Py); 8.69-8.74 (m, 4H, H_{3',5',6,6'}Py); 8.77 (s, 2H, H_{3',5'}Py). MS (EI, m/e) = 333 (M⁺).

Bis[(2,2':6',2''-terpyridin-4'-yl)phenyl]ethyne (18)

To a stirred solution of 4'-(4-ethynylphenyl)-2,2':6',2''-terpyridine (17) (1.0g, 3.0 mmol) and 4'-(4''-bromophenyl)-2,2':6',2''-terpyridine (15) (1.17, 3.0 mmol) in *n*-propylamine (180 ml) was added a solution of Pd[P(Ph)₃]₄ (0.21g, 0.18 mmol) in *n*-propylamine (30 ml). The mixture was refluxed at 60 °C overnight during which a yellow solid precipitated. The yellow solid was filtered off and washed several times with *n*-propylamine to give bis[(2,2':6',2''-terpyridin-4'-yl)phenyl]ethyne (18) (1.82g, 2.84 mmol, 95%) as a light yellow solid. MS (EI, m/e) = 640 (M⁺).

1,4-Bis[1,5-dioxo-1,5-bis(2-pyridyl)pentan-3-yl]benzene (19)

Acetylpyridine (43.6 ml, 0.36 mol) was added to a stirred solution of benzene-1,4-dicarbaldehyde (10.7g, 0.08 mol) in warm ethanol (800 ml). After

2 min, aqueous sodium hydroxide (1M, 40 ml) was added. The solution immediately darkened in color and a white precipitate was formed. After stirring for 8 hours at room temperature, the precipitate was collected by filtration, washed well with ethanol (3 x 100 ml) to give the tetraketone 1,4-bis[1,5-dioxo-1,5-bis(2-pyridyl)pentan-3-yl]benzene (**19**) (22.1g, 0.038 mol, 48%) as a white solid. MS (EI, m/e) = 582 (M^+); 476 (M^+ - PyCO).

1,4-Bis(2,2':6',2''-terpyridin-4'-yl)benzene (**20**)

A suspension of 1,4-bis[1,5-dioxo-1,5-bis(2-pyridyl)pentan-3-yl]benzene (**19**) (10g, 17.24 mmol) and ammonium acetate (50 g) in ethanol (500 ml) was heated to reflux for 5 days. After this time, the reaction mixture was cooled, and the solid product collected by filtration, washed well with ethanol (3 x 100 ml) and dried in vacuo to yield 1,4-bis(2,2':6',2''-terpyridin-4'-yl)benzene (**20**) (1.7g, 3.1 mmol, 19%) as a brown solid. $^1\text{H-NMR}$ (CDCl_3): δ 7.37 (dd, $J = 4.8, 7.5$ Hz, 4H, H_5); 7.92 (dd, $J = 1.8, 7.5$ Hz, 4H, H_4); 8.06 (s, 4H, ph); 8.68 (d, $J = 7.5$ Hz, 4H, H_3); 8.75 (d, $J = 4.8$ Hz, 4H, H_6); 8.80 (s, 4H, H_3). MS (EI, m/e) = 540 (M^+).

1,4-Dibromo-2-(3,7-dimethyloctyl)-5-methoxybenzene (**21**)

1-(3,7-Dimethyloctyl)-4-methoxybenzene (26.4g, 0.1 mol) and NBS (53.4g, 0.15 mol) were dissolved in CHCl_3 (120 ml) and acetone (120 ml) and refluxed for 24 hours. NBS (4g, 11.2 mmol) was added and the mixture refluxed for another 16 hours. The reaction mixture was poured into H_2O (200 ml), the layers separated and the organic layer washed successively with Na_2SO_3 (2 x 100 ml), Na_2CO_3 (2 x 100 ml), diluted HCl, and H_2O until pH = 7. The solvent was evaporated and chromatographic separation on silicagel with CHCl_3 /hexane (3:7) gave 1,4-dibromo-2-(3,7-dimethyloctyl)-5-methoxybenzene (**21**) (31.9g, 75.6 mmol, 76%) as a colourless oil. $^1\text{H-NMR}$ (CDCl_3): δ 0.84, 0.86 (s, (2x3)H, CH_3); 0.91, 0.93 (s, 3H, CH_3); 1.12-1.85 (m, 10H, CH_2); 3.82 (s, 3H, OMe); 3.97 (m, 2H, OCH_2); 7.07, 7.08 (s, 2H, ph). MS (EI, m/e) = 422 (M^+); 282 (M^+ - $\text{C}_{10}\text{H}_{21}$); 267 (M^+ - $\text{C}_{10}\text{H}_{21}$ -Me).

1,4-Di[4'-(4-ethynylphenyl)-2,2':6',2''-terpyridine]-2-(3,7-dimethyloctyl)-5-methoxybenzene (22)

To a stirred solution of 4'-(4-ethynylphenyl)-2,2':6',2''-terpyridine (**17**) (2.37g, 7.11 mmol) and 1,4-dibromo-2-(3,7-dimethyloctyl)-5-methoxybenzene (**21**) (1.0g, 2.37 mmol) in *n*-propylamine (300 ml) was added a solution of Pd[P(Ph)₃]₄ (0.4g, 0.347 mmol) in *n*-propylamine (60 ml). The mixture was refluxed at 60 °C overnight during which a yellow solid precipitated. The yellow solid was filtered off and washed with *n*-propylamine. The filtrate was partly evaporated and the precipitate was filtered off. Chromatographic separation of the solids on silicagel with chloroform as eluens gave 1,4-di[4'-(4-ethynylphenyl)-2,2':6',2''-terpyridine]-2-(3,7-dimethyloctyl)-5-methoxybenzene (**22**) as a yellow solid (2.39g, 2.58 mmol, 93%). ¹H-NMR (CDCl₃): δ 0.83, 0.85 (s, (2x3) H, CH₃); 0.99, 1.02 (s, 3H, CH₃); 1.16-1.93 (m, 10H); 3.94 (s, 3H, OMe); 4.10 (m, 2H, OCH₂); 7.06, 7.08 (s, 2H, ph); 7.38 (dd, J = 5.1, 7.2 Hz, 4H, H₅,H_{5''}); 7.67 (d, J = 8.7 Hz, 2H, ph); 7.70 (d, J = 8.7 Hz, 2H, ph); 7.92 (m, 8H, H₄,H_{4''},ph); 8.68-8.75 (m, 8H, H₃,H_{3''},H₆,H_{6''}); 8.78 (s, 4H, H_{3'},H_{5'}). MS (EI, m/e) = 926 (M⁺); 786 (M⁺- C₁₀H₂₁); 771 (M⁺-C₁₀H₂₁-Me). UV-VIS 382 nm. MALDI-TOF-MS: m/z: 926.

6.4 SYNTHESIS OF ADAMANTANES

1,1'-Biadamantane (23)

1-Bromoadamantane (10 g, 46.5 mmol) was heated under reflux in diethylether (100 ml) with magnesium (0.565 g, 23.25 mmol) for 48 hours under stirring. Silver bromine (202 mg, 1.07 mmol) was added and the reaction mixture refluxed for a further hour. Water was added at 0°C. The aqueous layer was washed with diethylether (2 x 200 ml) and the combined organic layers were evaporated. The residue was recrystallized in benzene to give 1,1'-biadamantane (**23**) (3.02g, 11.2 mmol, 47%) as a white solid. ¹H-NMR (CDCl₃): δ 1.59 (m, 6H); 1.74 (s, 12H); 1.90 (m, 12H). MS (EI, m/e) = 270 (M⁺); 135 (M⁺- adamantane).

3,3'-Dibromo-1,1'-biadamantane (24)

1,1'-Biadamantane (**23**) (3.75g, 13.88 mmol) was charged into a flask fitted with a reflux condenser and bromine (20 ml) was added with stirring. After 15 minutes the reaction mixture was heated to reflux for two hours. The cooled reaction mixture was diluted with carbon tetrachloride (75 ml) and separated. The carbon tetrachloride layer was washed with ice water. Sodium bisulfite was added until excess bromine was destroyed. The organic layer was separated and the water layer extracted with carbon tetrachloride (2 x 50 ml). The combined organic layers were dried over magnesium sulfate and the solvent evaporated. The reaction product was precipitated with methanol, filtered off and recrystallized from dioxane to give 3,3'-dibromo-1,1'-biadamantane (**24**) (2.35g, 5.49 mmol, 40%) as white crystals. ¹H-NMR (CDCl₃): δ 1.53-1.61 (m, 12H); 2.16-2.31 (m, 16H). ¹³C-NMR (CDCl₃): δ 32.49 (4C, CH); 33.59 (4C, CH₂); 35.15 (2C, CH₂); 42.58 (2C, C-C); 47.54 (2C, CH₂); 48.90 (4C, CH₂); 68.09 (2C, C-Br). MS (EI, m/e) = 427 (M⁺); 347 (M⁺-Br); 213 (M⁺-adamantane-Br).

3,3',5,5'-Tetrabromo-1,1'-biadamantane (25)

A mixture of 1,1'-biadamantane (**23**) (0.81g, 3.0 mmol) and AlBr₃ (250mg) was stirred with Br₂ (30 ml) for 4 hours at room temperature. The catalyst was destroyed by the addition of ice, and the reaction mixture was poured into a well-stirred mixture of CCl₄ (80 ml) and ice (150 ml). The excess bromine present was destroyed by the addition of solid NaHSO₃. The phases were separated, and the aqueous phase was extracted with additional CCl₄ (50 ml). The extract was combined with the organic phase and dried over anhydrous MgSO₄. Evaporation of the solvent and crystallization from CHCl₃/acetone gave 3,3',5,5'-tetrabromo-1,1'-biadamantane (**25**) (1.4g, 2.4 mmol, 80%) as an off-white solid. ¹H-NMR (CDCl₃): δ 1.53-1.57 (m, 4H); 2.11-2.31 (m, 18H); 2.72-2.83 (m, 4H). ¹³C-NMR (CDCl₃): δ 32.17 (2C, CH₂); 34.21 (2C, CH); 45.68 (4C, CH₂); 46.05 (2C, C-C); 46.41 (4C, CH₂); 58.36 (2C, CH₂); 62.05 (4C, C-Br). MS (EI, m/e) = 585 (M⁺); 505 (M⁺-Br).

3,3',5,5',7,7'-Hexabromo-1,1'-biadamantane (26)

A mixture of 1,1'-biadamantane (**23**) (1.0g, 3.7 mmol) and anhydrous AlCl₃ (0.75g) was stirred with Br₂ (20 ml) for 24 hours at 70 °C. The reaction

mixture was triturated with aqueous sodium sulphite (to remove excess bromine) with hydrochloric acid added (to dissolve aluminium salts). The layers were separated and the solids were removed by filtration, washed and dried to give 3,3',5,5',7,7'-hexabromo-1,1'-biadamantane (**26**) (0.86g, 1.1 mmol, 30%) as an off-white solid. $^1\text{H-NMR}$ (CDCl_3): δ 2.22 (d, $J = 3.0$ Hz, 12H); 2.76 (s, 12H). MS (EI, m/e) = 664 ($\text{M}^+ - \text{Br}$); 584 ($\text{M}^+ - \text{Br}_2$); 504 ($\text{M}^+ - \text{Br}_3$).

3,3',5,5',7,7'-Hexachloro-1,1'-biadamantane (**27**)

To a solution of 1,1'-biadamantane (**23**) (1.0g, 3.7 mmol) in carbon tetrachloride (40 ml) was added AlCl_3 (1.0g, 7.5 mmol). The reaction mixture was heated under reflux for three days, cooled, and quenched with water (10 ml). The liquid was decanted and the tarry residue was washed with dichloromethane (2 x 30 ml). The combined organic extracts were washed successively with saturated sodiumhydrogen carbonate (50 ml), water (40 ml) and saturated sodium chloride (40 ml) and dried with MgSO_4 to give 3,3',5,5',7,7'-hexachloro-1,1'-biadamantane (**27**) (0.99g, 2.1 mmol, 57%) as an off-white solid. MS (EI, m/e) = 476 (M^+); 441 ($\text{M}^+ - \text{Cl}$); 406 ($\text{M}^+ - \text{Cl}_2$); 202 ($\text{M}^+ - \text{adCl}_4$).

1,3,5,7-Tetraphenyladamantane (**28**)

A dry three-neck flask was fitted, under nitrogen, with two condensers running to a 30% NaOH solution. The flask was placed in an ice bath and cooled. To this flask was added 1-bromoadamantane (50.0g, 0.233 mol), benzene (500 ml), and *t*-butylbromide (65.0 ml, 0.476 mol). AlCl_3 (3.4g, 0.025 mol) was added in three portions over 15 min to the chilled, stirred solution. The solution was allowed to warm to room temperature and afterward refluxed for 2 hours. The heterogeneous reaction mixture was cooled to room temperature and poured into acidic ice. Benzene (500 ml) was added and the slurry stirred for 1 hour. The solution was filtered to remove the 1,3,5,7-tetraphenyladamantane (**28**) and washed with acetone. The solid was Soxhlet extracted overnight with chloroform. The desired product was insoluble in chloroform (67.0g, 0.152 mol, 66%). 1-Phenyl-, 1,3-diphenyl-, and 1,3,5-triphenyladamantane were isolated as a mixture from the combined benzene and chloroform solutions. 1-Phenyl- and 1,3-diphenyladamantane were very

soluble in ether, while 1,3,5-triphenyladamantane was not. 1,3,5-Triphenyladamantane was isolated by washing the mixture with ether. It can be purified by recrystallization from benzene. MS (EI, m/e) = 440 (M^+).

1,3,5,7-Tetrakis(4-iodophenyl)adamantane (29)

1,3,5,7-Tetraphenyladamantane (28) (25g, 56.25 mmol) and iodine (28.75g, 112.5 mmol) were ground together in a mortar. The finely ground pink solid was transferred to a 500-ml one neck round-bottom flask under nitrogen. The mortar was rinsed with chloroform (250 ml) which was also transferred to the flask. [bis-(trifluoroacetoxy)iodo]benzene (BFIB) (48.75g, 112.5 mmol) was added and the reaction mixture flushed with nitrogen. A static atmosphere of nitrogen was maintained while the dark red mixture was stirred for 6 hours, after which the mixture was filtered to remove a pink solid (mix of product and starting material). The solid was Soxhlet extracted with chloroform overnight. The chloroform solutions were combined and washed sequentially with 5% NaHSO₃ (to remove the iodine), water, and saturated NaCl solution. The solvent was removed under reduced pressure to give a yellow solid which was washed with diethylether and recrystallized from CHCl₃/MeOH (4:1) to give 1,3,5,7-tetrakis(4-iodophenyl)adamantane (29) (61.6g, 65.25 mmol, 58%) as a white crystalline product. ¹H-NMR (CDCl₃): δ 2.03 (s, 12H); 7.16 (d, J = 8.7 Hz, 8H); 7.65 (d, J = 8.7 Hz, 8H). MS (EI, m/e) = 944 (M^+); 818 ($M^+ - I$).

3,3',5,5',7,7'-Hexaphenyl-1,1'-biadamantane (30)

A flask was filled with 3,3'-dibromo-1,1'-biadamantane (24) (0.5g, 1.17 mmol) *t*-butylbromide (0.45 ml, 3.28 mmol) and benzene (20 ml), under nitrogen. The flask was placed in an ice bath and cooled. To this chilled, stirred solution was added AlCl₃ (0.23g, 0.17 mmol). The solution was allowed to warm to room temperature and refluxed for 24 hours. The heterogeneous reaction mixture was cooled to room temperature and poured into acidic ice (50 ml). Benzene (40 ml) was added and the slurry stirred for 1 hour. The layers were separated and the organic layer was dried in vacuo. The crude reaction product was again treated at the same manner as described above and after work up recrystallized in *o*-dichlorobenzene to give 3,3',5,5',7,7'-hexaphenyl-1,1'-biadamantane (30) (0.18g, 0.25 mmol, 21%) as a white solid. ¹H-NMR (CDCl₃): δ 1.88 (s, 12H); 1.99 (d, J = 12.0 Hz, 6H); 2.13 (d, J = 12.0

Hz, 6H); 7.20 (m, 6H); 7.33 (m, 12H); 7.44 (m, 12H). MS (EI, m/e) = 726 (M^+); 649 (M^+ - ph); 363 (M^+ - $adph_3$).

1,3,5,7-Tetrakis(4''-trimethylsilyl-1,4'-biphenyl)adamantane (31)

1,3,5,7-Tetrakis(4-iodophenyl)adamantane (**29**) (4.72g, 5 mmol) and 4-trimethylsilylbenzene-1-boronic acid (5.82g, 30 mmol) were dissolved in toluene (100 ml). The solution was degassed and flushed with nitrogen. An aqueous solution of Na_2CO_3 (1M, 80 ml) was added and the solution was degassed again. Tetrakis(triphenylphosphine)palladium (200 mg) was added and the mixture was refluxed for 24 hours. The mixture was allowed to cool to room temperature, the layers were separated, the aqueous layer was washed twice with toluene (50 ml) and the combined organic layers once with water (50 ml). The organic layer was dried over $MgSO_4$. Chromatographic separation on silicagel with a) hexane b) hexane/ $CHCl_3$ (4/1) gave 1,3,5,7-tetrakis(4''-trimethylsilyl-1,4'-biphenyl)adamantane (**31**) as a white yellow powder (3.84g, 3.72 mmol, 74%). Recrystallization in toluene gave white crystals. 1H -NMR ($CDCl_3$): δ 0.29 (s, 36H, TMS); 2.28 (s, 12H, adamantane); 7.59 (m, 32H, ph). ^{13}C -NMR ($CDCl_3$): δ -0.37 (12C, $SiCH_3$); 39.90 (4C, C-ad); 48.06 (6C, CH-ad); 126.22 (8C); 127.10 (8C); 127.83 (8C); 134.51 (8C); 139.76 (8C); 141.95 (4C); 149.19 (4C). MS (EI, m/e) = 1034 (M^+); 808 (M^+ - TMS- ph_2).

1,3,5,7-Tetrakis(4''-trimethylsilyl-2'',5''-di-*n*-hexyl-1,4'-biphenyl)-adamantane (32)

1,3,5,7-Tetrakis(4-iodophenyl)adamantane (**29**) (0.472g, 0.5 mmol) and 2,5-di-*n*-hexyl-4-trimethylsilylbenzene-1-boronic acid (1.086g, 3.0 mmol) were dissolved in toluene (10 ml). The solution was degassed and flushed with nitrogen. An aqueous solution of $Ba(OH)_2$ (1M, 10 ml) was added and the solution was degassed again. Tetrakis(triphenylphosphine)palladium (40mg, 0.0174 mmol) was added and the mixture was refluxed for 24 hours. The mixture was allowed to cool to room temperature, the layers separated, the aqueous layer washed with toluene (2 x 10 ml) and the combined organic layers with water (5 ml). The organic layer was dried over $MgSO_4$. Chromatographic separation on silicagel with a) hexane b) hexane/ $CHCl_3$ (9/1) gave 1,3,5,7-tetrakis(4''-trimethylsilyl-1,4'-biphenyl)adamantane (**32**) as a white yellow solid (0.47g, 0.276 mmol, 55%). 1H -NMR ($CDCl_3$): δ 0.38 (s,

36H, TMS); 0.86 (m, 24H, CH₃); 1.20-1.63 (m, 48H, CH₂); 2.34 (s, 12H, adamantane); 2.58 (t, J = 8.1 Hz, 8H, CH₂); 2.71 (t, J = 8.1 Hz, 8H, CH₂); 7.09 (s, 4H, ph); 7.35 (d, J = 8.4 Hz, 8H, ph); 7.37 (s, 4H, ph); 7.60 (d, J = 8.4 Hz, 8H, ph). MS (EI, m/e) = 1706 (M⁺).

1,3,5,7-Tetrakis(4-{2-trimethylsilyl}-1-ethynyl)-phenyladamantane (33)

To a stirred solution of 1,3,5,7-tetrakis(4-iodophenyl)adamantane (**29**) (2g, 2.12 mmol) and trimethylsilylacetylene (1.66g, 16.96 mmol) in *n*-propylamine (180 ml), was added a solution of Pd[P(Ph)₃]₄ (0.58g, 0.50 mmol) in *n*-propylamine (150 ml). The mixture was refluxed overnight and the solvent evaporated. Chromatographic separation through silica gel with a mixture hexane/CHCl₃ (3/1) as eluents and recrystallization from CHCl₃/Hexane gave 1,3,5,7-tetrakis(4-{2-trimethylsilyl}-1-ethynyl)-phenyladamantane (**33**) (1.53g, 1.85 mmol, 87%) as white powder. ¹H-NMR (CDCl₃): δ 0.23 (s, 36H, Si(CH₃)₃); 2.07 (s, 12H, adamantane); 7.36 (d, J = 8.4 Hz, 8H, ph); 7.42 (d, J = 8.4 Hz, 8H, ph). ¹³C-NMR (CDCl₃): δ 0.73 (9C, Si(CH₃)₃); 39.94 (4C, quaternary-ad); 47.39 (6C, secondary-ad); 94.66 (4C, C≡C); 105.67 (4C, C≡C); 121.76 (4C, C-ph); 125.60 (8C, CH-ph); 132.74 (8C, CH-ph); 150.06 (4C, C-ph). MS (EI, m/e) = 825 (M⁺); 809 (M⁺ - CH₃); 793 (M⁺ - 2CH₃); 721 (M⁺ - TMS-2CH₃).

1,3,5,7-Tetrakis(4-ethynyl)-phenyladamantane (34)

To a stirred solution of 1,3,5,7-tetrakis(4-{2-trimethylsilyl}-1-ethynyl)-phenyladamantane (**33**) (0.5g, 0.61 mmol) in methanol/THF (25ml/35ml) was added KF (0.176g, 3.03 mmol) as a solid. After stirring overnight the solution was concentrated by rotary evaporation to give a crude product which was dissolved in CHCl₃ to precipitate the K-salts which were filtered off. Recrystallization from CHCl₃/hexane gave 1,3,5,7-tetrakis(4-ethynyl)-phenyladamantane (**34**) (0.30g, 0.56 mmol, 92%). ¹H-NMR (CDCl₃): δ 2.10 (s, 12H, ad); 3.04 (s, 4H, H-C≡C); 7.40 (d, J = 8.4 Hz, 8H, ph); 7.47 (d, J = 8.4 Hz, 8H, ph). MS (EI, m/e) = 536 (M⁺).

Product (35)

A mixture of 1,3,5,7-tetrakis(4-ethynyl)-phenyladamantane (**34**) (0.1g, 0.186 mmol) and 6 eq tetraphenylcyclopentadienone (0.43g, 1.12 mmol) was

refluxed in *o*-xylene (3 ml) for 8 hours. The mixture was cooled and the solvent evaporated. The solid was precipitated in ethanol until the red colour almost disappeared and recrystallized in a mixture of CHCl_3 and ethanol to give (35) (0.33g, 0.17 mmol, 91%) as a white solid. $^1\text{H-NMR}$ (CDCl_3): δ 6.70 (m); 6.82 (m); 6.90(m); 6.98(m); 7.13 (s); 7.52 (s). IR (KBr, cm^{-1}) ν 3054, 3024, 1600, 1509, 1243, 699. UV-Vis (CHCl_3): 254 nm.

1,3,5,7-Tetrakis[[4'-[4-{2-(phenyl)-1-ethynyl}phenyl]-2,2':6',2''-terpyridine]adamantane (36)

To a stirred solution of 1,3,5,7-tetrakis(4-iodophenyl)adamantane (29) (0.50g, 0.53 mmol) and 4'-[4-(4-ethynylphenyl)-2,2':6',2''-terpyridine (17) (1.412g, 4.24 mmol) in *n*-propylamine (180 ml) was added a solution of $\text{Pd}[\text{P}(\text{Ph})_3]_4$ (0.24g, 0.208 mmol) in *n*-propylamine (40 ml). The mixture was refluxed at 60 °C and a yellow solid precipitated during the night. The yellow solid was filtered off and washed with *n*-propylamine. The filtrate was evaporated and chromatographic separation on silicagel with chloroform as eluents gave another fraction, which was combined with the yellow solid. The combined fractions were recrystallized twice in chloroform to give 1,3,5,7-tetrakis[[4'-[4-{2-(phenyl)-1-ethynyl}phenyl]-2,2':6',2''-terpyridine]-adamantane (36) as a white solid (0.56g, 0.317 mmol, 60%). $^1\text{H-NMR}$ (CDCl_3): δ 2.19 (s, 12H, adamantane); 7.37 (m, 8H); 7.50 (d, $J = 8.4$ Hz, 8H); 7.57 (d, $J = 8.4$ Hz, 8H); 7.67 (d, $J = 8.4$ Hz, 8H); 7.90 (m, 16H); 8.69-8.74 (m, 16H); 8.76 (s, 8H). $^{13}\text{C-NMR}$ (CDCl_3): δ 39.67, 47.14, 89.25, 91.05, 119.02, 121.38, 121.66, 124.07, 124.46, 125.36, 127.45, 132.04, 132.38, 137.23, 138.24, 149.19, 149.71, 156.13, 156.29. MS (EI, m/e) = 1767 (M^+); 884 (M^{+2}); 589 (M^{+3}); 442 (M^{+4}). MALDI-TOF-MS: m/z : 1766.36.

1,3,5,7-Tetrabromoadamantane (37)

Adamantane (19.44g, 143 mmol) was added in small portions over 30 min. to a stirred solution of bromine (90 ml) and anhydrous aluminium chloride (20g, 150 mmol) at 0°C. The mixture was then slowly heated to 70°C and held at that temperature for 24 h. The reaction mixture was treated subsequently with aqueous sodium sulphite and hydrochloric acid. The resulting solid was filtered, dried in vacuo, and recrystallized from acetonitrile to give 1,3,5,7-tetrabromoadamantane (37) (30.76g, 68.2 mmol, 48%) as tan crystals. $^1\text{H-NMR}$

(CDCl₃): δ 2.68 (s, 12H). MS (EI, m/e) = 451 (M⁺); 371 (M⁺- Br); 293 (M⁺- Br₂); 213 (M⁺- Br₃).

1,3,5,7-Tetrakis(1,3-dibromophenyl)adamantane (38)

A dry three-neck flask was fitted with a water condenser, a magnetic stirrer, a nitrogen inlet and outlet to a NaOH solution. The flask was placed in an ice bath. To this chilled flask was added 1,3,5,7-tetrabromoadamantane (37) (2.5g, 5.5 mmol), 1,3-bromobenzene (50 ml), and AlBr₃ (0.7g, 2.5 mmol). The reddish-brown mixture was stirred at 0°C for 5h, allowed to warm to room temperature overnight, and finally heated at 60°C for 6h. The mixture was poured onto acidic ice. After the ice melted, the layers were separated and the organic layer was washed with water and a saturated NaCl solution. The product was isolated by precipitation into methanol. Chromatographic separation on silicagel with a mixture of hexane/chloroform a (1/10) and b (1/1) as eluents and recrystallization in chloroform gave 1,3,5,7-tetrakis(1,3-dibromophenyl)adamantane (38) (1.88g, 1.76 mmol, 32%) as a white solid. ¹H-NMR (CDCl₃): δ 2.01 (s, 12H); 7.49 (t, 8H); 7.56 (m, 4H). ¹³C-NMR (CDCl₃): δ 39.32, 46.05, 123.27, 127.01, 132.34, 151.53. MS (EI, m/e) = 1073 (M⁺); 837 (M⁺- phBr₂); 603 (M⁺- 2(phBr₂)); 391 (M⁺- 3(phBr₂)).

1,3,5,7-Tetrakis[1,3-di-(4'-phenyl-1-ethynyl-2,2':6',2''-terpyridine)-phenyl]adamantane (39)

To a stirred solution of 1,3,5,7-tetrakis(1,3-dibromophenyl)adamantane (38) (0.10g, 0.093 mmol) and 4'-(4-ethynylphenyl)-2,2':6',2''-terpyridine (17) (0.497g, 1.49 mmol) in *n*-propylamine (50 ml) was added a solution of Pd[P(Ph)₃]₄ (0.08g, 0.051 mmol) in *n*-propylamine (10 ml). The mixture was refluxed at 60 °C overnight during which a yellow solid precipitated. The yellow solid was filtered off and washed with *n*-propylamine. The filtrate was evaporated and chromatographic separation on silicagel with a) chloroform and b) chloroform/MeOH as eluents gave 1,3,5,7-tetrakis[1,3-di-(4'-phenyl-1-ethynyl-2,2':6',2''-terpyridine)phenyl]-adamantane (39) as a yellow solid (0.137g, 0.047 mmol, 50%). ¹H-NMR (CDCl₃): δ 2.20 (s broad, ad); 7.18-7.26 (m); 7.58-7.77 (m); 8.49-8.60 (m). MS (EI, m/e) = 1546.9 (M²⁺); 1032.1 (M³⁺); 774.2 (M⁴⁺); also hepta-substituted present: 1420.7 (M²⁺); 947.8 (M³⁺); and hexa-substituted 1294.7 (M²⁺); 863.7 (M³⁺).

6.5 SYNTHESIS OF SILSESQUIOXANES

Octaphenylpentacyclo[9.5.1.1^{3,9}.1^{5,15}.1^{7,13}]octasiloxane (40)

Phenyltrichlorosilane (21.6g, 0.1 mol) was dissolved in benzene (100 ml) and shaken with water until hydrolysis was complete. After removing the acid layer and washing with water, methanolic 40% benzyltrimethylammonium hydroxide solution (3.32 ml, 0.006 mol) was added. The mixture was refluxed for 4 hours, allowed to stand 4 days, refluxed another 24 hours and then cooled and filtered to give octaphenylpentacyclo[9.5.1.1^{3,9}.1^{5,15}.1^{7,13}]octasiloxane (40) as a white powder (7.36g, 7.15 mmol, 57%). Purification by recrystallization was possible in hot *o*-dichlorobenzene. ¹H-NMR (CDCl₃): δ 7.73 (dd, *J* = 7.8, 1.2 Hz, 2H); 7.42 (m, 1H); 7.34 (m, 2H). MS (EI, *m/e*) = 1032 (M⁺); 955 (M⁺-ph); 877 (M⁺-2ph). IR (KBr, cm⁻¹) ν 3073 (C-H aromatic); 3028 (C-H aromatic); 1594 (benzene ring); 1457 (benzene ring); 1431, 1136, 1114 (ν_{as} O-Si-O); 745 (monosubstituted aromatic ring); 697 (monosubstituted aromatic ring); 608, 497 (δ O-Si-O). Melting point > 400°C.

4-Chlorophenyltrichlorosilane (41)

To magnesium turnings (36.0g, 1.5 mol) and dry diethyl ether (100 ml) a solution of 1-bromo-4-chlorobenzene (236.25g, 1.24 mol) in dry diethyl ether (480 ml) was added dropwise, in the course of 3 hours. The reaction mixture was refluxed for another 3 hours and was added dropwise to silicontetrachloride (224.25g, 151.2 ml, 1.34 mol) in diethyl ether (375 ml) in the course of 1 hour. The reaction mixture was refluxed overnight. The ethereal solution was decanted from the insoluble magnesium salts and the residue extracted several times with boiling diethyl ether (3 x 300 ml). The combined ethereal solutions were dried under reduced pressure. Purification of the residue was done by vacuum distillation (bp 119-120°C / 35 mm Hg) to give 4-chlorophenyltrichlorosilane (41) as a colorless, highly air and moisture sensitive, liquid (160g, 0.65 mol, 52%). ¹H-NMR (CDCl₃): δ 7.46 (d, *J* = 8.0 Hz, H_{3,5}); 7.71 (d, *J* = 8.0 Hz, H_{2,6}). MS (EI, *m/e*) = 246 (M⁺); 211 (M⁺-Cl); 133 (M⁺-phCl).

Octa(*p*-chlorophenyl)pentacyclo[9.5.1.1^{3,9}.1^{5,15}.1^{7,13}]octasiloxane (42)

4-Chlorophenyltrichlorosilane (41) (20g, 81.3 mmol) was dissolved in benzene (150 ml) and shaken with brine until hydrolysis was complete. The solution was washed once with water and a methanolic 40% benzyltrimethylammonium hydroxide solution (1 ml) was added. The solution was refluxed for 6 hours and allowed to stand at room temperature until no more crystals were formed (\pm 72 hours). The crystals were recovered by filtration and chromatographic separation on silica (eluens CH₂Cl₂) gave pure octa(*p*-chlorophenyl)pentacyclo[9.5.1.1^{3,9}.1^{5,15}.1^{7,13}]octasiloxane (42) (7.45g, 5.71 mmol, 61%). ¹H-NMR (CDCl₃): δ 7.54 (d, J = 8.1 Hz, 2H); 7.60 (d, J = 8.1 Hz, 2H). ¹³C-NMR (CDCl₃) δ 128.11 (C-Si); 129.18 (C-H); 136.09 (C-H); 138.45 (C-Cl). ²⁹Si-NMR (79.6 MHz, TMS, 25° C) δ -78.2. MS (EI, m/e) = 1307 (M⁺); 1196 (M⁺ - pCl). IR (KBr, cm⁻¹) ν 3038 (C-H aromatic); 1585 (benzene ring); 1489 (benzene ring); 1384, 1138, 1104, 1082 (ν_{as} O-Si-O); 1015, 813 (*p*-disubstituted benzene ring); 760 (C-Cl); 710, 526 (δ O-Si-O). Melting point > 400°C.

X-ray Crystal Structure Determination of octa(*p*-chlorophenyl)pentacyclo[9.5.1.1^{3,9}.1^{5,15}.1^{7,13}]octasiloxane (42)

The colorless single crystals obtained by slow evaporation from a CH₂Cl₂ solution belong to the triclinic space group P-1 (No. 2) with cell parameters $a = 12.216(2)\text{\AA}$, $b = 12.141(2)\text{\AA}$, $c = 12.388(2)\text{\AA}$, $\alpha = 90.05(3)^\circ$, $\beta = 76.90(3)^\circ$, $\gamma = 65.71(3)^\circ$, $Z = 1$. The transparent crystals collapsed within a few seconds when exposed to air. The data were measured at 100K using a MAR345 image plate detector ($\lambda = 0.71073\text{\AA}$) and a crystal of size 0.35 x 0.35 x 0.20 mm³. In total 29153 reflections were collected resulting in 6387 independent reflections ($R_{merge} = 0.070$). The structure was solved by direct methods and refined by full-matrix least squares on F^2 using the SHELXTL program package. The asymmetric unit consists of half a molecule plus one molecule CH₂Cl₂. Non-hydrogen atoms were anisotropically refined and the hydrogen atoms in the riding mode with isotropic temperature factors fixed at 1.2 times $U(eq)$ of the parent atoms. The final refinement parameters were $R_1 = 0.0657$ for 5543 observed reflections ($F_o > 4\sigma(F_o)$), $wR_2 = 0.1856$ for all data (weighting scheme $w^{-1} = \sigma^2(F_o^2) + (0.0987P)^2 + 3.9187P$, where $P = [\text{Max}(F_o^2, 0) + 2F_c^2]/3$), GOF = 1.043.

4-Methyl-biphenyl (43)

An oven dried flask was purged with argon and charged with tris(dibenzylideneacetone)dipalladium (0) ($\text{Pd}_2(\text{dba})_3$) (0.11g, 0.12 mmol), phenylboronic acid (1.45g, 11.9 mmol), 3-bis(2,4,6-trimethylphenyl)-imidazolium chloride (81mg, 0.24 mmol), Cs_2CO_3 (5.18g, 15.9 mmol) (Cs_2CO_3 was grind, prior to use, with mortar and pestle and dried thoroughly) dry dioxane (20 ml) and 4-chlorotoluene (1g, 7.94 mmol) and refluxed for 3 hours. The reaction mixture was cooled to room temperature diluted with diethyl ether (20 ml) and washed with NaOH (1M, 20 ml). The layers were separated and the aqueous layer was extracted with diethyl ether (2 x 20 ml). The combined organic layers were dried over anhydrous magnesium sulphate. The solvent was evaporated and chromatographic separation through silica gel with hexane gave 4-methyl-biphenyl (43) (1.23g, 7.3 mmol, 92%) as a white solid. $^1\text{H-NMR}$ (CDCl_3): δ 2.39 (s, 3H, CH_3); 7.25 (d, $J = 8.1$ Hz, 2H); 7.34 (m, 1H); 7.42 (m, 2H); 7.49 (d, $J = 8.1$ Hz, 2H); 7.59 (m, 2H).

4,4'-Biphenyldiboronic acid (44)

To a solution of 4,4'-dibromobiphenyl (25g, 0.08 mol) in tetrahydrofuran (500 ml) at -78°C , *n*-butyllithium (100 ml, 0.25 mol, 2.5 M solution in hexane) was added dropwise. The mixture was allowed to warm up to room temperature and stirred at 25°C for 1h. The solution was cooled once again and triisopropylborate (75.2g, 92 ml, 0.40 mol) was added. The reaction was allowed to warm up to room temperature, stirred overnight, diluted with diethylether (200 ml) and added to a stirred mixture of crushed ice and concentrated sulphuric acid (6 ml). The addition of ether and water facilitated the separation of the layers. The layers were separated and the aqueous layer washed with diethylether (4 x 100 ml). The combined organic layers were dried over MgSO_4 and evaporated. The white solid was washed twice with cold diethylether and dried in vacuo to give 4,4'-biphenyldiboronic acid (44) (12.0g, 49.6 mmol, 62%) as a white solid. $^1\text{H-NMR}$ (DMSO): δ 7.66 (d, $J = 8.1$ Hz, 4H, ph); 7.88 (d, $J = 8.1$ Hz, 4H, ph); 8.09 (s, 4H, $\text{B}(\text{OH})_2$). $^1\text{H-NMR}$ (CDCl_3): δ 7.21 (d, $J = 8.1$ Hz, 4H, ph); 7.47 (d, $J = 8.1$ Hz, 4H, ph).

4,4'-Biphenyldiboronic acid pinacol ester (45)

4,4'-Biphenyldiboronic acid (**44**) (2g, 8.26 mmol) and pinacol (2.44g, 20.65 mmol) were refluxed in toluene (90 ml) under a Dean-Stark head. Toluene was evaporated after completion of the reaction and chromatographic separation through silica gel with chloroform gave 4,4'-biphenyldiboronic acid pinacol ester (**45**) (3.18g, 7.85 mmol, 95%) as a white powder. This powder was recrystallized in hexane to give white crystals. $^1\text{H-NMR}$ (CDCl_3): δ 1.34 (s, 24H, CH_3); 7.61 (d, $J = 8.1$ Hz, 4H, ph); 7.86 (d, $J = 8.1$ Hz, 4H, ph). MS (EI, m/e) = 406 (M^+); 391 ($\text{M}^+ - \text{CH}_3$).

6.6 SYNTHESIS OF COMPLEXES **RuCl_3 -Complex (46)**

A solution of $\text{RuCl}_3 \cdot 3\text{H}_2\text{O}$ (0.34g, 1.30 mmol) and 4'-[4-{2-(trimethylsilyl)-1-ethynyl}phenyl]-2,2':6',2''-terpyridine (**16**) (0.5g, 1.23 mmol) in ethanol (70 ml) was refluxed for 3 hours. After cooling the brown precipitate was filtered, washed sequentially with ethanol (2 x 20 ml), H_2O (2 x 20 ml), diethylether (2 x 30 ml) and dried in vacuo yielding RuCl_3 -complex (**46**) (0.71g, 1.16 mmol, 95%) as a brown solid. UV-Vis (CH_3CN): 286, 390 nm.

Bis[4'-[4-{2-(trimethylsilyl)-1-ethynyl}phenyl]-2,2':6',2''-terpyridyl]-ruthenium(II) hexafluorophosphate (47)

To a suspension of compound (**46**) (0.1g, 0.165 mmol) and 4'-[4-{2-(trimethylsilyl)-1-ethynyl}phenyl]-2,2':6',2''-terpyridine (**16**) (0.067g, 0.165 mmol) in a mixture MeOH/chloroform (2/1) (30 ml) was added N-ethylmorpholine (4 drops) and the mixture was refluxed for 6 hours until it turned into a clear red solution. After cooling to room temperature an excess $[\text{NH}_4][\text{PF}_6]$ was added and the red precipitate was filtered off and washed sequentially with H_2O (2 x 20 ml) and diethylether (2 x 30 ml) to give bis[4'-[4-{2-(trimethylsilyl)-1-ethynyl}phenyl]-2,2':6',2''-terpyridyl]-ruthenium(II)-hexa-fluorophosphate (**47**) (0.144g, 0.12 mmol, 87%) as a red solid. $^1\text{H-NMR}$ (CD_3CN): δ 0.32 (s, 18H, TMS); 7.19 (ddd, $J = 1.5, 5.7, 8.7$ Hz, 4H, H_5, H_5'); 7.44 (d, $J = 5.7$ Hz, 4H, H_6, H_6'); 7.81 (dd, $J = 1.8, 8.4$ Hz, 4H, ph); 7.95 (ddd, J

= 1.5, 8.1, 8.7 Hz, 4H, H₄,H_{4'}); 8.23 (dd, J = 1.8, 8.4 Hz, 4H, ph); 8.65 (d, J = 8.1 Hz, 4H, H₃,H_{3'}); 9.01 (s, 4H, H₃,H₅). ¹³C-NMR (CD₃CN): δ 0.15 (TMS); 98.06 (2C, C≡C); 105.37 (2C, C≡C); 122.76 (4C); 125.85 (4C); 126.00 (4C); 128.77 (4C); 129.24 (4C); 134.03 (4C); 138.21 (2C); 139.32 (4C); 148.34 (2C); 153.72 (4C); 156.75 (4C); 159.35 (4C). FAB⁺ (matrix nitrobenzylalcohol) *m/z* = 1057 (M-PF₆)⁺; 912 (M-2PF₆)²⁺. UV-Vis (CH₃CN): 313, 495 nm.

Bis[4'-(4-ethynylphenyl)-2,2':6',2''-terpyridyl] zinc(II) hexafluorophosphate (48)

To a suspension of 4'-(4-ethynylphenyl)-2,2':6',2''-terpyridine (17) (100mg, 0.300 mmol) in a mixture of MeOH (20 ml) and CHCl₃ (5 ml) was added Zn(II)acetate (32.9mg, 0.150 mmol) and the mixture was refluxed 8 hours. After cooling to room temperature an excess [NH₄][PF₆] was added and the precipitate was filtered off and washed sequentially with H₂O (2 x 20 ml) and Et₂O (2 x 30 ml) to give bis[4'-(4-ethynylphenyl)-2,2':6',2''-terpyridyl]zinc(II) hexafluorophosphate (48) (0.141g, 0.276 mmol, 92%) as a white solid. ¹H-NMR (CD₃CN): δ 3.67 (s, 2H, C≡H); 7.41 (m, 4H, H₅,H_{5'}); 7.86 (m, 8H, H₆,H_{6'},ph); 8.19 (m, 8H, H₄,H_{4'},ph); 8.72 (d, J = 7.8 Hz, 4H, H₃,H_{3'}); 8.98 (s, 4H, H₃,H₅). ¹³C-NMR (CD₃CN): δ 86.66 (2C, C≡C); 88.39 (2C, C≡C); 127.58, 129.23, 130.72, 133.54, 134.26, 139.06, 142.47, 147.25, 153.76, 154.04, 155.89, 161.24. FAB⁺ (matrix nitrobenzylalcohol) *m/z* = 875 (M-PF₆)⁺; 730 (M-2PF₆)²⁺. UV-Vis (CH₃CN): 287, 313 nm.

Bis[4'-(4-ethynylphenyl)-2,2':6',2''-terpyridyl]cobalt(II) hexafluorophosphate (49)

To a suspension of 4'-(4-ethynylphenyl)-2,2':6',2''-terpyridine (17) (100mg, 0.300 mmol) in a mixture of MeOH (20 ml) and CHCl₃ (5 ml) was added Co(II)acetate (37.3mg, 0.15 mmol) and the mixture was refluxed 8 h. After cooling to room temperature an excess [NH₄][PF₆] was added and the precipitate was filtered off and washed sequentially with H₂O (2 x 20 ml) and Et₂O (2 x 30 ml) to give bis[4'-(4-ethynylphenyl)-2,2':6',2''-terpyridyl]cobalt(II) hexafluorophosphate (49) (0.121g, 0.119 mmol, 80%) as a deep maroon solid. ¹H-NMR (CD₃CN): δ 4.91 (s); 9.06 (d, J = 6.3 Hz); 9.54 (s). FAB⁺ (matrix nitrobenzylalcohol) *m/z* = 870 (M-PF₆)⁺; 725 (M-2PF₆)²⁺. UV-Vis (CH₃CN): 286, 308, 450-550 nm (weak).

Heteroleptic Complex (50)

To a suspension of compound (46) (0.1g, 0.165 mmol) and 4'-(4'''-bromophenyl)-2,2':6',2''-terpyridine (15) (0.064g, 0.165 mmol) in MeOH (30 ml) was added N-ethylmorpholine (4 drops) and the mixture was refluxed for 4 hours until it turned into a clear red solution. After cooling to room temperature an excess $[\text{NH}_4][\text{PF}_6]$ was added and the red precipitate was filtered off and washed sequentially with H_2O (2 x 20 ml) and Et_2O (2 x 30 ml) to give the heteroleptic complex (50) (0.152g, 0.128 mmol, 78%) as a red solid. $^1\text{H-NMR}$ (CD_3CN): δ 0.31 (s, 9H, TMS); 7.18 (m, 4H, $\text{H}_5, \text{H}_{5'}$); 7.41 (d, $J = 5.7$ Hz, 4H, $\text{H}_6, \text{H}_{6'}$); 7.82 (d, $J = 8.4$ Hz, 2H, ph); 7.94 (m, 4H, $\text{H}_4, \text{H}_{4'}$, ph); 8.12 (d, $J = 8.4$ Hz, 2H, ph); 8.21 (d, $J = 8.4$ Hz, 2H, ph); 8.64 (m, 4H, $\text{H}_3, \text{H}_{3'}$); 8.99 (s, 2H, $\text{H}_3, \text{H}_{5'}$); 9.00 (s, 2H, $\text{H}_3, \text{H}_{5'}$). FAB^+ (matrix nitrobenzylalcohol) m/z 1039 (M-PF_6) $^+$; 894 (M-2PF_6) $^{2+}$. UV-Vis (CH_3CN): 311, 490 nm.

RuCl₃-Complex (51)

To solution of $\text{RuCl}_3 \cdot 3\text{H}_2\text{O}$ (88.4 mg, 0.35 mmol) in MeOH (10 ml) was added dropwise a solution of 1,16-bis(2,2':6',2''-terpyridin-4'-yloxy)-hexadecane (0.1g, 0.139 mmol) in CHCl_3 (2 ml) and the mixture was refluxed for 5 hours. After cooling to room temperature the brown precipitate was filtered, washed sequentially with CHCl_3 (2 x 5 ml), H_2O (2 x 10 ml), Et_2O (2 x 10 ml) and dried in vacuo yielding RuCl_3 -complex (51) (0.14g, 0.123 mmol, 89%) as a brown solid. UV-Vis (CH_3CN): 275, 394 nm.

Bi-Complex (52)

A suspension of 4'-[4-{2-(trimethylsilyl)-1-ethynyl}phenyl]-2,2':6',2''-terpyridine (16) (21.4mg, 0.053 mmol), RuCl_3 -complex (51) (30mg, 0.026 mmol) and N-ethylmorpholine (3 drops) in MeOH (8ml) was refluxed for 5 hours. After cooling to room temperature an excess $[\text{NH}_4][\text{PF}_6]$ was added and the precipitate was filtered off and washed sequentially with H_2O (2 x 10 ml) and Et_2O (2 x 20 ml) to give bi-complex (52) (51mg, 0.0294 mmol, 83%) as a red solid. $^1\text{H-NMR}$ (CD_3CN): δ 0.32 (s, 18H, TMS); 1.3-1.8 (m, 24H, CH_2); 2.04 (m, 4H, CH_2); 4.53 (t, $J = 6.3$ Hz, 4H, OCH_2); 7.14 (t, $J = 6.3$ Hz, 4H, $\text{H}_5, \text{H}_{5'}$); 7.22 (t, $J = 6.3$ Hz, 4H, $\text{H}_5, \text{H}_{5'}$); 7.40 (m, 8H, $\text{H}_6, \text{H}_{6'}$); 7.81 (d, $J = 8.1$ Hz, 4H, ph); 7.93 (m, 8H, $\text{H}_4, \text{H}_{4'}$); 8.21 (d, $J = 8.1$ Hz, 4H, ph); 8.32 (s, 4H,

H₃,H₅); 8.50 (d, J = 7.8 Hz, 4H, H₃,H₃); 8.65 (d, J = 8.1 Hz, 4H, H₃,H₃); 8.99 (s, 4H, H₃,H₅). UV-Vis (CH₃CN): 240, 273, 304, 492 nm.

RuCl₃-complex (53)

To a solution of RuCl₃·3H₂O (0.18g, 0.69 mmol) in EtOH (60 ml) was added dropwise a solution of 1,4-di[4'-(4-ethynylphenyl)-2,2':6',2''-terpyridine]-2-(3,7-dimethyloctyl)-5-methoxy-benzene (**22**) (0.3g, 0.324 mmol) in CHCl₃ (15 ml) and the mixture was refluxed for 4 hours. After cooling to room temperature the brown precipitate was filtered, washed sequentially with CHCl₃ (2 x 10 ml), H₂O (2 x 20 ml) and Et₂O (2 x 20 ml) then dried in vacuo yielding compound (**53**) (0.36g, 0.272 mmol, 84%) as a brown solid. UV-Vis (CH₃CN): 287, 324, 375 nm.

Bi-complex (54)

A suspension of 4'-[4-{2-(trimethylsilyl)-1-ethynyl}phenyl]-2,2':6',2''-terpyridine (**16**) (35.6mg, 0.088 mmol), RuCl₃-complex (**53**) (50mg, 0.037 mmol) and N-ethylmorpholine (5 drops) in MeOH (15ml) was refluxed for overnight. After cooling to room temperature an excess [NH₄][PF₆] was added and the precipitate was filtered off and washed sequentially with CHCl₃ (2 x 10 ml), H₂O (2 x 10 ml) and Et₂O (2 x 20 ml) to give bi-complex (**54**) (80.1mg, 0.0318 mmol, 85%) as a red solid. ¹H-NMR (CD₃CN): δ 0.33 (s, 18H, TMS); 0.90 (s, 6H, CH₃); 1.1-1.9 (m, 13H, CH₂); 4.05 (s, 3H, OCH₃); 4.24 (m, 2H, OCH₂); 7.32 (m, 10H, H₅,H₅,ph); 7.56 (m, 8H, H₆,H₆); 7.93 (d, J = 8.4 Hz, 8H, ph); 8.06 (m, 8H, H₄,H₄); 8.32-8.42 (m, 8H, ph); 8.78 (m, 8H, H₃,H₃); 9.15 (m, 8H, H₃,H₅). ¹³C-NMR (CD₃CN): δ 20.19, 22.99, 25.67, 28.84, 30.82, 37.11, 38.00, 40.06, 57.24, 68.91, 95.35, 97.93, 105.14, 122.56, 125.65, 125.87, 128.58, 129.02, 129.15, 133.56, 133.86, 137.94, 139.16, 148.16, 153.53, 156.58, 159.16. UV-Vis (CH₃CN): 284, 312, 496 nm.

Tetra-Complex (55)

To a suspension of the RuCl₃-complex of 4'-heptyloxy-[2,2';6',2'']-terpyridine (78.6 mg, 0.14 mmol) and N-ethylmorpholine (4 drops) in MeOH (15 ml) was added 1,3,5,7-tetrakis[[4'-[4-{2-(phenyl)-1-ethynyl}phenyl]-2,2':6',2''-terpyridine]adamantane (**36**) (50 mg, 0.028 mmol) dissolved in CHCl₃ (8 ml) and the mixture was refluxed overnight. After cooling to room

temperature the mixture was filtered and the filtrate treated with an excess $[\text{NH}_4][\text{PF}_6]$. The red precipitate was filtered off and washed sequentially with H_2O (2 x 20 ml) and Et_2O (2 x 20 ml) to give complex (**55**) (78,1 mg, 0.016 mmol, 58 %) as a red solid. The product was purified via chromatographic separation with bio-beads SX-1 with DMF as eluents. $^1\text{H-NMR}$ (CD_3CN): δ 0.94 (s, 12H, CH_3); 1.41-1.71 (m, 24H, CH_2); 1.89-2.30 (m, 28H, CH_2 , ad); 4.54 (t, $J = 6.9$ Hz, 8H, OCH_2); 7.15 (t, $J = 6.3$ Hz, 8H, H_5, H_5'); 7.21 (t, $J = 6.3$ Hz, 8H, H_5, H_5'); 7.39 (d, 8H, H_6, H_6'); 7.45 (d, 8H, H_6, H_6'); 7.68-7.77 (m, 16H, ph); 7.89-7.98 (m, 16H, H_4, H_4' , ph); 8.28 (d, $J = 8.1$ Hz, 8H, ph); 8.33 (s, 8H, H_3, H_3'); 8.49 (d, $J = 7.8$ Hz, 8H, H_3, H_3'); 8.66 (d, $J = 8.1$ Hz, 8H, H_3, H_3'); 9.02 (s, 8H, H_3, H_3'). $^{13}\text{C-NMR}$ (CD_3CN): δ 18.6, 27.5, 30.7, 33.9, 36.7, 44.7, 51.2, 75.5, 93.5, 96.7, 116.2, 125.5, 126.5, 129.6, 130.2, 131.0, 132.5, 133.1, 136.8, 137.6, 141.8, 143.0, 143.1, 151.6, 155.9, 157.5, 157.7, 161.0, 161.2, 163.3, 163.4, 171.6 ppm. UV-Vis (CH_3CN): 240, 273, 285, 304, 493 nm. MALDI-TOF-MS: m/z : 4568 (M-PF_6) $^+$; 4424 (M-2PF_6) $^+$; 4280 (M-3PF_6) $^+$; 4136 (M-4PF_6) $^+$.

6.7 SYNTHESIS OF PRODUCTS CHAPTER FIVE

1,4-Didodecanoxybenzene (**56**)

Hydroquinone (55g, 0.5 mol), 1-bromododecane (274g, 1.10 mol) and KOH (56g, 1.0 mol) were refluxed for 10 hours in acetone (500 ml). Water was added (400 ml), the layers separated and the water layer extracted with diethyl ether (3 x 100 ml). The combined organic phases were washed successively with 10% aq NaOH (60 ml) and brine (3 x 50 ml), dried with MgSO_4 and the solvent evaporated. Recrystallization from diethyl ether gave 1,4-didodecanoxybenzene (**56**) (143g, 0.32 mol, 64%) as white crystals. $^1\text{H-NMR}$ (CDCl_3): δ 0.87 (t, $J = 6.9$ Hz, 6H, CH_3); 1.25-1.44 (m, 36H, CH_2); 1.73 (m, 4H, OCH_2CH_2); 3.88 (t, $J = 6.6$ Hz, 4H, OCH_2); 6.80 (s, 4H, ph). MS (EI, m/e) = 446 (M^+); 278 ($\text{M}^+ - \text{C}_{12}\text{H}_{25}$).

1,4-Didodecanoxy-2,5-diiodobenzene (**57**)

A mixture of 1,4-didodecanoxybenzene (**56**) (60g, 0.1345 mol), iodine (30.8g, 0.1211 mol), HIO_3 (14.2g, 0.0807 mol), 30% H_2SO_4 (40 ml) and CCl_4

(55 ml) in AcOH (240 ml) was heated for 3 hours at 75 °C. The mixture was cooled with an ice bath, the crystals were filtered out and washed with a large amount of methanol and then recrystallized twice from ethanol to give 1,4-didodecanoxy-2,5-diiodobenzene (**57**) (77g, 0.1103 mol, 82%) as a white powder. ¹H-NMR (CDCl₃): δ 0.86 (t, J = 6.6 Hz, 6H, CH₃); 1.28 (m, 32H, CH₂); 1.47 (m, 4H, CH₂); 1.78 (m, 4H, OCH₂-CH₂); 3.90 (t, J = 6.3 Hz, 4H, OCH₂); 7.15 (s, 2H, ph). MS (EI, m/e) = 698 (M⁺); 530 (M⁺ - C₁₂H₂₅); 362 (M⁺ - 2C₁₂H₂₅).

